RAMSES PROJECT

Grant Agreement n° 308497

WP 3: Small-scale vulnerability and risk analysis for cities and sectors

Deliverable 3.1: High level quantified assessment of key vulnerabilities and priority risks for urban areas in the EU

Reference code: RAMSES – D3.1

This project has received funding from the European Union's Seventh Programme for Research, Technological Development and Demonstration under Grant Agreement No. 308497 (Project RAMSES).

Project Acronym: RAMSES

Project Title: Reconciling Adaptation, Mitigation and Sustainable Development for Cities

Contract Number: 308497

Title of report: D3.1: High level quantified assessment of key vulnerabilities and priority risks for urban areas in the EU

Reference code: RAMSES – D3.1

Short Description:

This report describes a high level climate risk analysis methodology for urban areas. The approach takes advantage of increased availability of European and global dataset and computing power to apply the method to 571 cities in the EU's Urban Audit database.

Authors and co-authors: Carlos Tapia[1], Selma Guerreiro[2], Richard Dawson[2], Beñat Abajo[1], Chris Kilsby[2], Efren Feliu[1], Maddalen Mendizabal[1], José Antonio Martinez[1], J. German Fernández[1], Vasilis Glenis[2], Chinedum Eluwa[2], Txomin Laburu[1], Adelaida Lejarazu[1]

[1] Tecnalia Research and Innovation

[2] Newcastle University

Partners owning: Tecnalia R&I, Newcastle University

Contributions: PIK

Made available to:

Versioning

Version	Date	Name, organization
0.1	31/10/2015	Tecnalia R&I, Newcastle University
0.2	15/04/2016	Tecnalia R&I, Newcastle University

Quality check

Internal Reviewers:

Giuseppe Forino (T6)

Diego Rybski (PIK)

Executive Summary

This report introduces a high level climate risk analysis methodology for urban areas that provides a top-down, and broad, view of climate risks to cities across Europe. The approach takes advantage of increasingly availability of European and global dataset and computing power to apply the method to 571 cities in the EU's Urban Audit database.

This high level cities risk analysis involved:

- Identification of stakeholder priorities for city-scale climate risk and vulnerability assessment;
- Development of a framework for city-scale climate risk analysis that uses EU-wide (or globally available) data so that it can be applied to give a baseline assessment of all EU cities in the Urban Audit database;
- Development of a suite of EU-wide climate hazard modelling tools for flooding, heatwaves and droughts;
- Development of an EU-wide exposure and vulnerability assessment of each city in the Urban Audit database;
- Integration of exposure, vulnerability and hazard datasets to evaluate risks.

The spatial database of vulnerability, exposure, hazard and risk indices for all 571 cities will be uploaded to the EU Climate Adapt (European Climate Adaptation Platform) and the EEA Climate Change Data Centre. The results provide information on hazard, exposure, vulnerability and risks to enable the prioritisation of national and EU-wide adaptation investments. Furthermore, by assessing the components of risk separately the results provide important insights into the nature of appropriate adaptation strategies– whether to focus on engineered adaptation and/or strengthening socio-economic capabilities.

Risk is not just a function of hazard, but also of socio-economic vulnerabilities. This risk assessment methodology can be used to assess the relative priorities for cities: in terms of the most significant risks for each city, and whether the relative contribution of hazard or vulnerability to that risk. Some cities have relatively low hazard scores but high exposure and/or vulnerability, whilst other cities have relatively high hazard and low exposure, and/or vulnerability. This enables climate risk managers to prioritise hazard management interventions, or approaches to reduce vulnerability and build adaptive capacity. The results provide information of use to national and EU policy makers to inform the prioritisation of investment in particular risks and across European regions.

Heat and drought risks are significant in a number of locations but show significant variability. Typically cities in Northern European latitudes are less likely to be exposed to significant drought hazard than those in Southern latitudes. Most notably, the variability in hazards exceeds those reported by previous analyses which have only been based upon a small number of model results. Under the high impact hazard results, increases in heatwave risk and peak temperatures are prevalent across all EU cities. The UK (and parts of Scandinavia) are expected to experience the greatest impacts in terms of changes in fluvial flooding hazard while much of the Mediterranean region is not expected to see an increase, even in the high impact scenario.

The pattern of exposure, vulnerability and risk varies across European cities. Drought risk management should be a priority for those cities located around the Mediterranean and Black sea basins. Heatwave risks are generally greatest for central European cities (mainly in the Danube and Rhine basins) due to both comparatively larger hazards and vulnerabilities. Pluvial and fluvial risks have no clear spatial pattern, as hazards, exposure and vulnerabilities are dominated by local context and geography. Similarly, risks to coastal floods are mostly driven by exposure, with low-lying cities in the Netherlands, France and Germany having the greatest risk.

The methods developed provide a number of important advances over previous high level assessments. This includes a focus here on urban risk analysis; consideration of over 50 climate model simulations from CMIP5 to explore the range of climate hazard uncertainties; application of high resolution process models using cloud computing; and development of a flexible, stable, scalable and transparent indicator-based vulnerability assessment and risk analysis method tested by combining 58 sources of information within 571 cities. The very nature of a high level approach makes it unsuitable for local risk analysis, or emergency planning. Further work in RAMSES WP3 is developing tools for detailed risk analysis.

Table of contents

List of Figures

List of Tables

List of Abbreviations

CC – Climate Change

CCA – Climate Change Adaptation

IBVA – Indicator-based Vulnerability Assessment

GCM – General Circulation Model

CMIP5 – Coupled Model Intercomparison Project Phase 5

RCP8.5 – Representative Concentration Pathway 8.5

1 Introduction

Most part of quantitative climate change risk assessments developed at the urban and sub-urban scales rely on the availability of accurate information on potential climate change hazards. This information is usually derived from General Circulation Models that are regionalised by means of dynamic or statistical downscaling techniques. On this basis, hazard information at the local level can be expressed as probabilistic distributions of climate events characterised in terms of return periods and intensities of occurrence. This information, together with value estimates of the exposed assets, allows the quantification of the expected losses linked to specific climate change threats. Potential losses are frequently communicated as 'damage' or 'vulnerability functions'.

However, the underlying data needed to produce probabilistic distributions of climatic events under climate change scenarios are not always available at the local level (Kunreuther et al., 2013). Furthermore, when hazard information is available accurate cost estimates linked to specific climate change threats are difficult to assess in the face of social and economic vulnerability factors. Although some works provide some solid estimates on the potential impacts of climate-driven events (see e.g. the work on floods by Kocornik-Mina et al., 2015), most of them rely on a limited number of dimensions that are directly linked to the physical characteristics of the events themselves, such as e.g. flood extension, depth and velocity in the case of floods, as well as to the structural characteristics of the building stock, like e.g. houses with lowest floor below ground level retrieved from remote sensing data or similar tools. Still, damage cost assessments derived from these calculations can also be quite context-specific, undermining comparability across spatial units.

In parallel, both the traditional climate change vulnerability assessments based on sensitivity and adaptive factors (Cutter et al., 2003; Turner, Kasperson, et al., 2003), as well as the resilience analyses that have proliferated over the last years basing on concepts like robustness, redundancy, resourcefulness and rapidity (Cutter et al., 2010), deliver estimates of urban vulnerabilities and resilience, respectively, based on multi-criteria assessments built upon a variable number of socio-economic dimensions. However, these assessments are rarely combined with climate information and/or integrated into broader risk analysis frameworks.

Still, in Europe continental scale risk analysis is increasingly possible as a result of increased availability of European and global dataset and computing power. However, the quality and detail of a vulnerability and risk analysis is contingent on the availability and quality of data to support the analysis. There are many datasets available across the EU (e.g. Urban Audit and the European Climate Assessment & Dataset programme) and globally (e.g. GRUMP: global land use data, WorldClim: climate observations and model outputs). Generally, these provide only a limited number of variables or are reported at low resolutions. Meanwhile, many countries and cities have bespoke data collection activities that provide opportunities for more detailed analysis.

To take advantage of the opportunities provided by 'the best available' data, whilst also providing a platform for 'comparable and transferable' risk analysis Work Package (WP) 3 of the RAMSES project is developing a suite, covering a range of levels of sophistication, of urban vulnerability and risk analysis tools – to provide different types of risk information to support a range of decisions, as shown in Table 1. This report describes the high level method for climate risk analysis of EU cities developed under WP3.1 of the RAMSES project.

Decreasing scales of analysis	Decisions to inform	Data and methods sources	Methods	Increasing resolution of monitoring and modelling
	Benchmarking Nationwide assessment of sustainability in cities Identification of national priorities Planning policy and national directives *Regional and urban planning* Spatial development strategies Strategic assessments *Detailed design* Neighbourhood planning Infrastructure design Building design and orientation	Satellite observations Energy generation Rainfall, temperature monitoring Traffic and local air quality monitoring Airborne lidar and photogrammetry Property location, land use and land cover Population and demographic information Travel, energy, consumption and waste surveys Smart sensors and building air quality, energy and water monitoring Terrestrial and mobile laser scan Individual and mobile phone sensors	Indicator and checklists GIS overlays Global and regional climate model outputs Accounting tools Quantified modelling of risks and sustainability Integrated assessment models Urban metabolism Land use and demand modelling Weather generators High resolution simulation and process models of selected urban functions Industrial ecology and life cycle analysis Engagement with individuals, community groups and other stakeholders	

Table 1 Hierarchy of methods, decisions they might be used to inform and the type of data and methods appropriate to the scale of analysis.

1.1 Aim and objectives

The aim of WP3.1 is to develop a climate risk evaluation methodology that can be applied to all EU cities to identify priorities for national and EU adaptation investments. This is done by combining hazard, exposure and vulnerability information in a coherent, flexible, stable, scalable, transparent and integrated risk analysis.

The objectives of WP3 are to:

- Identify stakeholder priorities for city-scale climate risk and vulnerability assessment.
- Develop a framework for city-scale climate risk analysis that uses only EU-wide (or global) data so can be applied to give a baseline assessment of all EU cities in the Urban Audit database;
- Develop a suite of EU-wide climate hazard modelling tools for flooding, heatwaves and droughts.
- Develop an EU-wide vulnerability assessment of each city in the Urban Audit database.

The results in the form of a spatial database of vulnerability, exposure, hazard and risk indices for each Urban Audit city, will be uploaded to the EU Climate Adapt (European Climate Adaptation Platform) and the EEA Climate Change Data Centre.

1.2 Risk analysis

Our analysis follows the conceptual framework proposed by the IPCC on the WGII AR5 (IPCC, 2014). As illustrated by Figure 1, the IPCC framework clearly identifies the three core components of climate change –driven *risk*, namely *hazard*, *exposure* and *vulnerability*: "risk results from the interaction of vulnerability, exposure, and hazard" (IPCC, 2014, glossary).

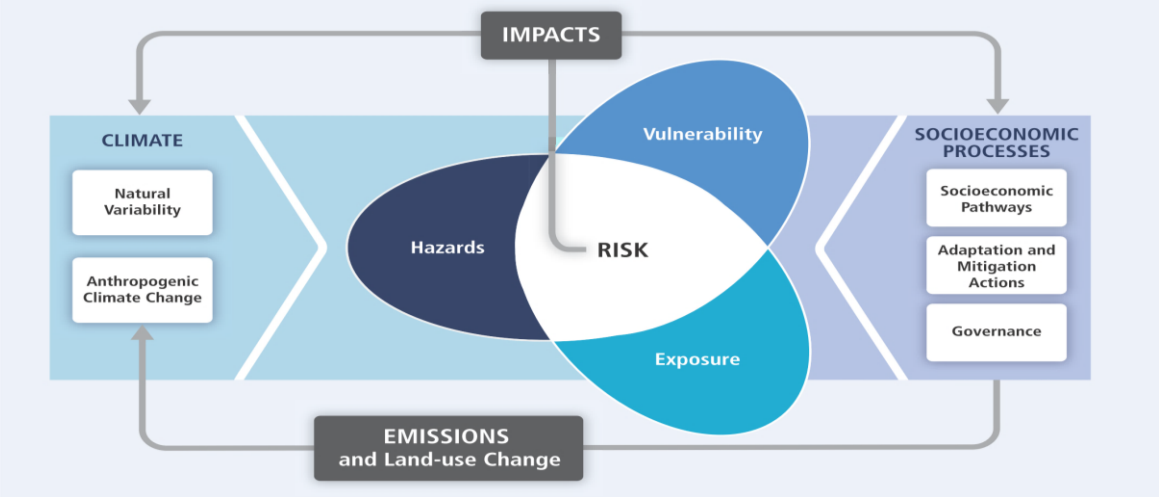

Figure 1: The conceptual framework proposed by the IPCC WGII-AR5 (2014).

Under this framework exposure remains a core component of risk, but it has been totally separated from the concept of vulnerability. This latter term is defined in the WGII AR5 as "the propensity or predisposition to be adversely affected". It is then mentioned that "vulnerability encompasses a variety of concepts and elements including sensitivity or susceptibility to harm and lack of capacity to cope and adapt" (IPCC, 2014, Glossary). In other words, the WGII AR5 recognises two core dimensions of vulnerability, namely *sensitivity* and *adaptive or coping capacity*[1].

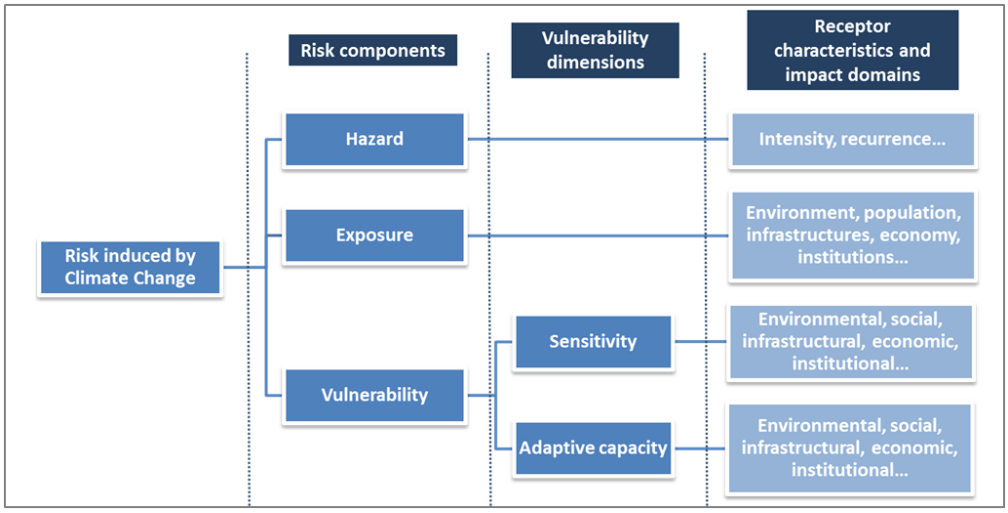

Figure 2: The operational framework developed within the high level' vulnerability and risk analysis for European cities.

[1] Sensitivity can be defined as "the degree to which a system is affected, either adversely or beneficially, by climate-related stimuli", and Adaptive capacity as "a system's ability to adjust to climate change (including climate variability and extremes), to moderate potential damage, to take advantage of opportunities or to cope with consequences" (IPCC, 2001).

Following this same rationale, *risk* will be characterised in this analysis as a function of three components *hazard*, *exposure*, and *vulnerability*, whereas vulnerability will be assessed as a function of two dimensions, *sensitivity* and response or *adaptive capacity*, as shown in the diagram included in Figure 1. The sensitivity and adaptive capacity dimensions are characterised in this work through a number of mutually exclusive socio-economic and physical attributes that shape the propensity or predisposition of citizens and cities to be adversely affected by climate change.

1.3 Overview of EU-wide analysis of urban risk linked to climate change

The high level vulnerability and risk analysis approach uses EU and global datasets to enable a universally-comparable climate change risk analysis of cities.

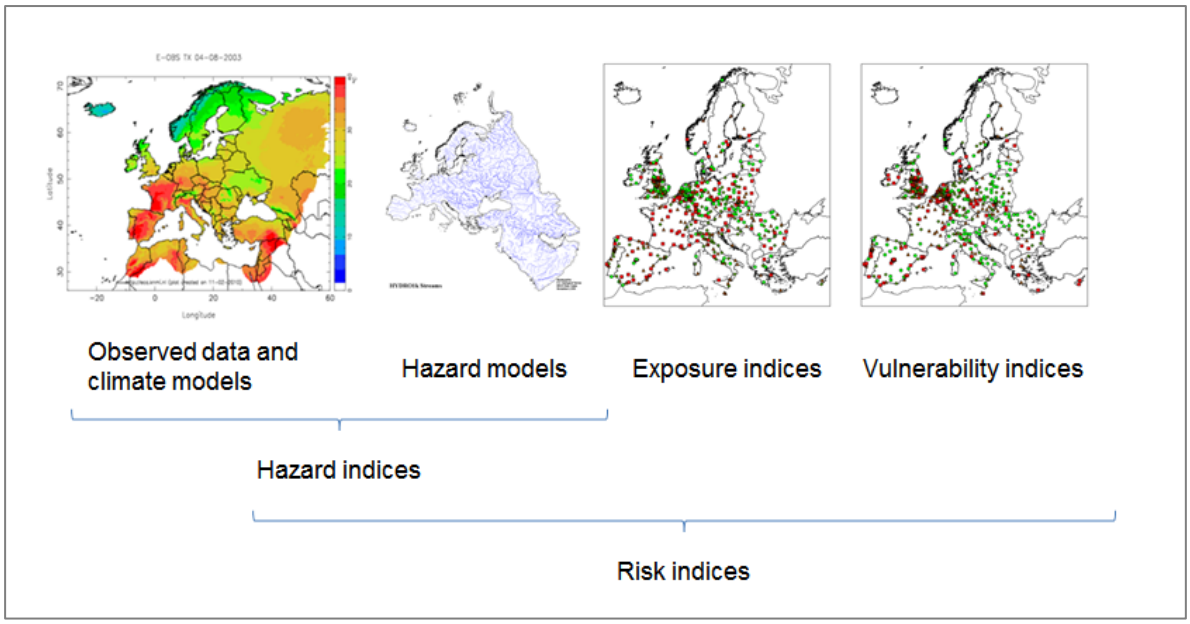

Figure 3: Overview of 'high level' vulnerability and risk analysis for European cities

An overview of the approach and some of the datasets that will be used are shown in Figure 3. Risk indices are calculated as a function of the climate change-driven hazards (Section 2), exposure (Section 3) and vulnerability (Section 4) of an urban area.

Our approach builds upon, and integrates, existing initiatives for hazard modelling of broad scale drought risk (Blenkinsop and Fowler, 2007), sea level rise (Nicholls and de la Vega-Leinert, 2008), fluvial flood risk (Barredo, 2007; Dankers and Feyen, 2009), heat risk (Fischer and Schär, 2010; Lissner et al., 2012), etc. Similarly, the vulnerability assessment builds upon previous EU research (Holsten and Kropp, 2012; Schauser et al., 2010; Stefan Greiving et al., 2011) whilst we also benefit from other RAMSES research, such as an assessment of climate change impacts in EU coastal cities (Boettle et al., 2016).

1.3.1 Scope

Cities shelter more than half of world's population. In the EU, over 75% of the population already lives within urban areas, and it is expected that this proportion will grow up to 82% by mid-century (UN-Habitat, 2011). Inevitably, a larger concentration of population, frequently achieved through rapid urbanization in previous decades, implies more risks derived from the potential impacts as climate change, as population, assets and economic activities concentrates on these areas (EEA, 2012; IPCC, 2014). Furthermore, urban areas are the direct or indirect cause of the largest share of the environmental impacts. In particular, cities are held responsible for over 75% of greenhouse gas emissions worldwide (UN-Habitat, 2011; World Bank, 2010).

Understanding these trends is thus crucial to avert potential damages linked to climate change and to minimise the impact of cities themselves on the global environment. But cities are not simple objects to analyse. Urban areas are shaped by the complex relations held among different sectors that integrate the coupled human-environment urban systems. These include the built environment, the infrastructures, the human, social and natural assets, the production systems, etc. (Liu et al., 2007; Turner, Matson, et al., 2003). Whereas these overlaps enable synergies between various elements, they also pose an enormous challenge in terms of adaptation planning (IPCC, 2014). From a climate risk management perspective (IPCC, 2012), the links and interactions among these components and between each of them and the hazardous climatic events that might trigger disasters shape the susceptibility of cities to harm and their capacity to resist and recover from such events (Cardona, 2005; Cutter et al., 2010).

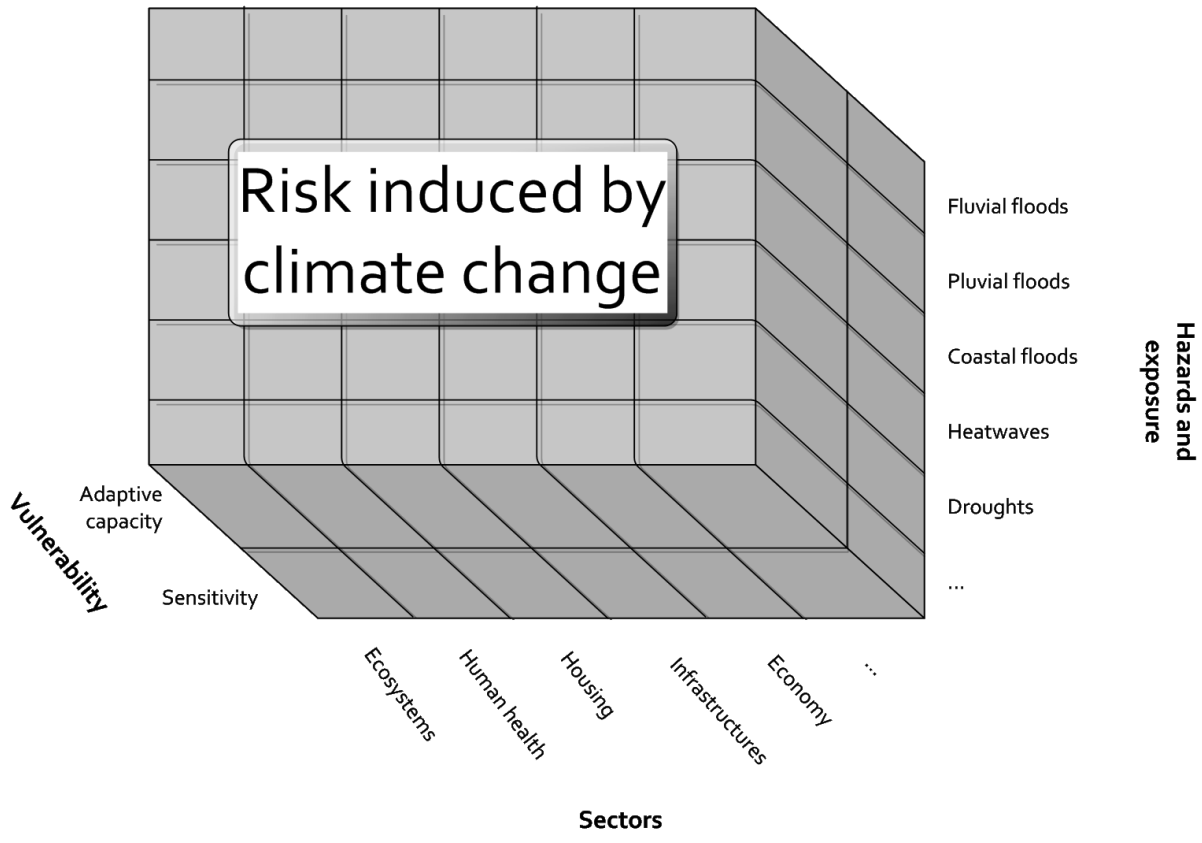

Figure 4: Managing complexity within a climate change risk analysis.

If these risk components are to be sufficiently characterised through indicators, it is crucial to understand how they interact within an urban context. In principle, this calls for the development of a

systematic inventory of all the potential threats, elements at risk and vulnerability factors. Still, there is an obvious trade-off between the number of dimensions considered and eventually combined within any indicator-based risk analysis and the interpretability and usability of its analytical outcomes. This stems from the following empirical considerations, that are expressed graphically in Figure 4:

- In areas affected by more than one threat the number of hazards to consider in the analysis could be large.
- There is a potentially limitless number of 'sectors', 'impact domains' or 'elements at risk' that could be assessed.
- The methodological alternatives to aggregate the indicators are also abundant.

Each one of the smaller cubes shown in Figure 4 represents a tri-dimensional space where the climate change threats, vulnerability d and elements at risk interface. Ideally, all these units could be individually characterised by means of indicators, as in a traditional multi-criteria assessment. In practice, though, characterising such small interaction spaces is very demanding in terms of data.

This calls for restricting the number of threats and sectors to analyse. In order to operationalise the process, we have first narrowed the assessment down to the most relevant climate change threats and the most relevant receptors of such threats within a European urban context. This has been done relying on a comprehensive literature review on previous risk and vulnerability assessments focusing totally or partially on the urban setting. The review included more than 170 peer-reviewed scientific papers and other relevant reports. Appendix B provides additional details on how literature review has been conducted.

Threat	Total number of papers reviewed
Multi-hazard	121
Heatwaves	19
Floods (fluvial and pluvial)	17
Coastal floods due to storm surges	9
Droughts	10

Table 2: Scoping of relevant indicators through a literature review.

Basing on this work, such urban sub-systems that are more likely to suffer damages under each impact chain – or that could be impacted on the first place and then 'transfer' impacts to other domains – were selected and associated to the relevant climate change-driven hazard. A restricted list of potential hazard-receptor combinations were thus formalised as a series of *impact chains* – or more simply *threats* – under analysis:

1. **Heatwaves (HW) on human health.**
2. **Flooding (pluvial [FLP], fluvial [FLF] and coastal [FLC]) on the socio-economic tissue and the urban fabric.**
3. **Drought (DR) on water planning.**

1.3.2 Data model

In coherence with the conceptual and operational frameworks described above, and taking into account the limitations imposed by data availability, a restricted number of hazard, exposure and vulnerability indicators have been selected as a basis for our EU-wide urban climate change risk analysis. This selection has been done in terms of the relevance and availability of the potential indicators, according to the scientific literature reviewed in this project, as described on Appendix B:

> ***Hazard indicators*** include indices that inform on the expected relative change of the potential climate change-driven threats in terms of the expected variation in the intensity and frequency of the potential events triggered by the underlying climatic conditions. Such events include floods (coastal, fluvial and pluvial), droughts and heatwaves. Most of the **hazard indicators** included in this assessment were explicitly produced for this study. These indicators have been mainly generated by means of modelling techniques basing on a new generation of general circulation models (GCMs) made available by the Coupled Model Intercomparison Project Phase 5 (CMIP5). A detailed description of these indicators and the methodology used to derive them can be found in Section 2.
>
> ***Exposure indicators*** characterise the degree to which cities' population and assets could be directly affected by climate change-driven threats. For some threats (e.g. floods), this implies providing estimates of the portion of the city that could be directly affected by such impacts under a number of climate scenarios. In other cases (e.g. heatwaves and droughts) it was assumed that the entire urban areas are equally exposed to climate change –driven threats. Section3 below provides a description on the exposure indicators used in this assessment.
>
> ***Vulnerability indicators*** include variables that illustrate the characteristics of the potential receptors of the climate change impacts in terms of their sensitivity to such impacts and their capacity to resist, cope or adapt to them. Vulnerability indicators have been thus classified into two separate groups influencing vulnerability in the opposite direction, labelled as 'sensitivity' – including those factors that increase vulnerability – and 'adaptive capacity' – comprising factors that reduce vulnerability –. Although some new adaptive capacity indicators have been produced relying on internet searches and other relevant sources, as accurately described in Section 4, most of the vulnerability indicators considered in this study have been obtained from the Urban Audit Database. Section 4 provides a detailed description of these indicators.

The assessment has been performed on the 571 cities included in the GISCO Urban Audit 2004 by April 2014.

2 Climate change Hazard Assessment

2.1 Overview

Following discussion with stakeholders regarding their priorities for high level risk information, and drawing from an extensive review of adaptation strategies in EU cities (Reckien et al., 2014) and work undertaken in RAMSES work package 9 (Terenzi and Wigström, 2014), and the EU Cities Adapt survey (Ricardo-AEA, 2013), flooding, heatwaves and drought were identified as the priorities for this assessment. Storms, fourth ranked on the priority list, have been identified as a priority for further work. Moreover, because climate models poorly represent storm processes, assessing future storm risks is highly uncertain.

The latest generation of general circulation models (GCMs) from the fifth phase of the Climate Model Intercomparison Project (CMIP5) were used to assess changes in heatwaves, floods and drought conditions for all cities in the European Urban Audit database. All available climate model runs were used in order to assess a wide range of possible futures, therefore providing the basis for risk analysis and thereafter identification of robust adaptation strategies.

While changes in heatwaves and droughts can be calculated directly from climate models' output, the assessment of flooding requires further modelling to convert changes in rainfall to changes in flooded area. Furthermore, the low spatial resolution of GCMs makes them unsuitable to model extreme rainfall and therefore their rainfall outputs cannot be used to assess changes in pluvial flooding directly. This report presents the results of the hazard assessment in terms of droughts and heatwaves but only a provisional methodology in terms of changes in pluvial and fluvial floods as this work is still ongoing.

2.2 Climate model outputs

A new generation of general circulation models (GCMs) are available from the fifth phase of the Coupled Model Intercomparison Project Phase 5 (CMIP5). Daily rainfall, maximum and minimum temperature outputs from CMIP5 models for RCP8.5 were downloaded from the British Atmospheric Data Centre (BADC). Sanderson *et al.* (2011) showed that RCP8.5 is similar to SRES A1FI and, although these are the highest emission scenarios considered by IPCC, they still assume emissions well below what the current energy mix would produce in the future.

Outputs from 39 GCMs were available to download, many of which had several runs with different initial conditions. These models have different projections, spatial resolutions and calendars (standard, no leap, or 360 days) and the period of data available also depended on the GCM. In the end, for the period 1951-2100, 54 model runs were available with both daily maximum and minimum temperature and 55 were available for daily rainfall.

However, questions remain on how to use the outputs of multi-model ensembles in impact studies. Averaging across models is widely used but is hard to interpret and defend (Knutti *et al.*, 2010a) and it may produce physically implausible results (Knutti, 2010). Furthermore, since a general all-purpose metric to evaluate climate models has not been found, and different metrics produce different rankings of models, excluding or weighting models might lead to overconfidence in the projections and unjustified convergence (Knutti *et al.*, 2010a). Building a probability density function (PDF) of change

implies the assumption that the models are independent, distributed around a "perfect model" and sample the range of uncertainty (Knutti, 2008). However, CMIP models are not independent, therefore model agreement might not be an indication of likelihood but a consequence of shared process representation and/or calibration on particular datasets (Knutti *et al.*, 2010a). Also the sampling of models is not random or systematic (Knutti, 2010).

On the other hand, choosing a few models that are representative of the range of climate model outputs from CMIP5 allows for an assessment of the uncertainties associated with the projections and permits different adaptation strategies to be studied for different possible futures leading to robust adaptation. Nonetheless, one has to consider that the extreme ends of the plausible range might not be sampled and that the chosen outcomes might be perceived as equally probable (Knutti *et al.*, 2010b).

For this study, indicators of droughts, floods and heatwaves were calculated for all the climate models outputs, for all European Urban Audit cities. However, for tractability results are only reported for three impact scenarios per city: "High, "Medium" and "Low" which correspond to the percentiles 90, 50 and 10 of the distribution of the indicator, calculated from the climate model runs, for each city. As explained above, these should not be interpreted as probabilities, and the three scenarios should only be seen as indicative of the range of outputs from CMIP5.

2.3 Data for broad scale climate hazard assessment

The data used for assessing climate hazards across European cities is:

- EU-DEM – a Digital Elevation Model over Europe "produced using Copernicus data and information funded by the European Union" available from http://www.eea.europa.eu/data-and-maps/data/eu-dem. The EU-DEM is a hybrid product based on Shuttle Radar Topography Mission (SRTM) and ASTER GDEM data with 25m resolution (projection 3035: EU-DEM-3035).
- Hydro1K Europe – geographic database produced by the US Geological Survey at a resolution of 1km (USGS, 2011). It includes a hydrologically corrected digital elevation map and several topographical derived datasets of which both the flow direction raster and flow accumulation raster were used for the assessment of fluvial flooding.
- Global Runoff Data Centre (GRDC) – international archive with observed discharge of gauges throughout the world available at http://www.bafg.de/GRDC/EN/Home/homepage_node.html used for the assessment of fluvial flooding.
- Urban Morphological zones 2000 (http://www.eea.europa.eu/data-and-maps/data/urban-morphological-zones-2000-2) defined as "set of urban areas laying less than 200m apart". This European Environment Agency (EEA) dataset was build based on the urban land cover classes of the CORINE LAND COVER dataset. This dataset was used to define "city area" in the calculations of percentage of city flooded for the pluvial flooding analysis.
- Urban Audit dataset "GISCO Urban Audit 2004" was used for delimitation of cities. 571 cities (city region level) were studied (see Figure 5).

Figure 5: Map of Europe with selected cities from Urban Audit that will be studied.

- Daily rainfall, maximum and minimum temperature from CMIP5, RCP8.5:
  - 39 GCMs with different projections, spatial resolutions and calendars (standard, no leap, or 360 days);
  - 131 model runs available to download (March 2014) from the BADC;
  - Time-periods available depend on the model run;
  - format of data: netCDF.

- e-obs, an European daily gridded data set for precipitation and maximum, and mean surface temperature from http://www.ecad.eu/download/ensembles/download.php:
  - 0.25 degree resolution
  - period 1950–2013;
  - based on observations;
  - format of data: netCDF

The maps of the gauge networks used to produce the e-obs dataset (see Figure 6) show uneven coverage throughout Europe, with the UK, Ireland, the Netherlands and Switzerland having a much higher gauge density. 2316 stations were available, although the number changes over time showing a sharp rise in the number of gauges from 1950 to 1960 and a dip in 1976 (for stations with less than 20% missing monthly data). The dataset was designed to provide best estimates of grid-cells averages (not point values) which was achieved by interpolating to a finer grid and then averaging to create a coarser grid (the one available).

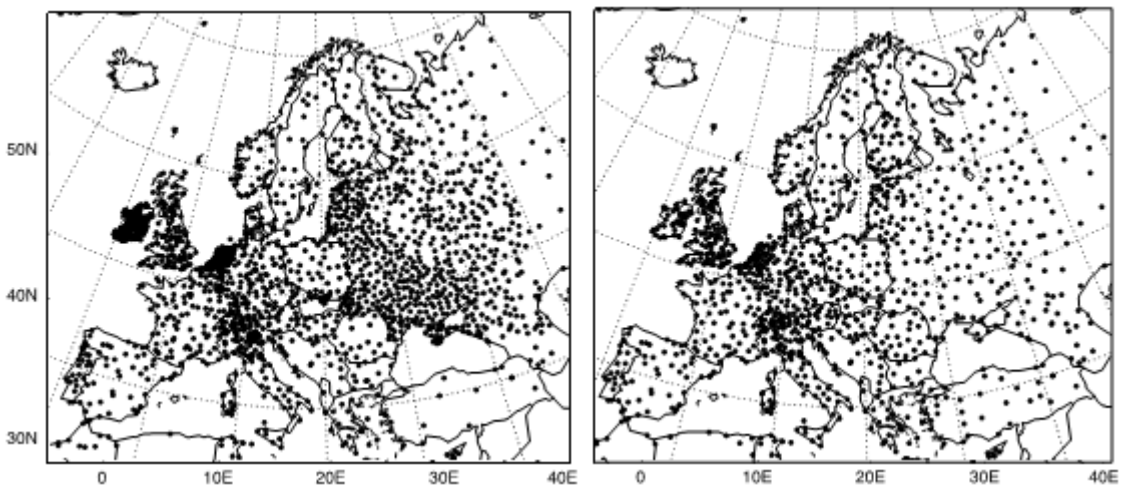

Figure 6: Map of Europe with the station network for precipitation (left) and mean temperature (right) used to produce the gridded dataset e-obs (adapted from M. R. Haylock et al. (2008)).

Using the e-obs dataset, European maps of annual and monthly rainfall were calculated, as well as mean monthly and mean maximum temperatures (Figure 7 - Figure 10).

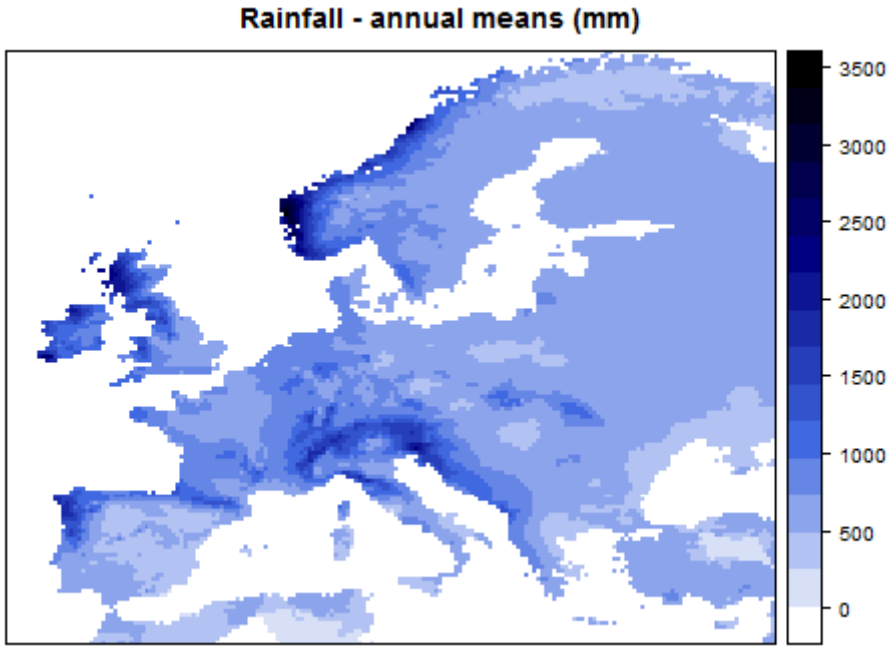

Figure 7: European map of mean annual rainfall (mm) calculated based on e-obs dataset.

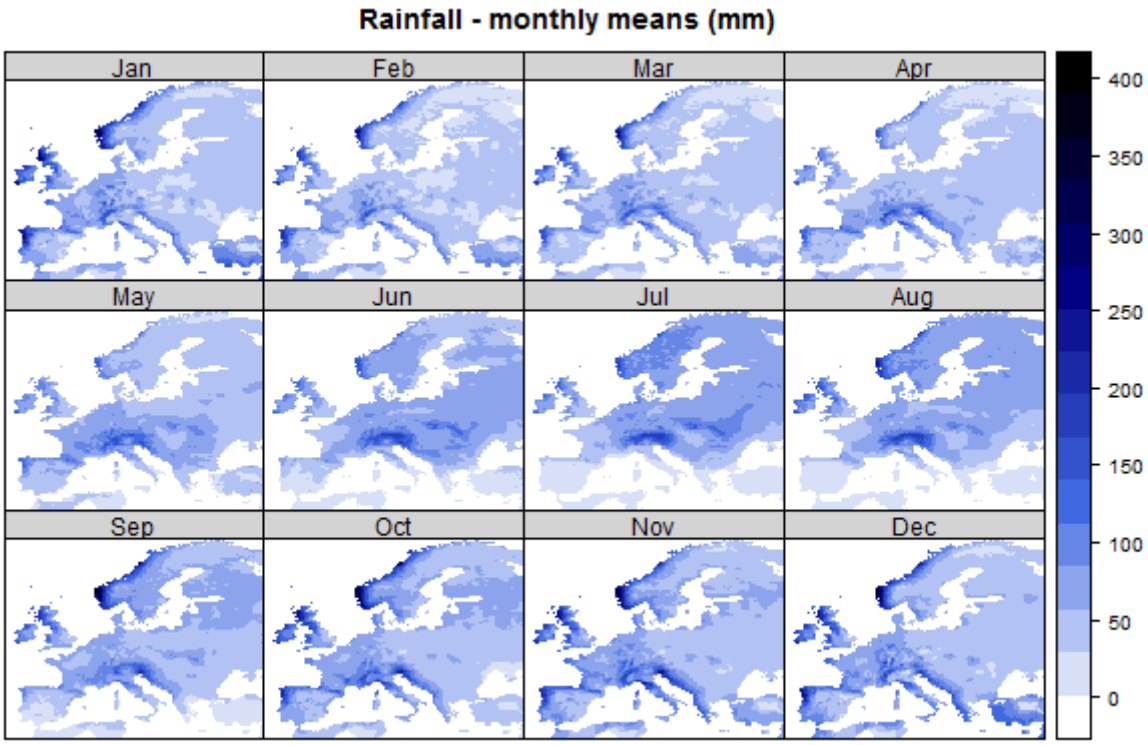

Figure 8: European maps of monthly mean rainfall (mm) calculated based on e-obs dataset.

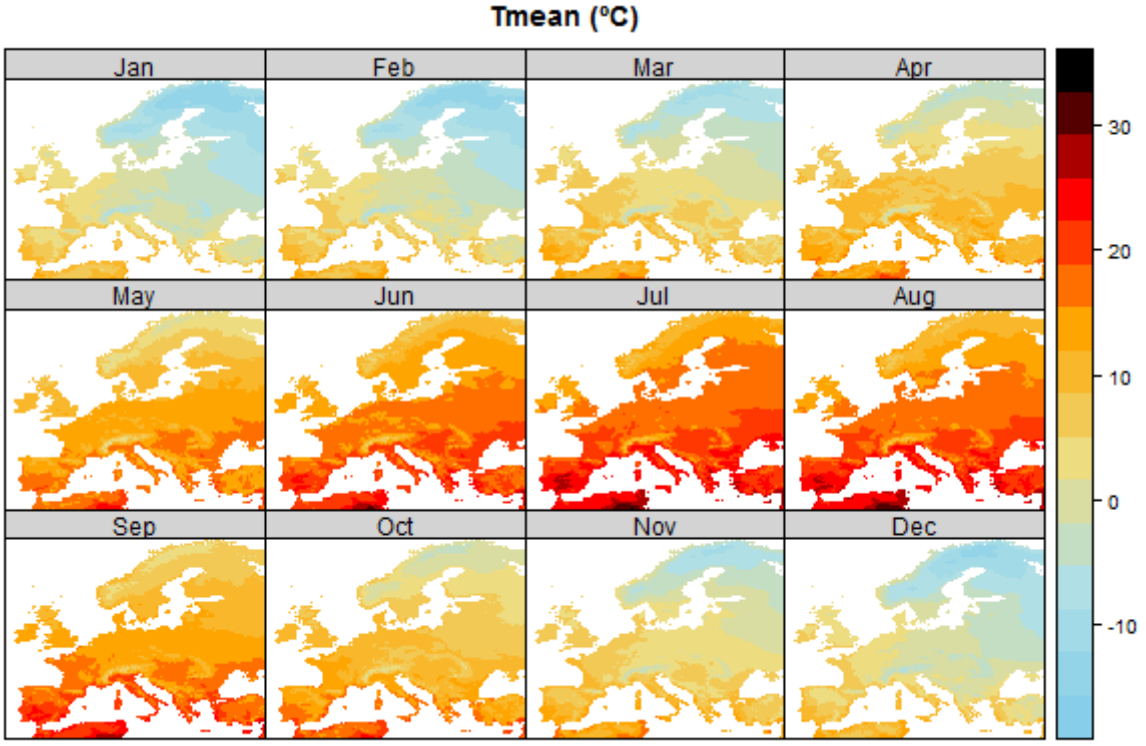

Figure 9: European maps of mean monthly mean temperature (°C) calculated based on e-obs dataset.

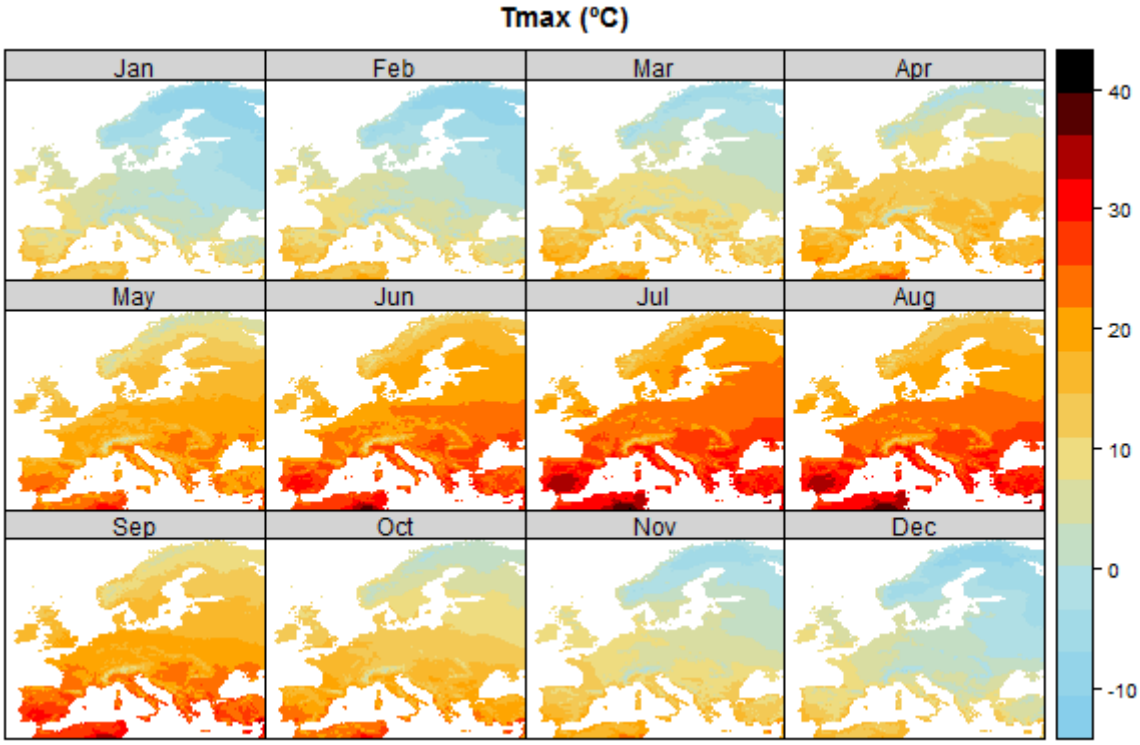

Figure 10: European maps of mean monthly maximum temperature (°C) calculated based on e-obs dataset.

- For the pluvial flooding analysis, several observed sub-daily rainfall datasets were combined:
  - 38 European gauges with time-series of annual maximum hourly rainfall, provided by Dr Panos Panago, from the Joint Research Centre, that were collected under the auspices of the REDES project (Panagos et al., 2015).
  - 192 UK gauges with time-series of annual maximum hourly rainfall, provided by Dr Stephen Blenkinsop from Newcastle University, that were collected under the auspices of the CONVEX project (Blenkinsop et al., submitted). These data was collected from three sources: the UK Met Office Integrated Data Archive System (MIDAS), the Scottish Environmental Protection Agency (SEPA) and the UK Environment Agency (EA). Not all of these gauges were used, since that would mean the density of gauges used in the UK would be well above the density of gauges in the rest of Europe, which would affect the results of the analyses.
  - One gauge (Catraia) with hourly time-series for the South of Portugal downloaded from the Portuguese National Water Resources Information System (http://snirh.pt/).
  - IDF curves were collated for:
    - Athens, Grece (Koutsoyiannis and Baloutsos, 2000);
    - Malaga, Spain (Ayuso-Muñoz *et al.*, 2015);
    - Ebre, Spain (Pérez-Zanón *et al.*, 2015)
    - Trondeheim, Norway (Hailegeorgis et al., 2013)

2.4 Heatwaves

2.4.1 Introduction

The late 20th and early 21st centuries in Europe have been the warmest of the last 500 years, with 2003 being by far the hottest summer (Luterbacher *et al.*, 2004). The last decade has seen record-breaking heatwaves throughout the world and summer temperature records have increase by more than a factor of 10 in parts of Europe, due to prolonged heatwaves (Coumou *et al.*, 2013).

A heatwave is a period of consecutive days with hot temperatures where both length and peak temperature are important. Heatwaves arise from the combination of large scale processes (like dry blocking conditions) and small scale process (for example, dry soils tend to favour anticyclonic conditions) whose interactions are not fully understood (Vautard *et al.*, 2013).

To assess the performance of RCMs from the EURO-CORDEX ensemble for simulating heatwaves in Europe, Vautard *et al.* (2013) used data from 8 simulations at 12km and 13 simulations at 50km for the period 1989–2008. They found that despite the large spread of results of RCMs (all using a historical reanalyses dataset – ERA-Interim – as boundary conditions), in general these models are simulating heatwaves that are too hot and too persistence, even after removing their temperature biases. Furthermore, interannual variability is generally also overestimated. Moreover, the higher resolution models only showed improvements in coastal areas, in other areas improvements were not observed, not even in mountainous areas.

Nevertheless, using the EURO-CORDEX model ensemble, Jacob *et al.* (2013) project that the mean number of heatwaves (defined as 3 consecutive days exceeding the 99th percentile of the daily maximum temperature for May to September for the period 1971–2000) will increase in all Europe for 2071-2100 (under RCP8.5). They found that the bigger increase will be in Southern Europe which will see more than 45 extra heatwaves. These increases are mostly robust and significant throughout the model ensemble but the change in the number of heatwaves depends considerably on the definition of heatwave. Using a different definition (more than 5 consecutive days with daily maximum temperature exceeding the mean maximum temperature for May–September of the control period by at least 5°C) the increase in the number of heatwaves in only seen in parts of the Southern Europe, and the changes are restricted to a maximum of 9 extra heatwaves.

Fischer and Schär (2010), looked at future projections of heatwaves in Europe using six RCMs driven by 3 GCMs from the ENSEMBLES project[2]. They conclude that Iberia and the Mediterranean region will see the biggest changes in number of heatwave days (from around 2 days per summer in 1961-1990 to 27 to 67 in 2071-2100). However, in terms of heatwave amplitude, the biggest increase are over south-central Europe (zonal belt along the northern Mediterranean coasts centred at about 45° N). For this region, warming in the extreme temperatures (99th percentile) is much higher than the warming in the mean summer temperatures (more than 50%). In contrast, in southern Europe the warming of the mean and extreme temperatures is similar. This is explained by a higher increase in temperature variability in south-central Europe due to circulation changes and due to a reduction in soil moisture. In this region, the changes in the 99th percentile, reach up to 7K. The authors also point out that this results are qualitatively consistent with the Prudence and Ensembles climate models.

[2] http://www.cru.uea.ac.uk/projects/ensembles/ScenariosPortal/Data3RCM.htm

2.4.2 Methodology

There is no standard definition of heatwave and the World Meteorological Organization (WMO) has not defined the term (WHO, 2004). Therefore different definitions of heatwaves are used, for example:

- The definition of heatwave for the EuroHEAT project for the summer period (June-August) is: days in which maximum apparent temperature (*Tappmax*) exceeds a threshold (90^{th} percentile of *Tappmax* for each month) for at least 2 days and continues as long as Tappmax is higher than its median value and minimum temperature (*Tmin*) exceeds its threshold (90^{th} percentile of *Tmin* for each month) (Michelozzi et al., 2007).
- Vautard et al. (2013), looking at heatwaves in the EURO-CORDEX RCMs, defined them as a period of at least six days with temperatures above the 90^{th} percentile of the simulated daily mean temperature for summer (JJA).
- Fischer *et al.* (2008) studied changes in European heatwaves using the ENSEMBLES dataset and defined heatwave as six consecutive days with maximum temperatures exceeding the local 90^{th} percentile of the control period (1961–1990) in summer (JJA).

A relative threshold (a percentile) has advantages over absolute thresholds since it accounts for the local climates while allowing the same definition of heatwave throughout Europe. Also, by using a relative threshold, heatwaves can be calculated directly with temperature from the climate models (without bias-correction) since the historical period simulation of the climate model is used for the definition of the threshold.

In this deliverable, the definition of heatwave is three consecutive days where both the maximum and the minimum temperature are above their respective historical 95 percentiles. The season of interest for the analysis of heatwaves was considered to be May to September. Despite this common definition of heatwave throughout the project, different definitions of historical and future periods are present due to different computational needs associated with different methodologies. For task 3.1, the historical period is defined as 1951-2000 and the future period is defined as 2051-2100.

The definition of which percentile to use was done based on the number of heatwaves for the historical period (1951-2000) projected by climate models for the low, medium and high impact scenarios for each city (see Figure 11 and Figure 12). Three thresholds were considered: 90^{th}, 95^{th} and 98^{th} percentiles. Using the 98^{th} threshold, three cities have no heatwaves in the historical period for the low impact scenario and therefore this definition of heatwave was considered too stringent. Like-wise, the 90^{th} was considered too yielding with all the European cities having more than one heatwave a year in the historical period for the highest impact scenario.

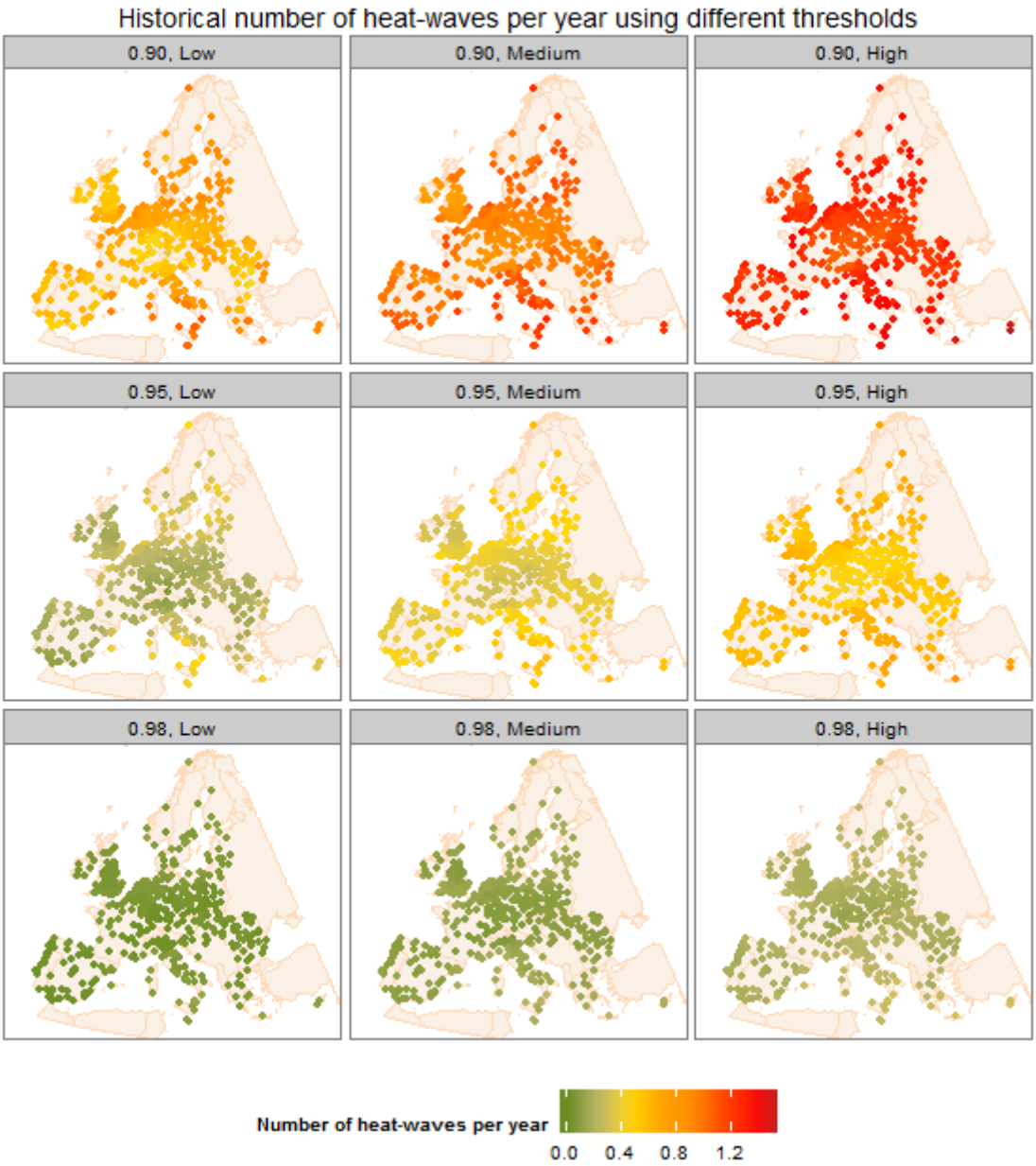

Figure 11: Maps of Europe with the number of historical (1951-2000) heatwaves per year calculated using a 90th, a 95th and a 98th percentile threshold (all with 3 days duration) shown for a low (10th percentile) impact scenario (left), a medium (50th percentile) impact scenario (middle) and a high (90th percentile) impact scenario (right) for each European city.

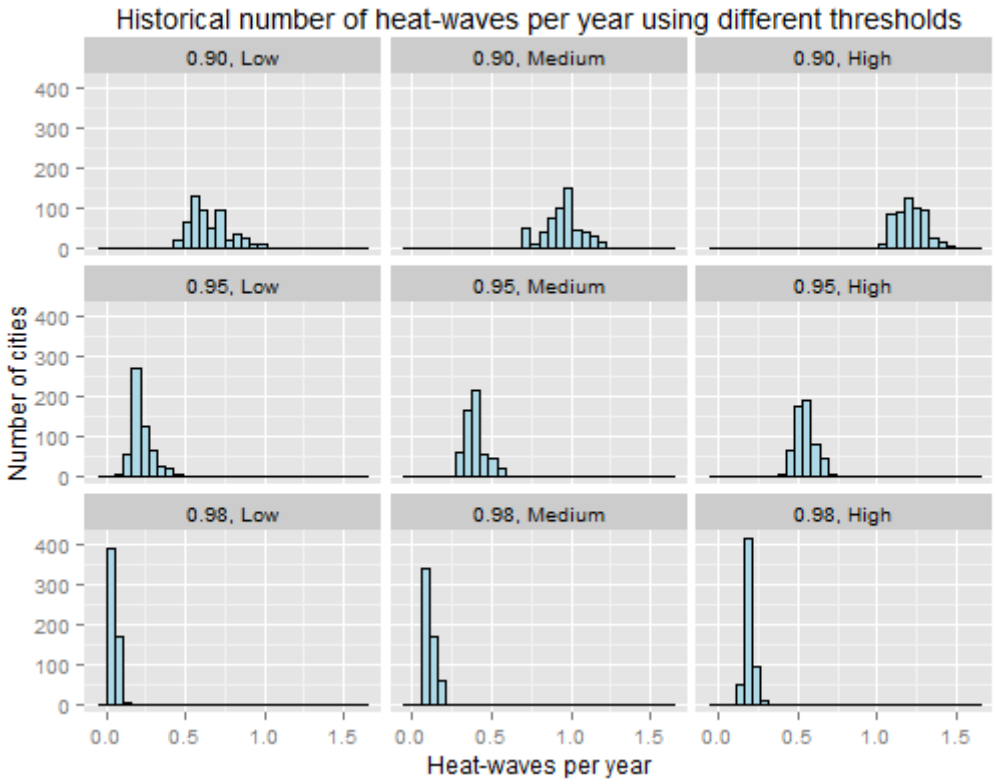

Figure 12: Histograms of historical (1951-2000) number of heatwaves per year calculated using a 90th, a 95th and a 98th percentile threshold (all with 3 days duration) shown for a low (10th percentile) impact scenario (left), a medium (50th percentile) impact scenario (middle) and a high (90th percentile) impact scenario (right) for each European city.

Climate model outputs were used directly to assess the change in number of heatwave days and changes in maximum temperature of heatwaves, between the historical (1951-2000) and the future (2051-2100) periods. Each European city was assigned the outputs of the climate model grid cell where it is located.

Two indicators were calculated, for each GCM and each city:

- change in the percentage of heatwave days (i.e. difference between future and historical percentage of heatwave days);
- and changes in maximum temperature of heatwaves (i.e. difference between the maximum temperature felt during a heatwave in the future period and in the historical period).

2.4.3 Results

There is a projected increase in the number of heatwave summer (May to September) days for all European cities under the three impact scenarios considered (Figure 13). These differences range from an extra 4% of summer days considered heatwave days in the low scenario in Norway to an extra 63% of summer days considered heatwave days in the high scenario in Malta. In general, the increases are higher in southern Europe, although some coastal northern European cities also see big increases (around 50% in the high impact scenario).

The maximum temperatures felt during heatwaves are also projected to increase for all European cities under all scenarios (Figure 13). This range from around 2°C in cities in Scandinavia and Scotland under the low impact scenario to an increase of 14°C in central Europe under the high scenario. The higher temperature increase are projected for the European mid latitudes (i.e. central Europe, parts of France and Northern Portugal and Spain).

This dichotomy of higher increases in frequency of heatwave days in Southern Europe but higher increases in maximum temperatures in European mid latitudes has been found in previous studies (Fischer and Schär, 2010) associated with higher increases in temperature variability in European mid latitudes. However, the increases in maximum heatwave temperature projected in the high impact scenario (reaching up to 14°C) have not, to the best of our knowledge, been analysed or reported before. These differences in results are possibly explained by the use of 54 GCM runs to assess possible changes in heatwaves, therefore investigating a much wider range of possible futures than previous studies.

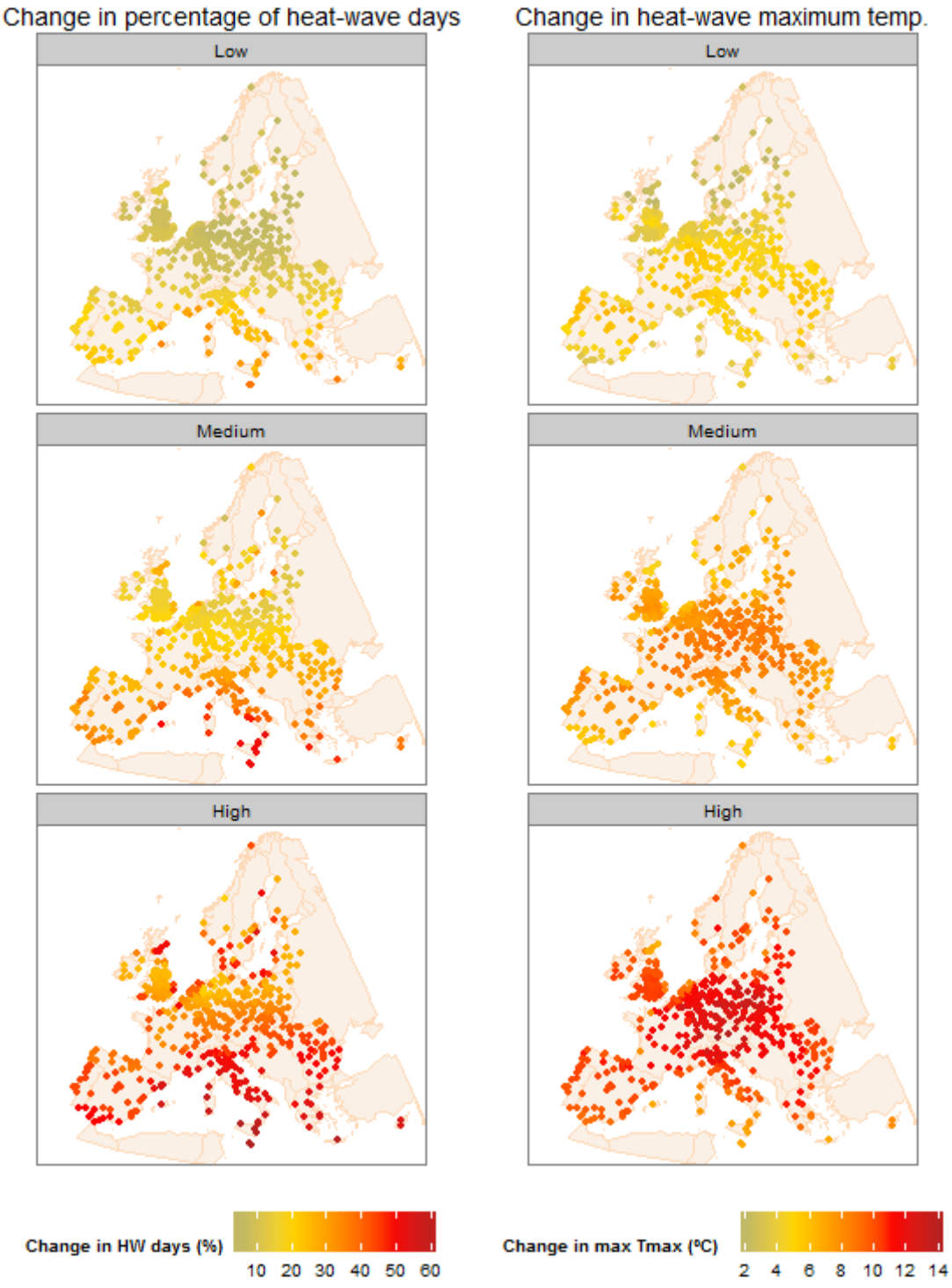

Figure 13: Change (difference) in the percentage of days classified as heatwaves days (left) and change in the maximum daily maximum temperature for days classified as heatwaves days (right). Both shown for a low (10^{th} percentile) impact scenario (top), a medium (50^{th} percentile) impact scenario (middle) and a high (90^{th} percentile) impact scenario (bottom) for each European city. The changes are calculated between the historical period (1951-2000) and the future period (2051-2100).

2.5 Drought

2.5.1 Introduction

There is no universally accepted definition of drought. It can be defined in terms of meteorological, hydrological, agricultural or socio-economic conditions and consequently a large number of different drought indices exist (Lloyd-Hughes and Saunders, 2002). The common ground between all definitions is the cause of drought – a deficit in precipitation. The problems arise in the determination of the time period over which this deficit accumulates and the relations between the deficit in rainfall with deficits in usable water sources and impacts therein (McKee *et al.*, 1993).

Drought is not a distinctive event; it might only be recognised several months after it starts, it might be interrupted by wet spells and depending on what type of drought is being considered it can terminate at different times (Phillips and McGregor, 1998). Bordi *et al.* (2009) define meteorological drought as abnormally low precipitation over a few months and hydrological drought as deficiencies in surface and sub-surface water supplies caused by a reduction in precipitation over the period of one year or more.

Assessment of changes in drought depends on the type of drought being studied (meteorological, agricultural, hydrological, socio-economic, etc.) and on the drought index chosen. Also, drought projections are still more uncertain than other aspects of the water cycle. Nevertheless, drying in the Mediterranean region, under RCP8.5 is likely, associated with changes in the Hadley Circulation, and reductions in runoff are also likely in Southern Europe, while increases in runoff are likely in high northern latitudes (IPCC, 2013). In central Europe and in the Mediterranean region, droughts are projected to become longer and more frequent (Jiménez Cisneros, 2014).

Forzieri *et al.* (2014) using 12 members of ENSEMBLES and a hydrological model (LISFLOOD), concluded that the discharge decreases in the South of Europe and the increases in the North of Europe are highly significant, but in between (the transition zone) the projections are more discordant.

2.5.2 Methodology

To characterize drought behaviour, the Drought Severity Index (DSI) was used. It was originally proposed by Bryant et al. (1992) and defined by Phillips and McGregor (1998), it is based on cumulative monthly precipitation anomalies and can be calculated for different time-scales. The time scale of 12 months (DSI-12) was chosen to reflect possible deficiencies in surface and sub-surface water supplies as defined by Bordi *et al.* (2009).

DSI-12 was calculated using the following procedure:

- If the rainfall anomaly in month *t* is negative (i.e. rainfall is below the mean for that month) and rainfall in the twelve previous months is lower than its twelve-monthly mean, a drought sequence is initiated in month *t*;
- DSI-12 for month *t* is then a positive value equal to the precipitation anomaly in month t.
- The DSI for the following month (*t*+1) is the rainfall anomaly of month *t* plus the rainfall anomaly of month *t*+1, but only if the twelve-monthly mean total for the months *t*-11, to *t*+1 has not been exceeded. When this mean is exceeded the drought sequence terminates and DSI-12 is assigned a value of zero.

To standardise the index, the absolute deficit (in mm) is divided by the mean annual rainfall and multiplied by 100. Therefore the final index value expresses the accumulated precipitation deficit as a percentage of the mean annual rainfall.

DSI-12 time-series were calculated for all cities and for all GCMs that had data from 1950 to 2100 (each city was assigned the outputs of the climate model grid cell where it is located). Subsequently, these DSI-12 time-series were subsetted for the historical period (1951-2000) and future period (2051-2100) and the maximum DSI-12 (for each GCM and each city) was calculated for both periods. Figure 14 and Figure 15 show the PDFs of these maximum DSI-12 values for the Newcastle-Upon-Tyne grid-cell and for Lisbon grid-cell (respectively), as examples of two cities with very different future drought behaviour.

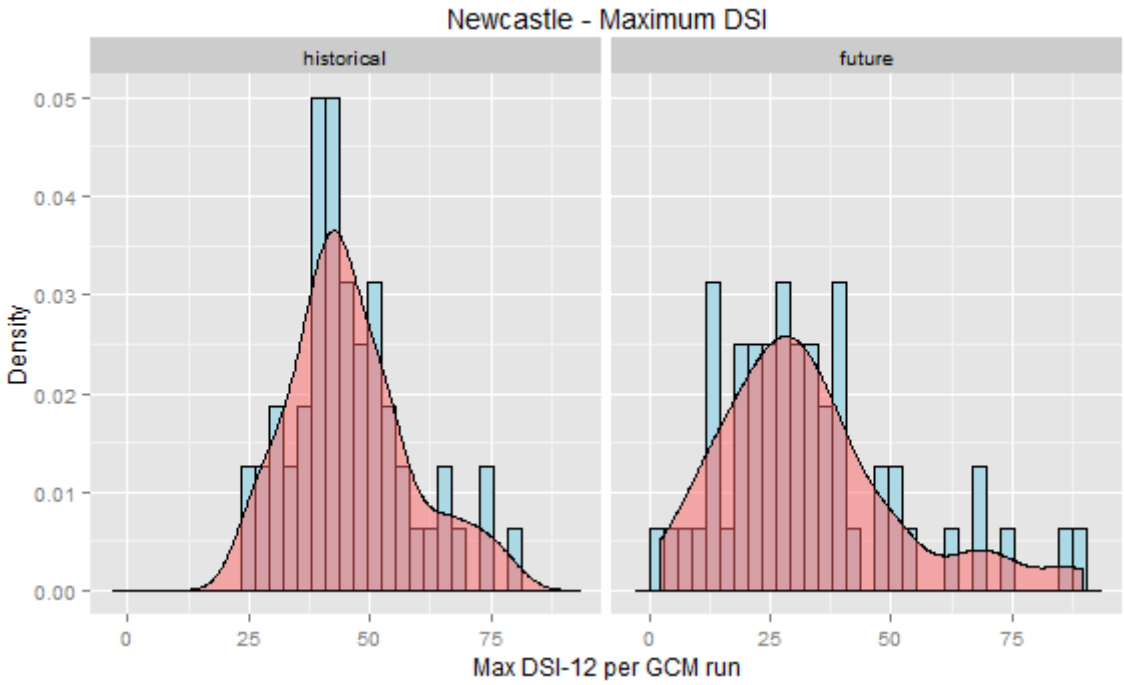

Figure 14: Histograms and PDFs of the maximum DSI-12 for each GCM for Newcastle-Upon-Tyne grid cell for both the historical (1951-2000) and future (2051-2100) periods.

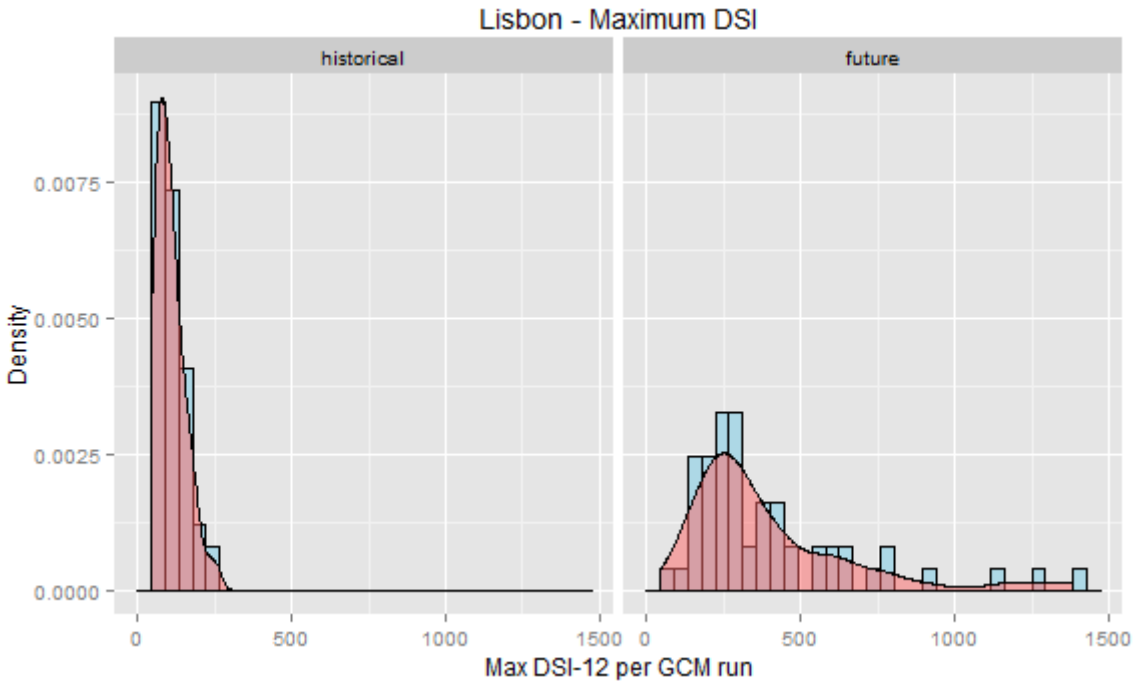

Figure 15: Histograms and PDFs of the maximum DSI-12 for each GCM for Lisbon grid cell for both the historical (1951-2000) and future (2051-2100) periods.

Two indicators were calculated, for each GCM and each city, based on these maximum DSI-12 values:

- the probability for any given month in the future to be above the maximum historical DSI-12; and,
- the change factor of maximum drought, i.e., future maximum DSI-12 divided by historical maximum DSI-12.

2.5.3 Results

The probability of having unprecedented droughts (shown by the probability for any given month in the future being above the historical maximum DSI-12 in Figure 16, left) in high and mid European latitudes is non-existent for the low impact scenario. For the medium impact scenario, this is only seen in Northern Europe, and for the high impact scenario, almost all Europe can experience unprecedented droughts. This northern expansion of possible worsening of drought conditions is not found in the literature, but our results are explained by the use of 55 GCM runs to assess possible changes in drought conditions, therefore investigating a much wider range of possible futures than previous studies.

Nevertheless, and in agreement with the publish literature (Forzieri et al., 2014; IPCC, 2013), the worse changes in drought conditions are projected for cities in Southern Europe, for all scenarios. For the higher impact scenario, some cities in Southern Europe in any given month have greater than 70% probability of being in an unprecedented drought and droughts can be up to 14 times worse than the worse historical drought. Even in the low impact scenario, the South of Iberia can see droughts that are up to 2.5 times worse than the worse historical drought (see Figure 16).

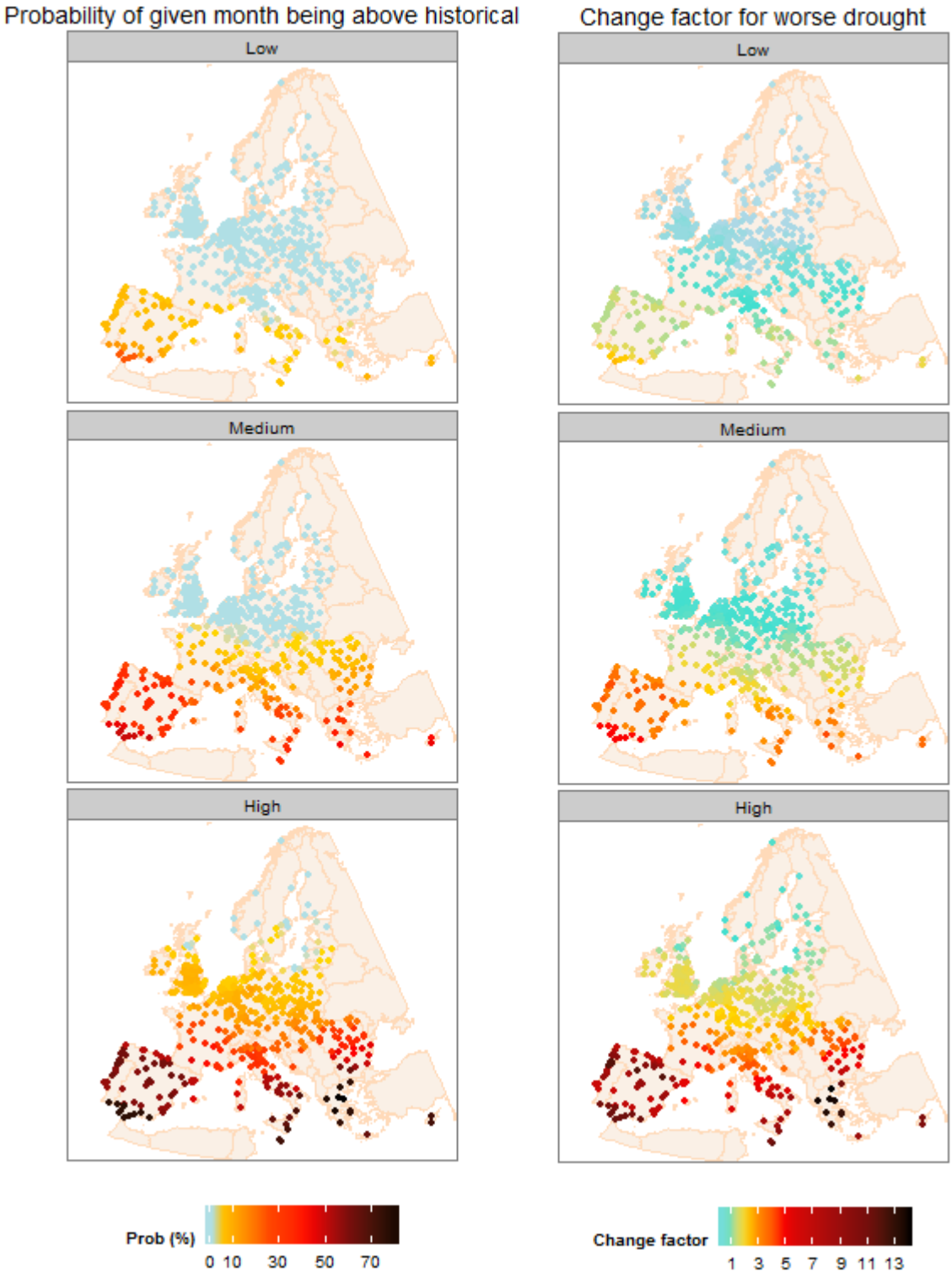

Figure 16: Probability for any given month in the future being above the historical maximum DSI-12 (left) and maximum DSI-12 change factor – future maximum DSI-12 divided by historical maximum DSI-12 (right). Both shown for a low (10th percentile) impact scenario (top), a medium (50th percentile) impact scenario (middle) and a high (90th percentile) impact scenario (bottom) for each European city. The historical period is 1951-2000 and the future period is 2051-2100.

2.6 Pluvial flood hazard

2.6.1 Introduction

Pluvial flooding is caused by intense rainfall above the capacity of the urban drainage system and is normally studied using flood models that can provide depth and velocity of surface water associated with rainfall events of specified severity (Glenis et al., 2013).

There are significant challenges associated with the assessment of future changes in pluvial flooding in all European cities. The first is the restricted availability of observed hourly rainfall records which, coupled with the spatial variability of intense rainfall regimes, hinders the definition of historical intense rainfall standards for each city. The second is the inability of climate models, run at standard resolution, to simulate intense hourly rainfall for present climates, which in turn means that credible future projections of changes in extreme rainfall are also not possible. Lastly, it is necessary to run a detailed, high resolution hydrodynamic model for each city in order to quantify which areas will flood for different rainfall events.

From all those challenges, the inability to simulate extreme rainfall by climate models is the one making it impossible to apply a similar methodology to the other impacts in this report. Both GCMs and RCMs simulate precipitation that is too frequent, and hourly events that are not intense enough, which can be ascribed to the inadequate representation of clouds, moist convection, and topography (Ban et al., 2014). The spatial resolution of conventional climate models is too coarse to allow for convective processes to be resolved, instead it has to be parametrized as a sub-grid process leading to an inability to represent extreme hourly precipitation (Ban et al., 2015). However, simulations with very high-resolution convection permitting models have been run recently, where convective processes are based on their governing dynamical equations without the need for parametrization. These "convection-permitting" models, more commonly used for nuerical weather prediction, resolve large storms and mesoscale convection but are still not able to represent convective plumes and small showers (Kendon et al., 2014). Due to their high demand on computational resources (Prein et al., 2015), these models are only run for short periods and for small areas. To run global models at convection permitting resolutions is so computationally expensive that, at the moment, those simulations are only run for a maximum of a month and it might take one or two decades to do long-term simulations with these models (Prein et al., 2015). Therefore these simulations are normally run as limited area simulations with boundary conditions provided by a GCM, or by reanalysis data (Prein et al., 2015).

Comparing a 12km convection-parametrizing model with a 2.2 km convection-permiting model for the Alpine region, Ban et al. (2014) found large differences in the simulation of hourly rainfall. While both models simulated reasonably well the frequency-intensity distribution of daily precipitation, for hourly precipitation the coarser model underestimated the frequency of extreme events. However, the 2.2km model simulated frequency-intensity distribution similar to the observed. Looking at future projections (2081-2090, using 1991–2000 as the control period) under RCP8.5 (Ban et al., 2015), intense hourly rainfall is projected to become more intense (3 to 6% increase in the 99.9th percentile) and more frequent (with an increase around 40% for intensities above 20mm/h).

Kendon et al. (2014) ran 1.5km and 12km climate models for southern UK for 1996-2009 and for 13 years in the 2100s for RCP8.5. The coarser model significantly underestimates heavy summer rainfall, while the 1.5km model gives a better representation of hourly rainfall but with a tendency for heavy rainfall to be too intense. For winter, both models show future increases in heavy rainfall (defined as the mean of the upper 5% of wet values) of around 40%. In summer, only the 1.5km model shows increases in intensity of extreme rainfall, which were around 36%.

The model projects fewer rain days in the future but a higher frequency of extreme events (above 28mm/h which corresponds to the 99.999th percentile of wet hours for the present-day).

These studies are at best indicative, as the simulations are for limited area regions and for time-periods too short to provide a large enough sample of events for a reliable frequency analysis or to be robust to the possible effects of natural variability). Furthermore, they are single representations of one GCM downscaled using one model and therefore there is no information about the uncertainty associated with these future projections whihc is usually addressed by running an enesemble of climate models with different formulations.

2.6.2 Methodology

2.6.2.1 Historical intense hourly rainfall

For the pluvial flooding analysis, the first step was to compile sub-daily rainfall datasets or IDF (Intensity-Duration-Frequency) curves for as many sites in Europe as possible (see section 2.3). Unfortunately these data are not readily available and we only were able to collate data for 46 gauges, many of them with short records, which limits the reliability of our methods.

After the compilation, hourly levels of rainfall for a 10 year return period were calculated for all available time-series. Considering the data available, hourly annual maxima were used instead of peaks-over-threshold. Following normal practice,a GEV distribution was assumed for all gauges and confidence intervals (95%) were calculated. A discretization correction factor (1.16) was applied to those data calculated from fixed window hourly time-series.

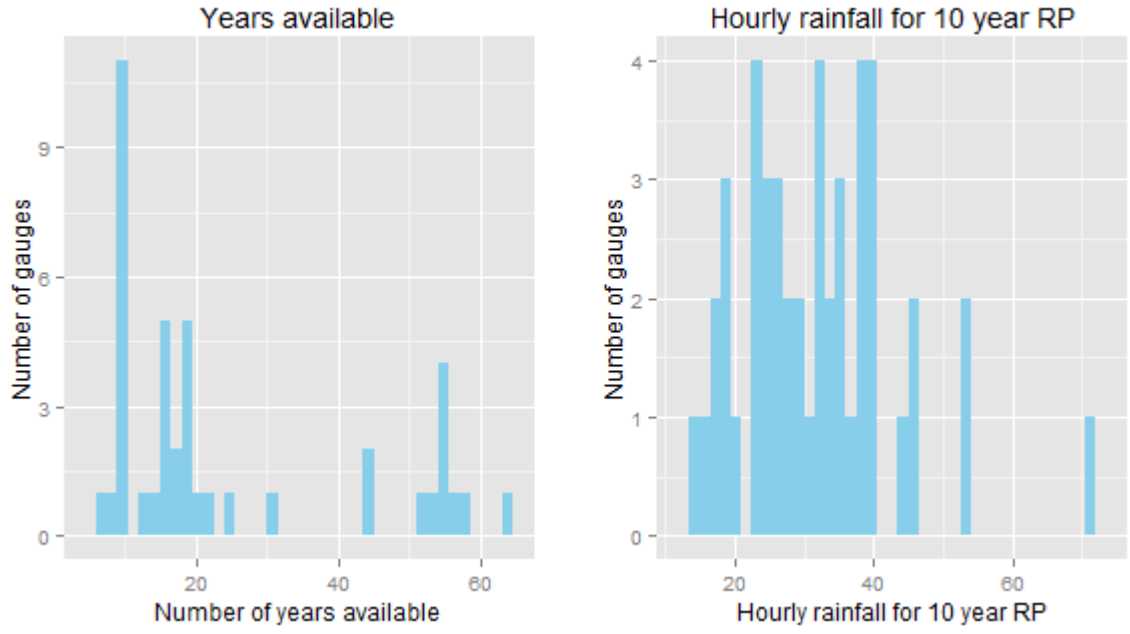

Figure 17: Number of years available for each gauge (left) and distribution of 10 year return period hourly rainfall (right).

Figure 17 shows the resulting hourly rainfall levels for a 10 year return period, as well as the number of years available per gauge for this calculation. Figure 18 shows the spatial distribution of the calculated hourly rainfall levels for the 10 year return period. It is clear that the gauge in Corsica

(Bastia) has a rainfall level for a 10 year return period (72 mm/h) well above all other gauges used in this study which vary between 14mm/h and 54mm/h.

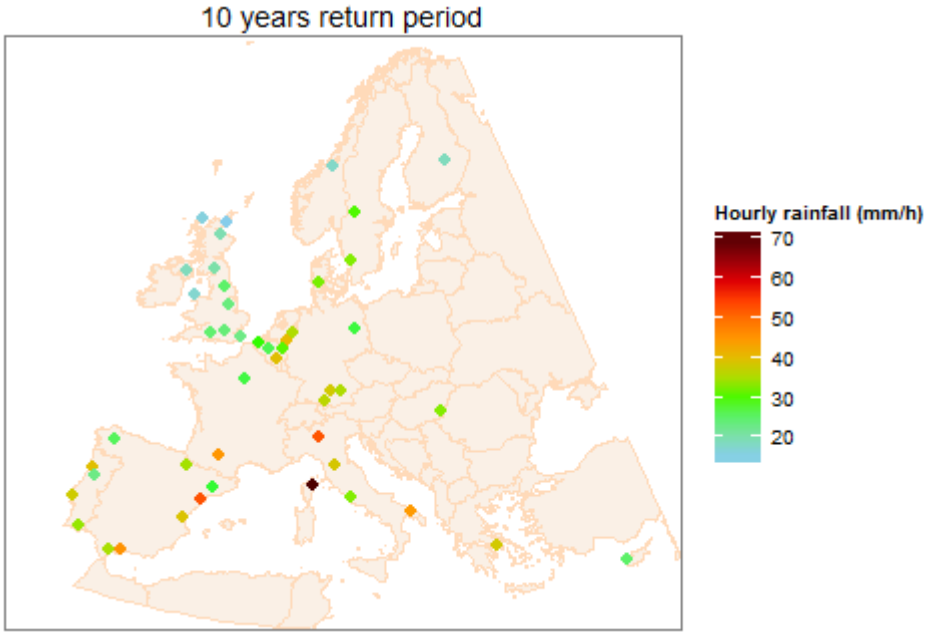

Figure 18: Map of Europe with the hourly rainfall for a 10 year return period for all available gauges. Return periods were calculated assuming a GEV distribution for all gauges. The number of years available for each gauge varied between 6 and 63 (median = 17 years).

Numerous regression models for hourly 10-year rainfall were explored using a variety of climatological variables from E-obs as well as elevation and location as predictor variables. Besides the usual statistical measures of goodness of fit (R-squared, correlation between variables, predictive power of the used variables, and statistics of the residuals) the robustness of the regression across possible ranges of values of predictors was carefully considered, since the model must be applied to all Europe. Therefore, lower R-squared values and higher errors at each gauge were preferred to overfitting the regression to the available gauge data, which could result in unrealistic hourly rainfall for the 10 year return period when the regression is applied throughout Europe.

The following regression equation was selected:

$$R_{1h,10yr} = 68.51252 + 1.01388R_{med} - 0.16297R_{max} - 0.94541\text{Latitude} - 1.21321T_{min}$$

With:

$R_{1h,10yr}$ – hourly rainfall for a 10 year return period R_{med} – median of the annual maximum daily rainfall	R_{max} – Maximum monthly mean rainfall T_{min}– minimum monthly maximum temperature

All the predictors were significant (all p-values bellow 0.006) and had low variance inflation factors (all bellow 4.4) meaning that multicolinearity was low (i.e. the variables of the regression are not correlated); therefore the model was considered robust. However, the R-

squared value was not very high (0.57) and the Bastia site has a large residual: 24.6mm. Maps of the residuals for all gauges are shown in Figure 19. Figure 20 shows the observed vs estimated $R_{1h,10yr}$ for all gauges with the confidence intervals for the observed values. Here it can be seen that the confidence intervals for Bastia (green square on the top-right corner of the plot) are very large (the 10 year return period can be between 16mm/h and 128mm/h) due to the high interannual variability of the Mediterranean climate and the low record length (only 10 years of data) available.

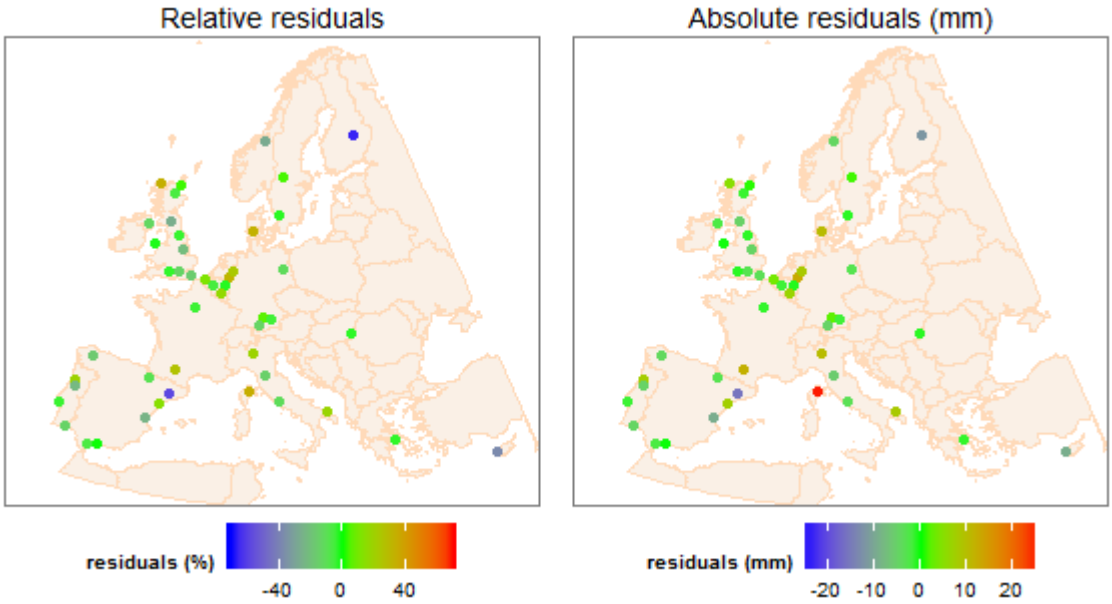

Figure 19: Maps of Europe showing the residuals of the linear regressions used to estimate the hourly rainfall for a 10 year return period. The plot in the left shows absolute residuals (in millimetres) while the plot on the right shows relative residuals (calculated as a percentage of the observed rainfall level for a 10 year return period).

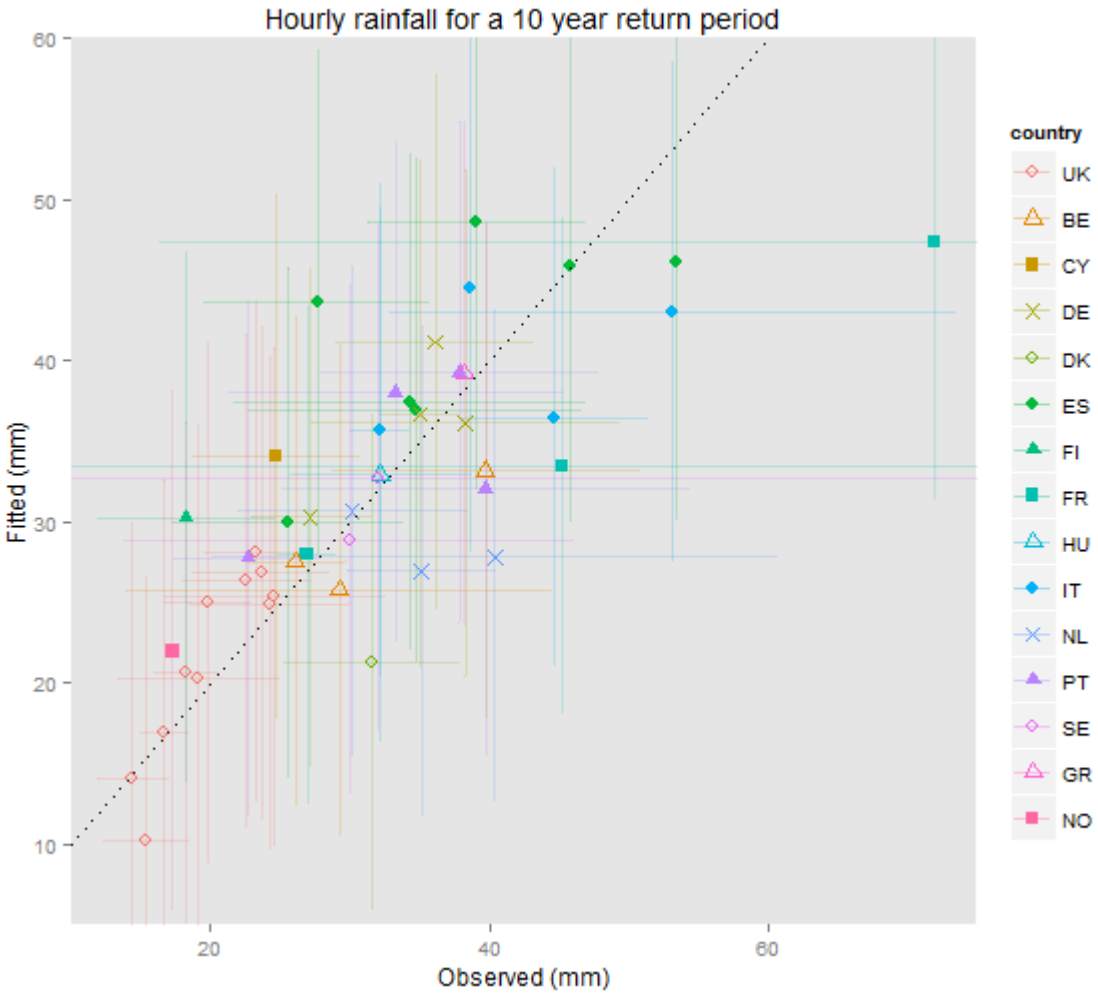

Figure 20: Observed Vs estimated hourly rainfall for a 10 year return period for all gauges. When possible, the observed values are shown with their respective 0.05 confidence interval (horizontal lines). For four gauges (Athens, Barcelona, Firenze and Malaga) confidence intervals are not available because the time-series for these gauges were not available and the rainfall levels for the 10 years return period were retrieved from the literature. Predictive intervals (0.95 level) are also shown (vertical lines). The diagonal dotted line shows the 1:1 line.

The results of the linear regression for all Europe are shown on Figure 21 and were used to calculate hourly rainfall for a 10 year return period for all European cities, except the two Maltese cities because e-obs does not cover Malta since the resolution of the dataset is not compatible with the small size of the island.

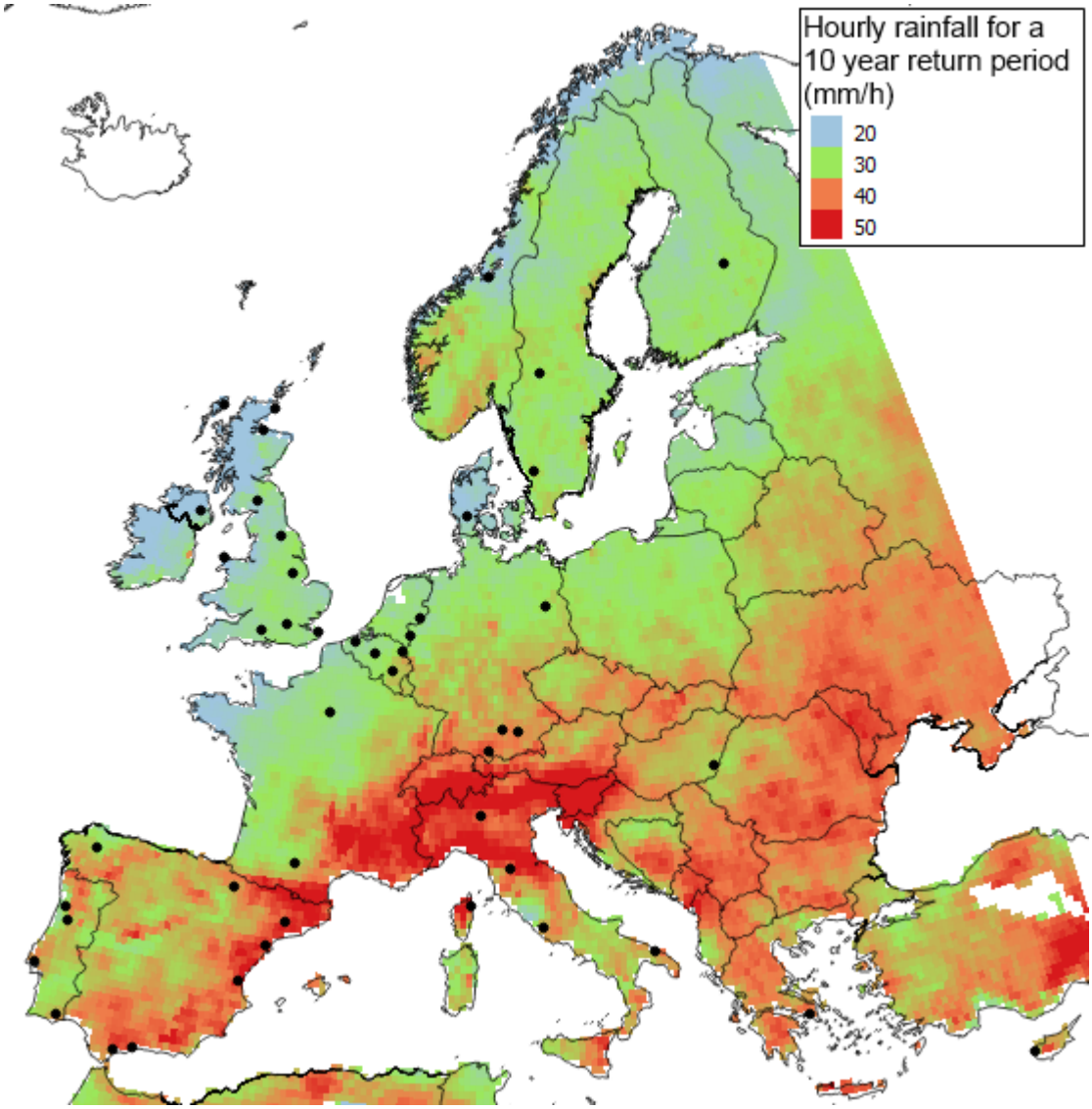

Figure 21: Map of Europe showing the estimates from the regression model for hourly rainfall for a 10 year return period based on e-obs climatological data. The locations of the gauges used are shown as black dots.

2.6.2.2 Future intense hourly rainfall

As explained in the introduction of this chapter there are no Europe-wide future climate model simulations at convection-permitting scales, therefore there are no reliable projections of future intense hourly rainfall for Europe. Also, the regression model developed for historical intense hourly rainfall for Europe is valid for the estimation of rainfall at any site, but there is no assurance that it would be valid for future climates when the range and inter-relationships of the predictor variables are likely to change.

Therefore, the assessment of future changes in pluvial flooding can only be done using a sensitivity analysis. Change factors will be applied to the historical hourly rainfall for a 10 year return period. The choice of change factors is somewhat subjective and we considered several sources of information to inform this decision:

- The convection-permitting simulation of the Alps (1991–2000 and 2081–2090 , RCP8.5) showing intensity of heavy hourly rainfall (99.9th percentile) increasing by 3% to 6% (Ban et al., 2015).
- The convection-permitting simulation of southern UK (1996-2009 and 13 years in the 2100s, RCP8.5) showing heavy rainfall (defined as the mean of the upper 5% of wet values) intensity increasing by around 40% in winter and 36% in summer (Kendon et al., 2014).
- Change factors calculated for daily Rmed (median of the annual maximum daily rainfall) shown in Figure 22. Daily extreme rainfall values are more credibly simulated by climate models and are available for the historic period in the e-obs data set. On the other hand, they are only a partial predictor of hourly extreme rainfall values: the correlation between daily Rmed and hourly rainfall for a 10 year return period (shown in Figure 23) is low (Pearson correlation of 0.5). The Rmed change factors are shown in Table 3.

Low impact scenario (10th percentile)		**Medium impact scenario (50th percentile)**		**High impact scenario (90th percentile)**	
Minimum	0.78	Minimum	0.95	Minimum	1.07
1st quartile	1.03	1st quartile	1.14	1st quartile	1.24
Median	1.06	Median	1.16	Median	1.26
Mean	1.04	Mean	1.14	Mean	1.26
3rd quartile	1.08	3rd quartile	1.17	3rd quartile	1.29
Maximum	1.13	Maximum	1.22	Maximum	1.36

Table 3: Summary statistics for change factors calculated for Daily Rmed for each european city for three impact scenarios.

Taking all the above information into consideration, the change factors chosen for the sensitivity analysis of future changes in pluvial flooding were 0.9, 1.2 and 1.5. This range is chosen so as to encompass the bulk of the likely range of changes. Note that a small decrease is considered possible within this range (0.9) and that there is no implication of any relatively greater probability in the middle of this range – rather, we consider this to be a uniform interval at this stage.

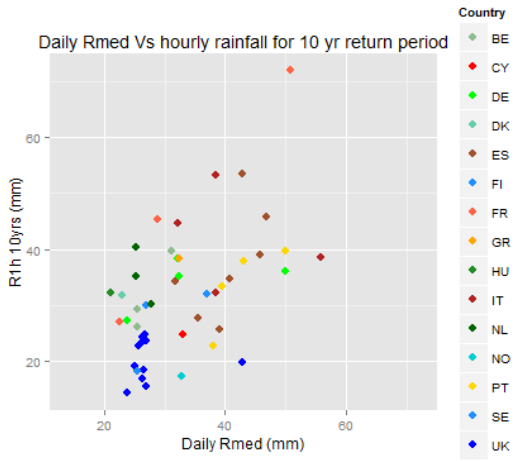

Figure 22: Historical daily Rmed plotted against the hourly rainfall for a 10 year return period for all gauges, color by country.

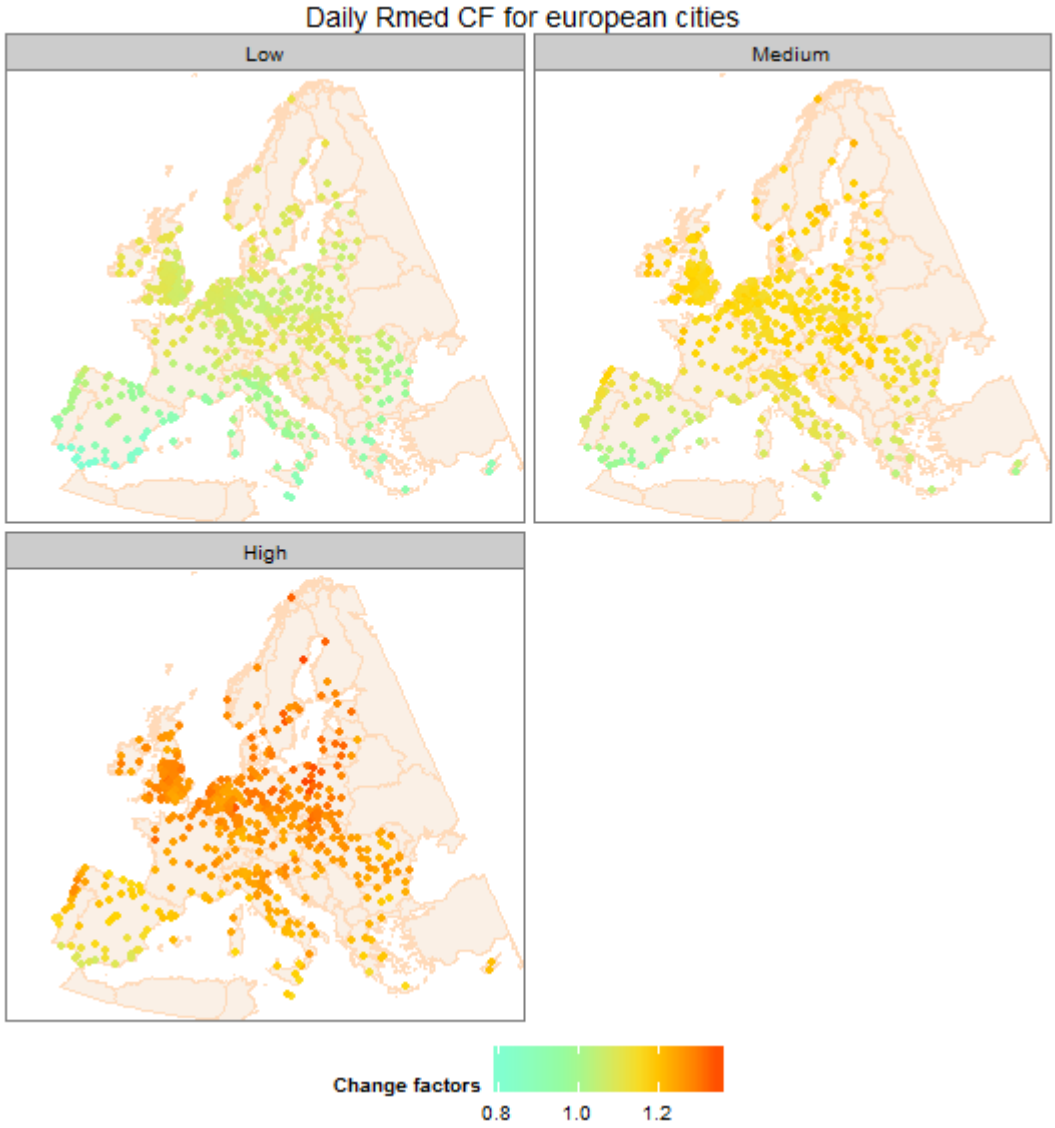

Figure 23: Change factors for daily Rmed for a low (10th percentile) impact scenario (top-left), a medium (50th percentile) impact scenario (top-right) and a high (90th percentile) impact scenario (bottom) for each european city.

2.6.2.3 Urban hydrodynamic model

In parallel to the calculation of historical and future intense hourly rainfall, flood modelling has been performed for all 571 cities using the urban flood model CityCat (City Catchment Analysis Tool) and the 25m resolution DEM. Newcastle University has developed the City Catchment Analysis Tool (CityCAT) model which provides rapid simulation of urban hydrodynamics based on the solution of the shallow water equations using the method of finite volume with shock-capturing schemes (Godunov, 1959; Harten et al., 1983; van Leer, 1979). The Osher Riemann solver (Dumbser and Toro, 2011; Osher and Solomon, 1982) was used to obtain a solution of the Riemann problem at the cell interfaces. Also, the MUSCL-Hancock finite-volume scheme (van Leer, 1984) was used to obtain a high resolution solution which is second order accurate in space and time in the smooth regions.

The CityCat model was deployed on the Microsoft Azure Cloud and a parameter sweep system previously developed (Glenis et al., 2013) was modified and used in order to simultaneously carry out simulations for 571 cities for the following hourly rainfall levels: 20mm/h, 30 mm/h,

40 mm/h, 50 mm/h, 60 mm/h, 70 mm/h, 80 mm/h, 100mm/h and 125 mm/h. With this approach the simulation time was reduced from around three months to just three to four days. As an example, the simulation result for Vienna for 70 mm/h event is shown in Figure 24.

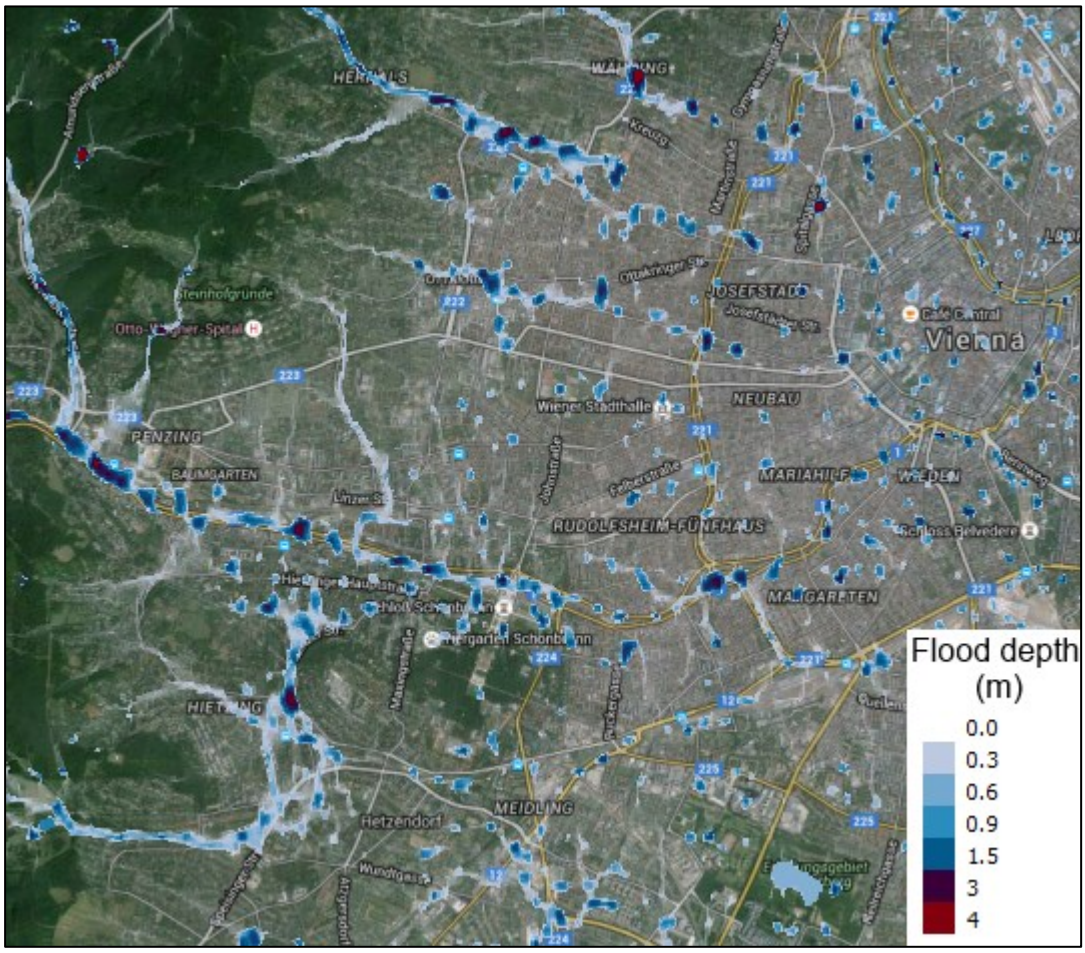

Figure 24: CityCat flood maps for Vienna using a 70mm/h storm.

The use of a coarse DEM (25m) and the lack of information about buildings means that there is low confidence in the spatial resolution of the flooded areas. Nevertheless, the model captures the movement of the water influenced by the natural elevation of the terrain.

The maximum water depth values for each rainfall event were calculated for all the grid cells in order to have a map of maximum flood depths for each city and each rainfall event. Subsequently, the percentage of city flooded for each event was calculated (plots shown in annex). For this, a threshold of 5cm of flood depth was considered to define the flooded area. This percentage was based only on the urban area (Urban Morphological Zones[3] calculated based on CORINE) inside the "city region" defined in the Urban Audit dataset. This was a necessary step since some "city regions" are not appropriate for this type of analysis, some even include estuary areas as shown in Figure 25.

[3] Urban Morphological zones 2000 (http://www.eea.europa.eu/data-and-maps/data/urban-morphological-zones-2000-2) defined as "set of urban areas laying less than 200m apart". This European Environment Agency (EEA) dataset was build based on the urban land cover classes of the CORINE LAND COVER dataset. This dataset was used to define "city area" in the calculations of percentage of city flooded for the pluvial flooding analysis.

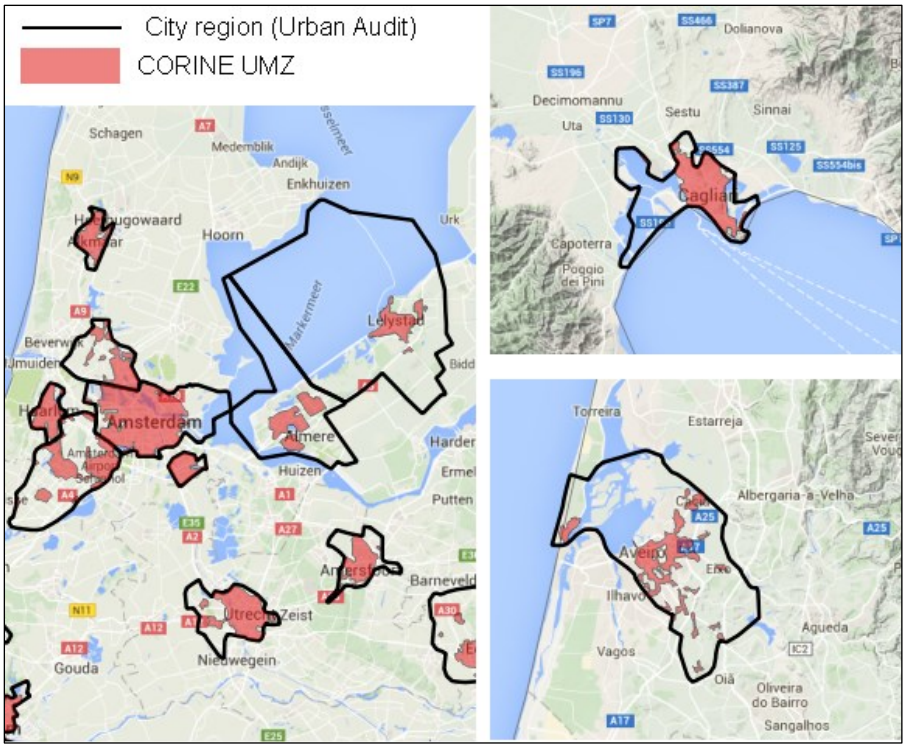

Figure 25: Examples of different definitions of "city". In black is the "city region" as defined in the Urban Audit dataset, in red are the Urban Morphological zones calculated based on CORINE. On the left several cities in the Amsterdam (NL002C) area are shown, the top-right shows Cagliari (IT027C) and the bottom right map shows Aveiro (PT008C).

To calculate the possible future changes in percentage of city flooded the following steps were used for each city:

1. Linear interpolation was performed between the modelled rainfall events and corresponding percentage of city flooded;
2. For the historical hourly rainfall for 10 year return period the corresponding percentage of city flooded was calculated based on the above interpolation (see Figure 26);
3. For the three different future hourly rainfall for 10 year return period (historical value multiplied by the three chosen change factors) the corresponding percentages of city flooded were calculated.
4. Differences and change factors between the future and the historical percentages of city flooded were calculated.

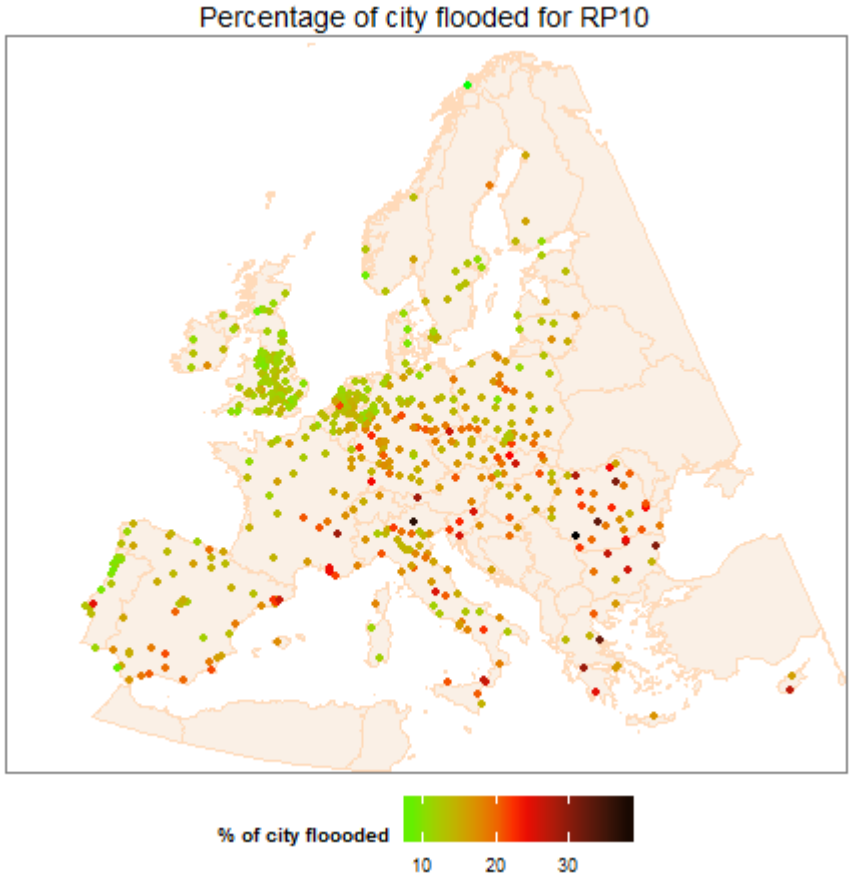

Figure 26: Percentage of city flooded for historical hourly rainfall for a 10 year return period. These percentages are based on the rainfall event and the elevation map used for each city and do not have in consideration adaptation measures already implemented in these cities (like sewer systems) which will be different in different cities.

2.6.3 Results

The changes in the percentage of city flooded using 0.9, 1.2 and 1.5 change factors for hourly rainfall for 10 year return period are shown in Figure 27. The indicator used for the risk analysis will be the ratio (or change-factor) of the percentage of city flooded, i.e. future percentage of city flooded divided by historical percentage of city flooded.

The changes in percentage of city flooded obviously follow the changes in the rainfall events and are therefore much bigger in the high impact scenario. However, since the elevation maps of each city are also taken into account, there is a wide spread of results in each scenario, particularly in the high impact scenario, that does not have a geographical pattern.

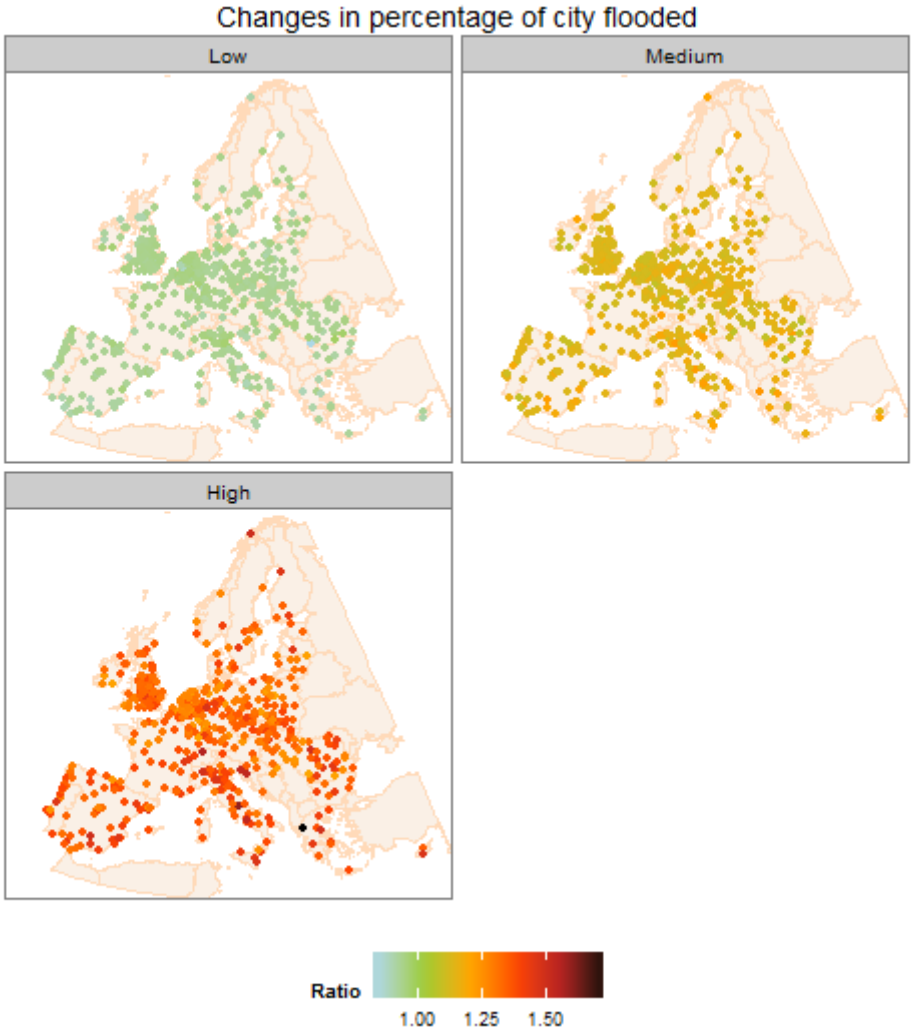

Figure 27: Changes in the percentage of city flooded (calculated as a ratio or change-factor: future percentage of city flooded divided by historical percentage of city flooded) shown for each European city. The changes are calculated assuming a 0.9, 1.2 and 1.5 change factors for hourly rainfall for 10 year return period respectively as low (top-left), a medium (top-right) and a high (bottom) impact scenarios.

Figure 28 shows that, for most cities, under the high impact scenario (and to a lesser extent in the medium scenario), the changes in terms of percentage of city flooded are smaller than the change factors that originated them. The opposite is true for the low impact scenario, which was done with a 0.9 rainfall change factor, but has a median percentage of city flooded change factor of 0.93. For the medium and high impact scenarios (rainfall change factors of 1.2 and 1.5) the median percentages of city flooded change factor are 1.14 and 1.34. Nevertheless, the differences between cities are quite large, especially for the high impact scenario where the minimum change factor is 1.18 and the maximum is 1.75, which means that the change in percentage of city flooded varies between an 18% to a 75% increase in area flooded for a 50% increase in rainfall.

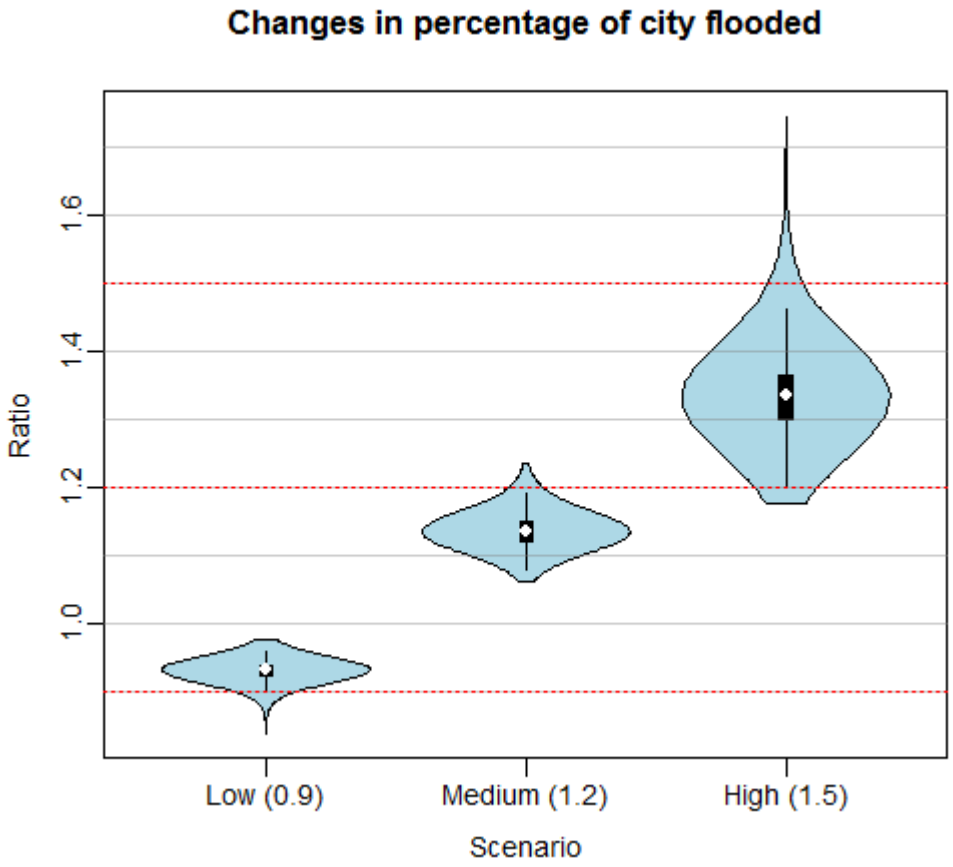

Figure 28: Violin plots (kernel density plots superimposed on boxplots, with median value shown in white) of ratio (or change factors) of percentage of city flooded (future percentage of city flooded divided by historical percentage of city flooded) for all European cities for a low (rainfall change factor=0.9), a medium (rainfall change factor=1.2) and a high (rainfall change factor=1.5) impact scenario. The rainfall (hourly rainfall for 10 year return period) change factors are also shown as dotted red lines.

2.7 Fluvial flood hazard

2.7.1 Introduction

Fluvial (or river) flooding affects numerous European cities, but data regarding river discharges are seldom available for city areas. The approach taken here is therefore to implement a regional flood frequency analysis: specifically, regression relations between flood characteristics and catchment and/or climatic characteristics are derived to ensure a consistent approach is applied to all EU cities.

A major benefit of regression based analyses is that there are no *a priori* assumptions about the interacting processes. All available data can be exploited to understand relationships with the variable of interest. It is also possible to derive some insight into individual correlations and interactions by exploring the residual plots against selected predictors. However, the linear assumptions do not appropriately represent the hydrological processes, and there are usually inter-site correlations. Resolving the issues related to nonlinearities usually involve data transformations, technique modification (from Ordinary Least Squares to Weighted Least Squares or Generalised Least Squares) and model structure redefinitions, thus voiding the earlier claim of minimal assumptions (Oudin et al., 2008).

Regression methods generally do not accurately estimate the flood quantiles due to the difficulty of relating runoff to a single/fixed set of catchment descriptors (Salinas et al., 2013). Nevertheless, regression studies carried out on clustered selections within the study region tend to perform better than global regressions (Salinas et al., 2013).

Smith et al. (2015) performed a regional flood frequency analysis at global scale using 703 discharge gauges from the Global Runoff Data Centre (GRDC) and a global annual average rainfall dataset from World-Clim (Hijmans et al., 2005), besides catchment area and slope. Regressions were used to calculate the mean annual flood and they concluded that the best regressions used just catchment area and annual average rainfall as estimators. Different exponents for the two estimators were calculated for different climatic areas based on the Koppen-Geiger classification, where Europe is mainly constituted by temperate and continental classes. The regressions performed better for temperate, tropical and polar regions than the drier continental and arid regions. Also, means and medians of the relative mean square errors were substantially different, demonstrating the strong effect of a small number of poorly performing gauges. The authors hypothesise that this might be due to basins with extensive water abstraction. The mean errors for the mean annual flood regression applied to temperate climate was 77% (median of 37%), for continental climate was 151% (44% median). The authors conclude that there is "some predictive skill" for the majority of the stations whilst pointing out that this methodology is not appropriate to provide estimates of detailed localized discharge.

An alternative methodology is to model the whole of Europe with a hydrological model, but this requires vast amounts of data, which is not readily easily accessible on a European scale (e.g. aquifer characteristics). Furthermore, both running and calibrating such a model would be very time consuming. Nonetheless, some studies of future flooding in Europe have tried to use simple hydrological or hydraulic models, e.g. Lisflood (van der Knijff et al., 2010). This model requires inputs representing precipitation, air temperature, potential evapotranspiration, and evaporation from open water bodies and bare soil surfaces and has been run for the whole Europe at 5km resolution (Rojas et al., 2012). The model has been calibrated with data from 258 European catchments for at least four years of observed discharge with a focus on the timing and magnitude of flood events. However, results for daily discharge were far from ideal,

with 70% of the percentage bias values between ±25%, 23% of the values below that interval (underestimation of discharges) and 7% above (overestimation of discharges).

Roudier et al. (2016) also used pan-European hydrological models for future flooding assessment, in this case Lisflood, E-Hype and VIC. The models were run with bias corrected climate variables (5 climate model runs bias corrected through quantile mapping using E-OBS). The median of the 100 year discharge level (Q100) modelled was assessed against the Q100 calculated from 428 gauges (from several sources). Root Mean Square Errors were lower for Lisflood (961 m^3/s) than E-Hype (1124m^3/s) or VIC (1279m^3/s) but these differences in performance might be partly explained by different calibration methodologies and datasets. Errors in simulation of pan-European historical discharges seem therefore to always be substantial whether regression methodologies or hydrological models are used.

Regarding the projection of future discharges, a few recent pan-European studies exist; Dankers and Feyen (2009) studied future changes in flood hazard in Europe for 2071-2100 relative to 1961-1990 using two GCMs (one with three different sets of initial conditions), two RCMs and two emission scenarios (SRES A2 and B2) to run Lisflood. They found that at regional level the choice of which combination of outputs was used resulted in large differences in the Q100, sometimes even without agreement in the sign of the change. However, they also found a decrease in extreme river discharge in North-eastern Europe common to all experiments. The extent of the area where that decrease was found varied with different experiments due to differences in the reduction of the snow pack (and therefore peak runoff during snowmelt) and how it was compensated by the increase of winter precipitation. The authors therefore questioned if their results could be explained by trying to estimate 100 year return levels from 30 year time-series of annual maximum discharges. Elsewhere in Europe, the different experiments showed mixed patterns partially due to a large internal variability in the climate model runs.

Rojas et al.(2012) assessed future flood hazard in Europe using 12 climate outputs of the ENSEMBLES project (SRES A1B scenario) for 1961-2100 corrected trough quantile-mapping (using the E-OBS dataset) to run Lisflood. The maximum annual discharges for the control period (1961-1990) showed reasonable results but lower discharges/smaller catchments tended to have bigger errors, extreme discharges tended to be underestimated and a small number of stations showed big discrepancies, probably partly due to the underestimation of the anthropogenic influence on high flows. Lisflood run with different future climate model projections showed very different estimates of changes in Q100, sometimes even without agreement in the sign of the change, especially in Scandinavia and North-eastern Europe. However, most simulations projected Q100 increases in western and central Europe, northern Italy, the British Isles and the upper basins of the rivers Rhine and Elbe. While decreases in Q100 are projected by most simulations in parts of Iberia, southern Italy, south-eastern Europe, north-eastern Germany, Poland, the Baltic region and some areas in Scandinavia. However, many of these changes were not statistically significant.

Alfieri et al. (2015) looked at projected relative changes in European floods between 1971-2100 using seven scenarios (a combination of 3GCMs and 4 RMCs) from EURO-CORDEX (RCP8.5). They used uncorrected (raw) climate model variables (temperature, precipitation, air pressure, specific humidity, wind speeds and downwelling shortwave radiation) to run the hydrological model Lisflood (at 5km spatial resolution and daily time step and modelled 22 European basins with area above 50 000 km^2) under the argument that bias correction does not improve the representation of the extremes and that the spatial resolution of the observed datasets is coarser than the EURO-CORDEX outputs. However, when using a physical based hydrological model, mean values are important in order to get a good representation of melting,

infiltration and evaporation processes and the choice of using uncorrected climatological variables might therefore induce strong biases in the discharges of these big basins.

Nevertheless, Alfieri et al. (2015) found that by 2100 both mean discharges and annual precipitation are projected to increase in north-eastern Europe and decrease in southern Europe (with no agreement in central Europe). In the seven scenarios used, the rainfall changes are in-line with the CMIP5 projections, although with added spatial detail. However, despite daily maximum rainfall being expected to increase in most of Europe (with higher and more significant increase when moving north and east), peak discharges show a different behaviour due to the effects of temperature increase affecting both evapotranspiration and snow accumulation. Mean annual daily peak flow is expected to decrease in southern Spain, Scandinavia and the Baltic countries and increase in central Europe and the UK. However, the uncertainty is large in most basins studied with trends showing a discontinuous pattern and with some showing good and other a lack of agreement between climate models.

Roudier et al. (2016) used 11 members of CORDEX (4 GCMs, 4 RCMs and three emission scenarios) and compared the 1971-2000 with a 30 year interval where the driving GCM reached +2ºC. Three pan-European hydrological models (Lisflood, E-Hype and VIC) were run with bias corrected climate variables (quantile mapping using E-OBS). Changes in river flooding were assess by calculating the magnitudes of 1 in 10 (Q10) and 1 in 100 year (Q100) flood using the daily maximum discharges of the 30 year periods and fitting a GEV distribution (using L-moments). For Q10, south of 60°N the median of the 33 projections range from no significant change to a significant 40% increase in magnitude. The Q100 showed the same type of behaviour but with more areas showing strong increases. North of 60°N there is more heterogeneity with large areas of no significant change, some increases in flooding in costal Scandinavian areas (rain-fed floods) and strong decreases in parts of Finland, NW Russia and parts of Northern Sweden due to decreases in snowpack. However, when looking at the 25th and the 75th percentile for the Q10 projections instead of just the median of the 33 projections, there are vast areas in Europe where there isn't an agreement even on the sign of change. This encompasses the majority of Scandinavia and Northeast Europe as well as the south of Iberia and other spotted areas throughout the continent.

There is a very wide range of projections for future changes in European river flooding with disagreement between different studies, or even within studies that used an ensemble of climate projections. Therefore, in this report the emphasis is on looking at the whole ensemble of climate projections from CMIP5 (54 climate model runs) to assess the range of possible future changes. Since this would be extremely time-consuming to do using a physically based hydrological model, a regression based methodology was applied.

2.7.2 Methodology

The Global Runoff Data Centre (GRDC) discharge records in Europe comprising at least 9 years of daily data between 1950 and 2013 and no missing data were initially selected. For each gauge an upstream basin was delineated in GIS in order to obtain its area and climatology. For this purpose the Hydro1K dataset was used[4]. First, the flow accumulation raster was used to correct the position of the GRDC gauges. This was necessary for two reasons: (i) there can be

[4] USGS (2011) *Hydro1K Europe*. Available at: http://eros.usgs.gov/#/Find_Data/Products_and_Data_Available/gtopo30/hydro/europe (Accessed: 09-02-2011).

errors with the coordinates of each gauge, and (ii) the hydro1K dataset has a resolution of 1km, therefore the location of the rivers is not always correct (especially in flat areas). This was done manually for all 225 gauges and involved the following steps:

1. Check if the gauge coordinates lies on a river, *i.e.* high flow accumulation zone in the hydro1k raster;
2. If not, and one river exists in the vicinity (<2km), adjust the gauge coordinates to lie on the river.
3. If more than one river exits in the vicinity, or if the river is further than 2km, further investigation was needed. The name of the river, from the GRDC metadata, and the coordinates of the gauge were used, with Google Maps to pinpoint the location of the gauge. With the exception of two cases, gauges were only moved when the distance was less than 3km. Also, when it was not obvious where the gauge should be moved to, it remained in its original place but was not excluded from the analysis.

The 225 basins were then delineated using a python script, the flow direction raster from hydro1K and the "corrected" location of the gauges as inputs. To assess the magnitude of the errors, the area of the calculated basins was compared with the area supplied in the GRDC metadata for each gauge (see Figure 29 and Figure 30). The errors were calculated as:

$$\text{Error} = (A_{calculated} - A_{metadata}) / A_{metadata} * 100$$

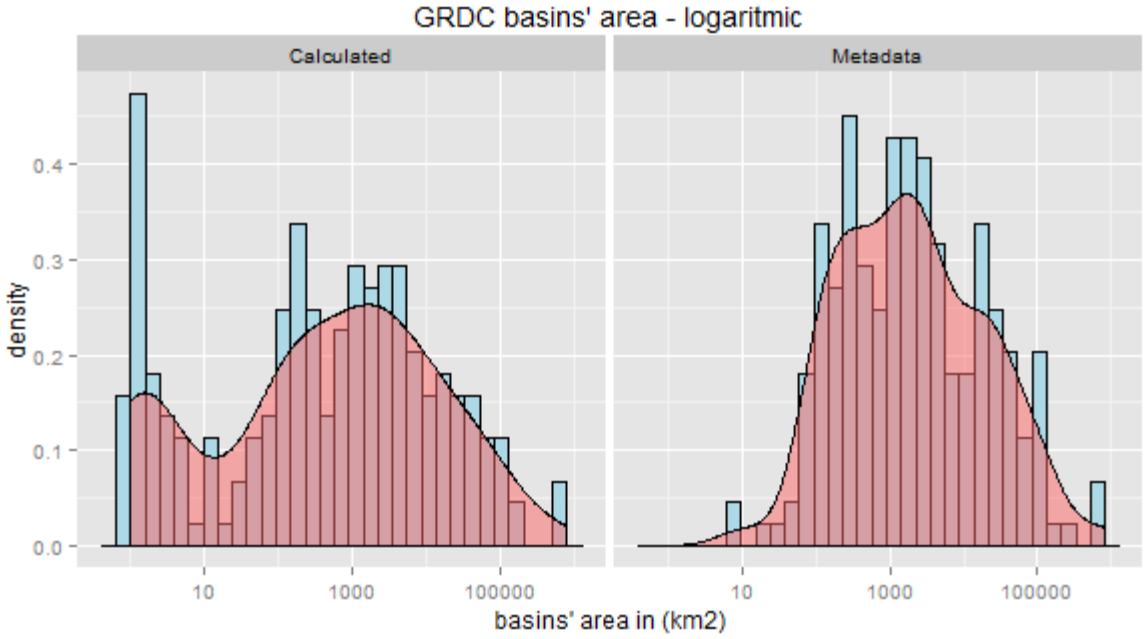

Figure 29: Histograms (blue) and PDFs (pink) of the areas of the basins of the 225 GRDC discharge gauges. The left plot shows the calculated areas using the methodology outline in the text. On the right are the areas of the same basins taken from the GRDC metadata.

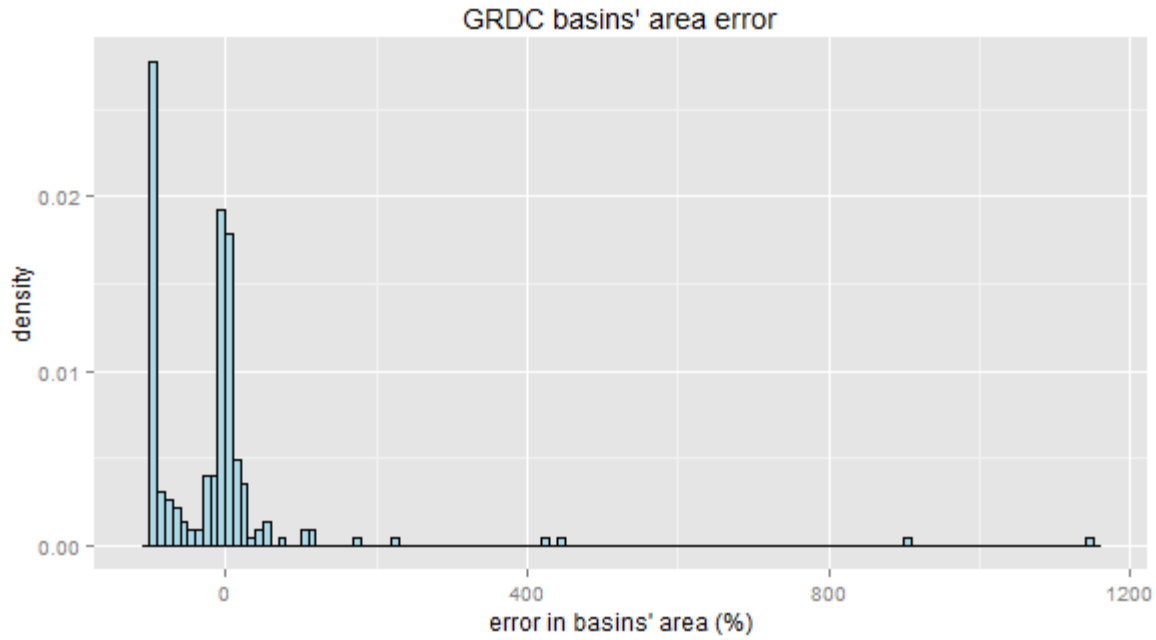

Figure 30: Histograms of the errors in basins' areas for 224 GRDC basins, the basin with the biggest error (44 736% is not shown because otherwise the plot would become illegible).

Basins with an area error over 25% were discarded. After this process, 114 catchments remained.

In Hydro1K the definition of a river was a water course with at least 1000 km^2 catchment area. We chose a smaller threshold – 500km^2 of catchment area – in order to keep a large number of basins, which is essential for a meaningful regression analysis. Nevertheless, the biggest basin in the dataset (gauge 6742900 in the Danube) which has an area of 807 000km^2 was discarded, since none of the European cities studied has a basin that big.

The 10 year return levels of annual maximum daily discharge (Q10) were calculated for all remaining basins. Following standard practice, a GEV distribution was fitted for all gauges and confidence intervals (95%) were calculated. Specific Q10 were also calculated by dividing Q10 by basin area, which gives a measure of the intensity of flow per unit area.

The basin shapefiles were used to subset the E-OBS dataset in order to extract basin average annual and monthly values for:

- precipitation,
- maximum, mean and minimum temperature, and
- a simplified measure of snow pack, calculated as the amount of mean monthly precipitation that falls when the minimum monthly temperature is negative for each E-OBS cell.

Potential evapotranspiration (PET) was also calculated for each basin using the Thornthwaite equation based on latitude and the basin mean monthly temperature. For simplicity, since the formula is not sensitive to small latitude changes, the latitude of the gauge was used instead of the latitude of the centroid of the basin.Figure 31and Figure 32 show some of the variables calculated.

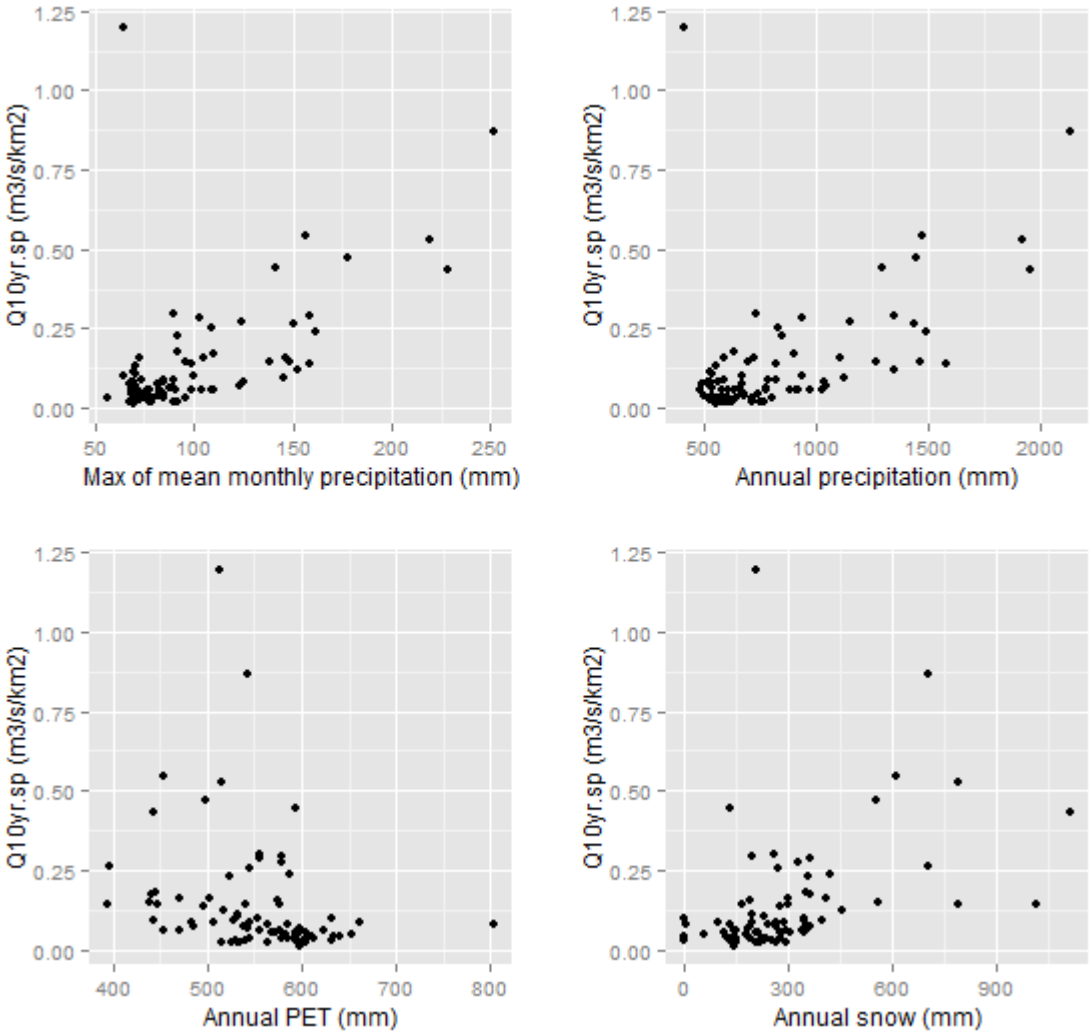

Figure 31: GRDC data exploratory plots

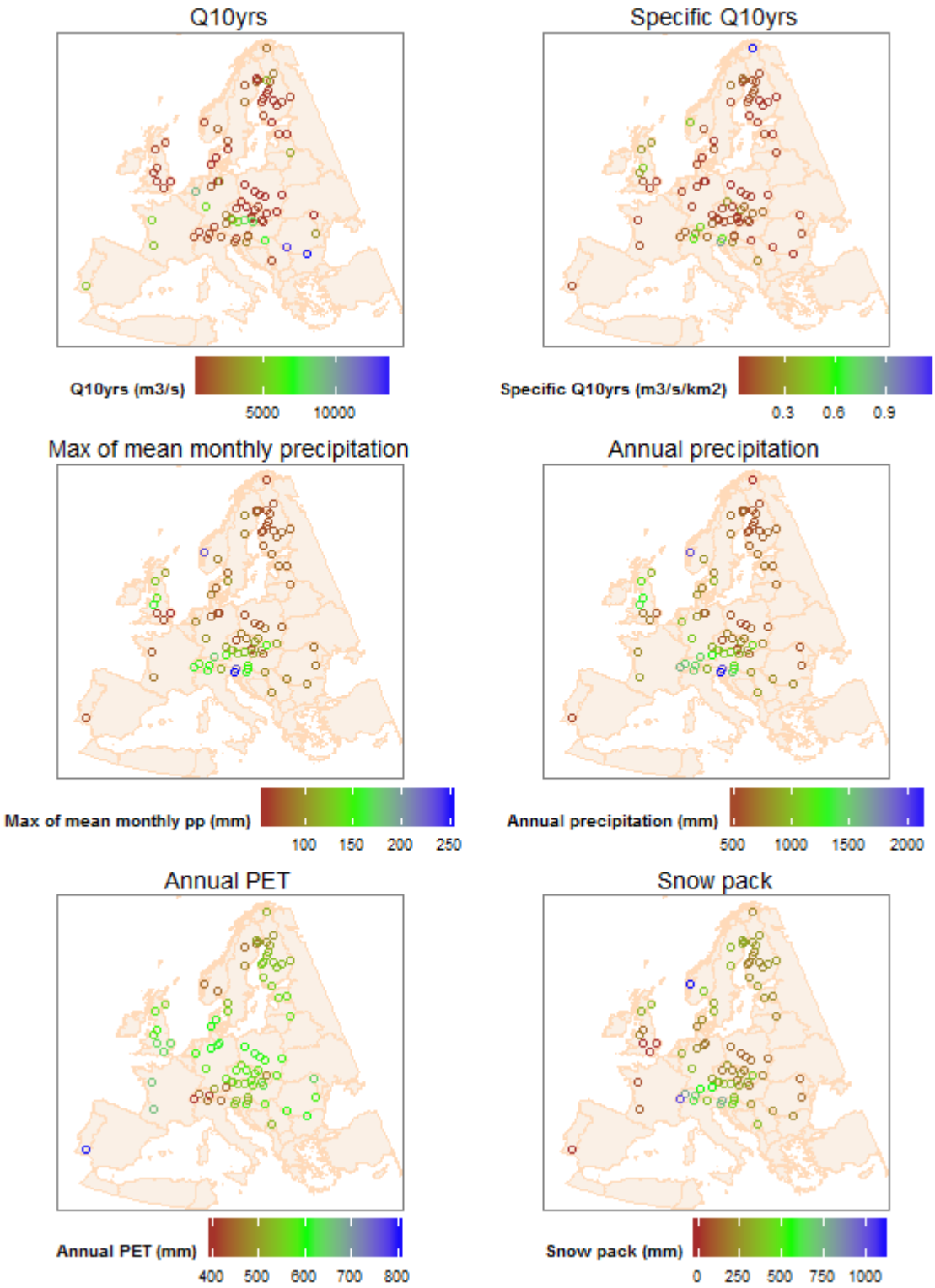

Figure 32: GRDC data exploratory maps

There is an obvious outlier (top-left point in the top plots of Figure 31 and top Finnish gauge in Figure 32) which has a specific Q10 of 1.2 $m^3/s/km^2$ despite having low annual precipitation (412mm) and an average annual PET (514mm). According to the metadata provided by GRDC, this gauge (6830510) should be in the Tana River which, at this location, makes the border between Finland and Norway. However, looking at Figure 33 the location of the gauge does not

seem to be correct since it is in a contributory stream of the Tana, instead of the Tana itself. Therefore this gauge was rejected.

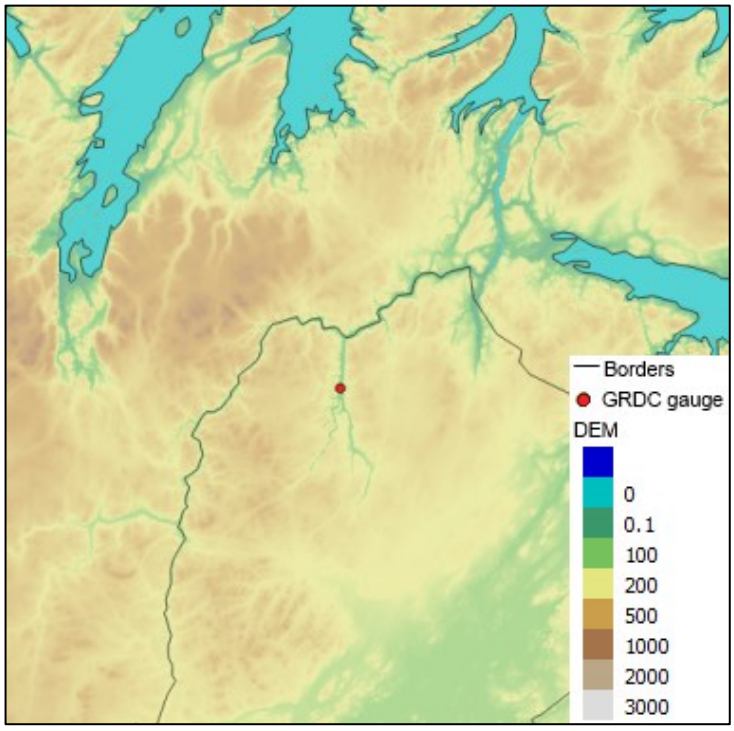

Figure 33: Elevation map with GRDC gauge number 6830510.

A European map with the basins used and rejected is shown inFigure 34. At the end of the selection process 82 basins remained to be used for the Q10 regression. The final selection of basins, although not uniform across Europe, still represents very different climates and a wide range of basin sizes.

Various regression models for specific Q10 (with and without transformations such as normalization and using logarithms) were trialled using monthly, seasonal and annual basin values of precipitation, PET, snow pack and rainfall (precipitation minus snow-pack). Specific Q10, was used instead of Q10 due to the dominance of basin area in the Q10 values as it dominates the regression and hides the contribution of the other variables. The dominance of basin area is aggravated by the large range of areas in the dataset (from 55 km^2 to 807 000 km^2, with a median of 2 535 km^2).

Besides the usual statistical measures of goodness of fit (R-squared, correlation between variables, predictive power of the used variables, and statistics of the residuals) the robustness of the regression across possible ranges of values of predictors was carefully considered, since the model must be applied to all Europe. Therefore, lower R-squared values and higher errors at each gauge were preferred to overfitting the regression to the available data. The following regression equation was selected:

$$Q10 = -2.424840 + 0.822813\text{Log}(\text{AREA}) + 0.015167P_{max}$$

With:

Q10 – 10 year return period of annual maximum daily discharge

P_{max} – Maximum monthly mean precipitation

AREA – basin area

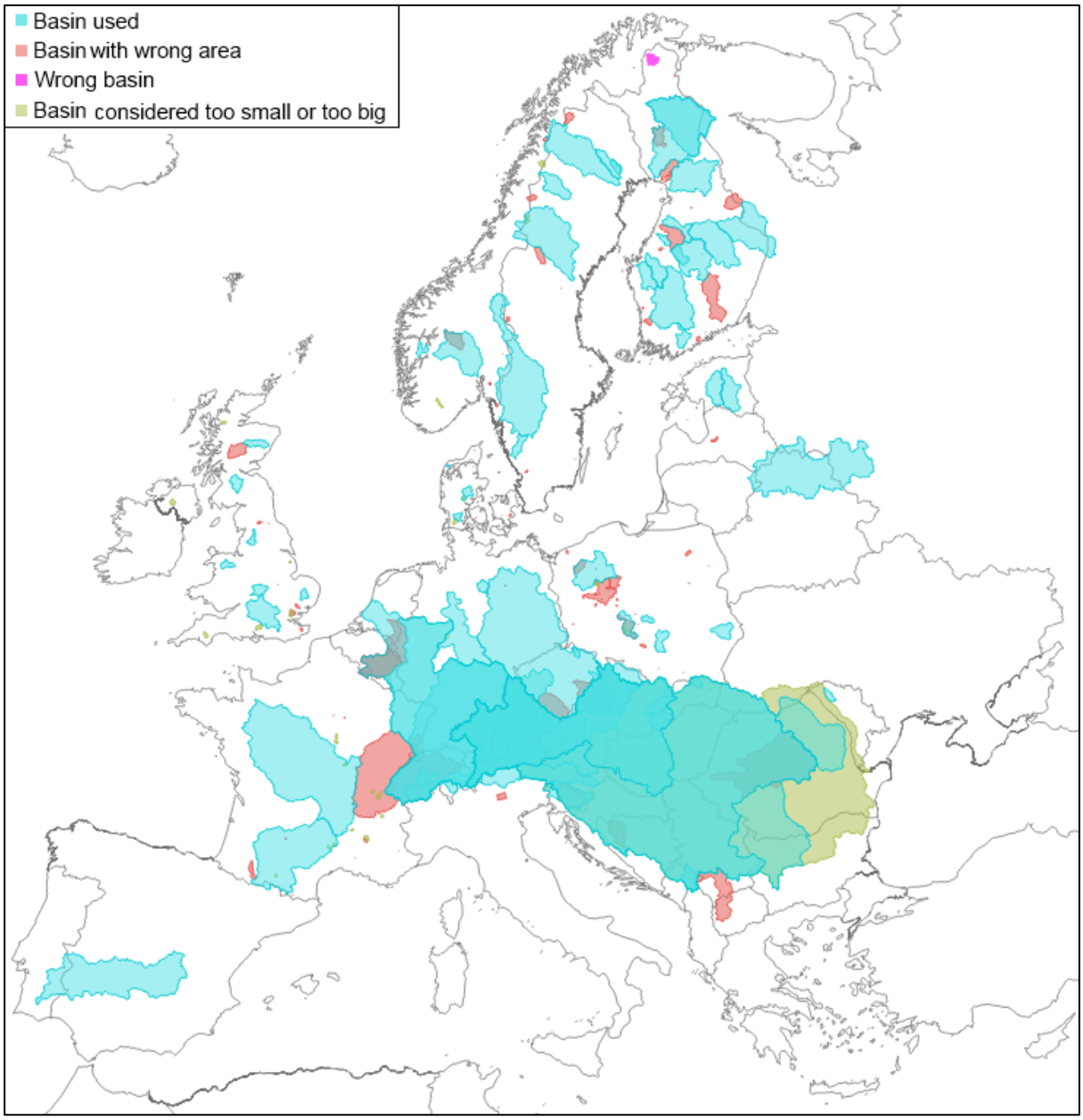

Figure 34: Map with all GRDC gauges' basins.

The adjusted R-squared for the regression was 0.84. Both predictors were significant (p-values bellow 1.41^{-13}) and had low variance inflation factors (1.05) meaning that multicollinearity was low (i.e. the variables of the regression are not correlated); therefore the model was considered robust. Absolute and relative errors are shown in Figure 35 and Figure 36. The biggest absolute errors correspond to rivers with very high discharge and do not correspond to big relative errors. The biggest relative error (280%), which is an outlier, is from the river Notec in Poland (GRDC gauge number 6457200).

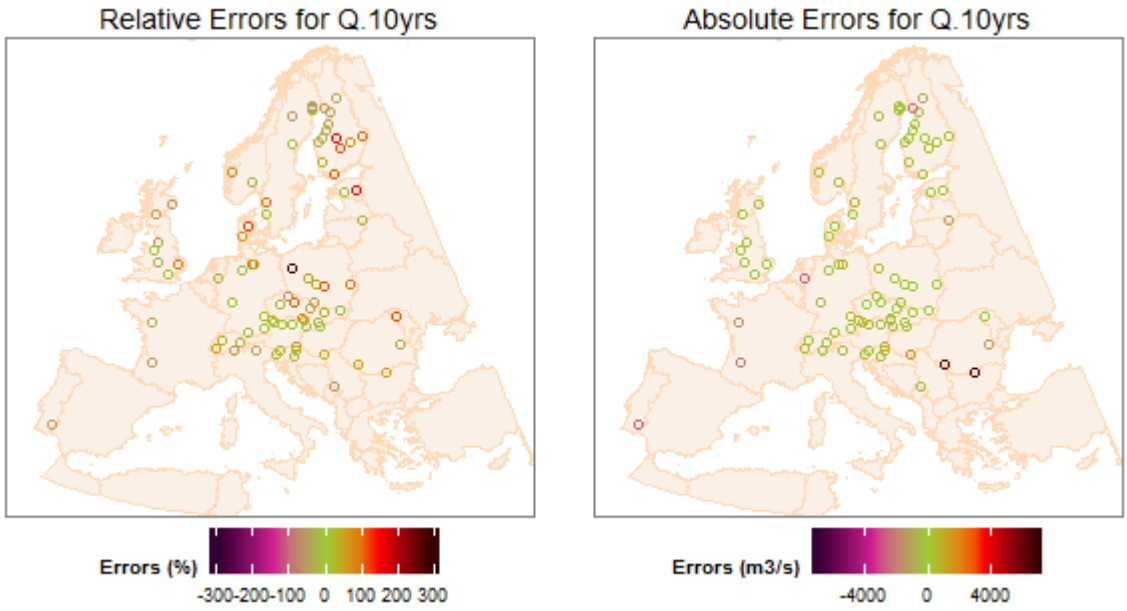

Figure 35: Maps of relative (left) and absolute (right) errors for the Q10 regression.

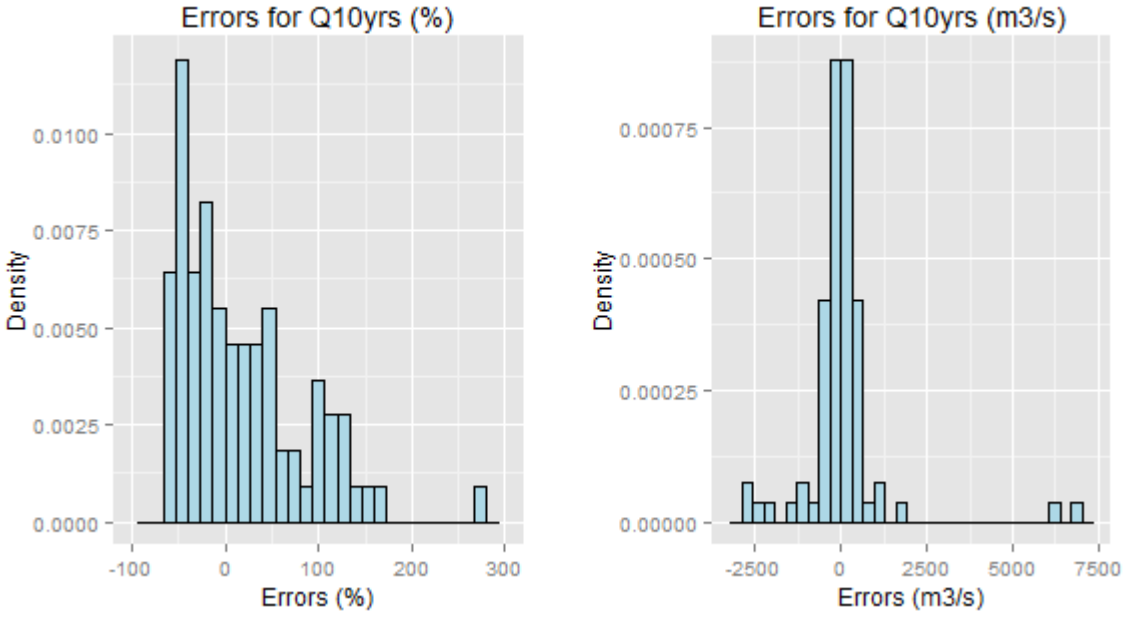

Figure 36: Maps of relative (left) and absolute (right) errors for the Q10 regression.

Figure 37 shows the observed vs estimated Q10 for all basins. The two Romanian basins of the Danube (top-right circles) stand out for their large discharge and large absolute error (despite the fact that the observed value is still within the predictive interval at 0.95 level). However, as mentioned before, they have small relative errors. The absolute errors can nevertheless be substantial and the prediction intervals for large discharges become very wide, meaning that the uncertainty in these estimates is high.

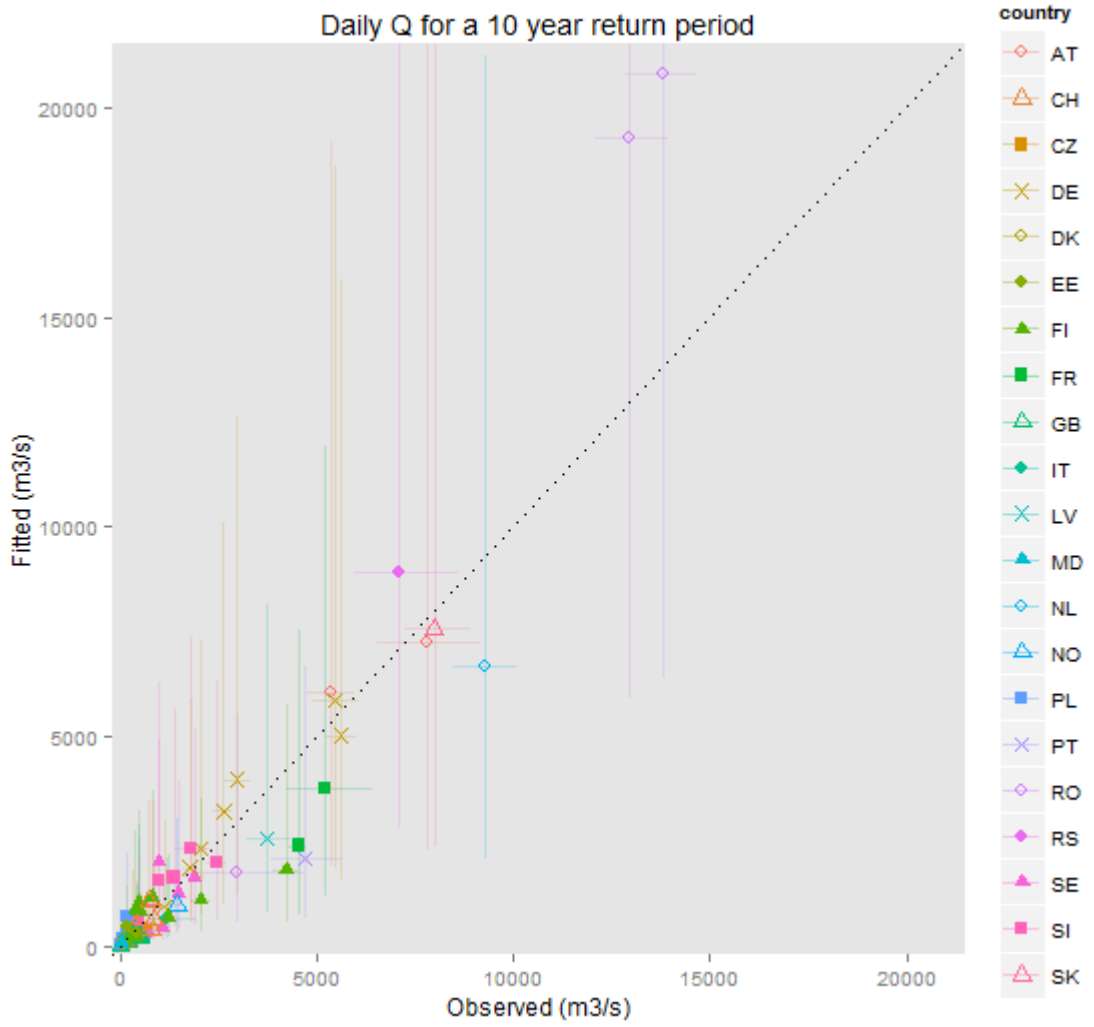

Figure 37: Observed Vs estimated Q10 for all basins. The observed values are shown with their respective 0.05 confidence interval (horizontal lines). Predictive intervals (0.95 level) are also shown (vertical lines). The diagonal dotted line shows the 1:1 line.

The results of the linear regression were used to calculate Q10 for rivers flowing through European cities. To do so, the maximum flow accumulation point inside each city (with a 1km buffer) was calculated using an R routine. Those points were than used to delineate the correspondent 571 basins using a python script with the flow direction raster from hydro1K (as done for the GRDC gauges). The resulting basins are shown in Figure 38. The calculated regression was than applied to every basin with more than 500km^2 in order to calculate Q10 for rivers flowing through European cities. Change factors for maximum monthly mean precipitation for each basin from the 54 climate model runs were than applied to the E-OBS precipitation values and the future Q10 were calculated using the same regression. The changes in discharge are presented as ratios.

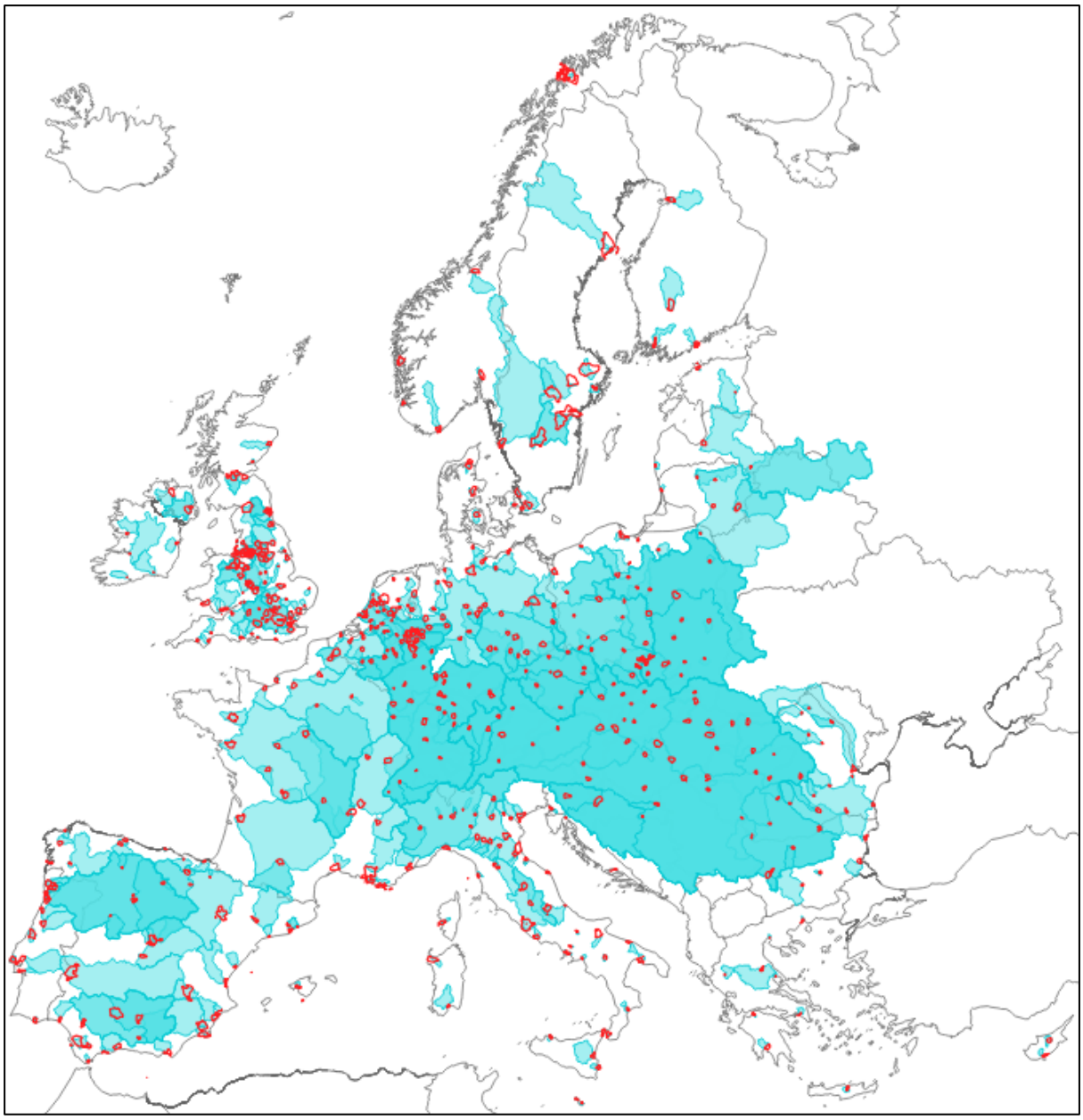

Figure 38: All 571 cities (red dots) with their respective basins.

2.7.3 Results

For the low impact scenario most cities show either no change or a reduction in Q10, with increases in Q10 (up to 30%) mainly in the UK, Belgium, Netherlands and Scandinavian countries (see Figure 39). The medium scenario shows a north-south divide with increases in Q10 in the north, especially high in the UK and Scandinavia (up to a 70% increase in Q10) while most of the south of Europe still sees no change or decreases. Only in the high impact scenario does most of Europe show increases in Q10 (up to 230%) with the most affected areas

being the UK, Norway and the north west of Iberia. Most of the Mediterranean region still sees no increases in Q10.

This wide range of possible future changes for most of Europe reflects the variety of results presented in previous pan-European studies that used climate ensembles to assess changes in flood severity (Alfieri et al., 2015; Dankers and Feyen, 2009; Rojas et al., 2012; Roudier et al., 2016). Although it is important to note that our simple regression model does not account for the effects of snowpack reduction and therefore floods due to snowmelt are not accounted for. This means we cannot add to the discussion of the interplay between reductions of snowpack with simultaneous increases in rainfall which may be important for northern latitudes and high elevations.

The British Isles are particularly at risk of an increase in river flooding with 43% of cities showing an increase in river flooding in the low impact scenario. In the medium scenario every city sees an increase in Q10 of at least 16% (27% in the high scenario). The mean change in these cities for the medium (high) scenario is 32% (55%) increase in Q10 and the maximum is 70% (118%) increase. North west Iberia also shows a strong increase in Q10 (up to 125%) but only in the high scenario. The two Norwegian cities considered (Trondeheim and Kristiansand) also show increases in all scenarios and a large increase in the high scenario (50% and 132%) but since snowpack is not accounted for in our methodology this result may not translate into an increase in real Q10.

Dankers and Feyen (2009) identified natural variability/internal variability in the climate models as the major cause of discrepancy of future changes in Q100 calculated using 30 year intervals. To minimize this source of uncertainty we used a longer period of analysis (50 year intervals) in order to characterize the climate better (not being as susceptible to decadal changes) and used a shorter return period for flood calculations (Q10 instead of Q100). Also, recalling that Dankers and Feyen (2009), Rojas et al. (2012), Alfieri et al. (2015) and Roudier et al. (2016) all find that for parts of Europe there is no agreement in the sign of projected change between scenarios, we argue that understanding the range of possible futures is more important than analysing the mean or median of a particular subset of possible futures.

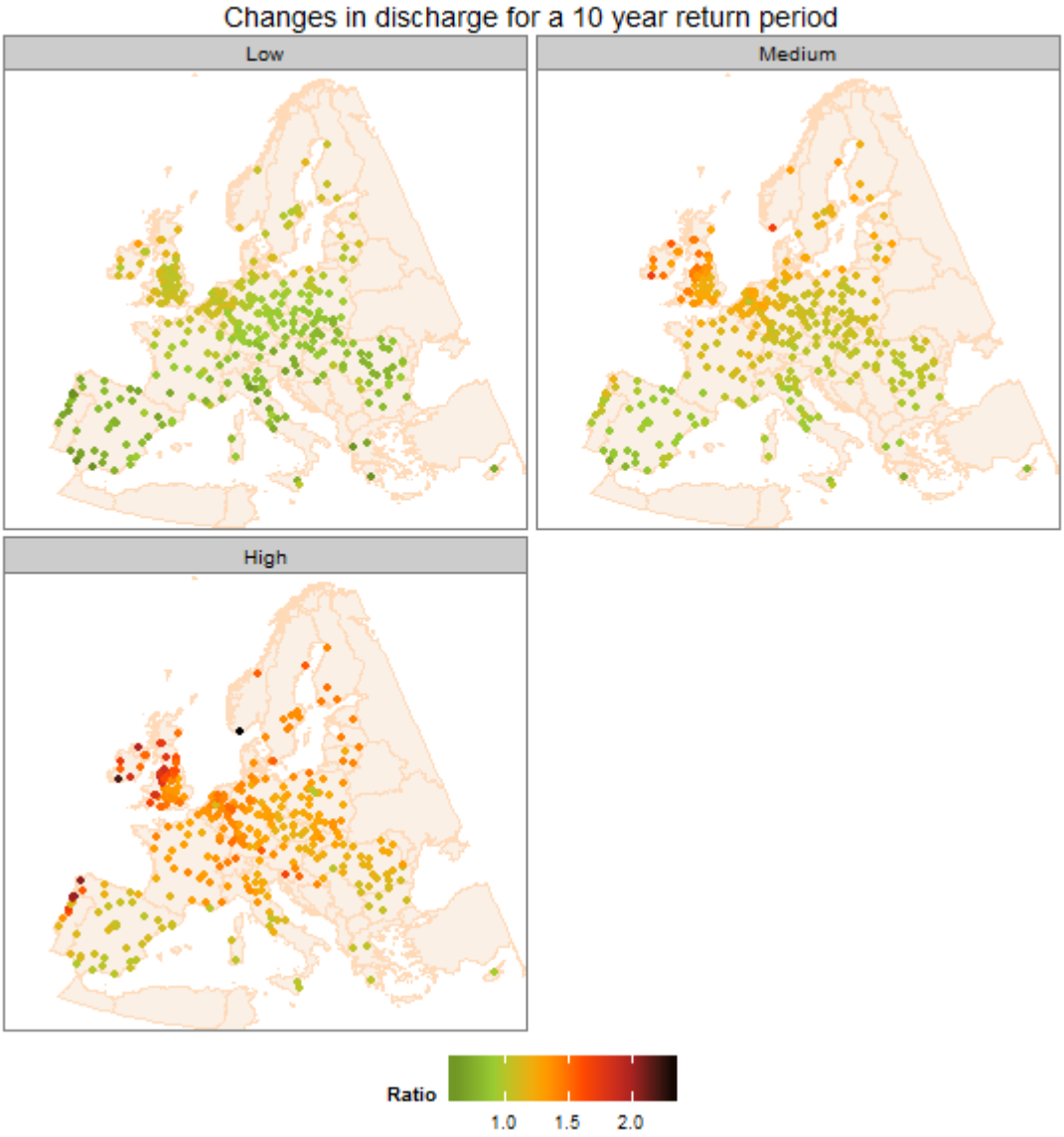

Figure 39: Changes in Q10 (calculated as a ratio: future Q10 divided by historical Q10) for each European city. The changes are shown for a low (10th percentile) impact scenario (top-left), a medium (50th percentile) impact scenario (top-right) and a high (90th percentile) impact scenario (bottom) for each European city. The changes are calculated between the historical period (1951-2000) and the future period (2051-2100).

2.8 Coastal flood hazard

Broad scale coastal flood risk analysis is reported in detail by Boettle et al. (2016) as part of RAMSES WP1.2. The key stages of the method involved derivation of exposure and hazard functions by:

- Processing elevation data to derive the relationship between storm surge level and inland flood extent.
- Relate land cover to land use to identify residential, commercial, industrial and agricultural zones.
- Identify a suite of land use damage functions
- Integrate damage functions with the flood maps to build depth-damage relationships for each urban area.
- Climate scenarios for sea level rise can be applied to increase the depth of flooding for given storm surge return periods.

2.9 Hazard scoring

2.9.1 Overview of the data model

As shown on previous sections, most of the **hazard indicators** used in the risk analysis are expressed as relative changes in intensities or probabilities of occurrence of specific climate –driven events. Uncertainty in climate projections has been managed by providing three alternative impact scenarios for each of these indicators:

- **Heatwave index:** change in the percentage of heatwave days (i.e. difference between future and historical percentage of heatwave days); and changes in maximum temperature of heatwaves (i.e. difference between the maximum temperature felt during a heatwave in the future period and in the historical period).
- **Drought stress index:** change in the probability for any given month in the future to be above the maximum historical DSI-12; and, the change factor of maximum drought, i.e., future maximum DSI-12 divided by historical maximum DSI-12.
- **Pluvial flood index**: change in the percentage of city flooded using 0.9, 1.2 and 1.5 change factors for hourly rainfall for 10 year return period (i.e. future percentage of city flooded divided by historical percentage of city flooded), generated using a sensitivity analysis
- **Fluvial flood index**: change in the 10 year return period of annual maximum daily discharge (Q10).

This was supplemented by one additional hazard index:

- **Intensity of the Urban Heat Island (UHI) effect** based on 8-day averaged daily mean land surface temperature (LST, i.e. skin surface temperature) data during summer months (June-August) 2006-2013. Data from MODIS (MOD11A2, MYD11A2) datasets (Zhou et al., 2013). This can be considered a compounding factor to changes in heatwave frequency.

Code	Description	Threat[5]	Source
Hazard indicators			
HWDAYSUNEWI	Relative change on the percentage of days classified as heatwaves days between 1951-2000 and 2051-2100 for low, medium and high impact scenarios	HW	Newcastle University
HWMAXUNEWI	Change in the maximum daily maximum temperature between 1951-2000 and 2051-2100 (units: ºC) for low, medium and high impact scenarios	HW	Newcastle University
UHIPIKI	UHI intensity based on 8-day averaged daily mean land surface temperature (LST, i.e. skin surface temperature) data during summer months (June-August) 2006-2013. Data from MODIS (MOD11A2, MYD11A2) datasets (Zhou et al., 2013).	HW	PIK
DSI12RCUNEWI	Relative change on the DSI-12 indicator (2051-2100 over 1951-2000) for low, medium and high impact scenarios	DR	Newcastle University

[5] DR: Droughts
FLF: Fluvial Flooding
FLP: Pluvial Flooding
FLC: Coastal Flooding
HW: Heatwaves

DSI12PROBUNEWI	Probability for any given month in the future to be above the maximum historical DSI-12 indicator (2051-2100 over 1951-2000) for low, medium and high impact scenarios	DR	Newcastle University
FLPUNEWI	Changes in the percentage of city flooded using 0.9, 1.2 and 1.5 change factors for hourly rainfall for 10 year return period (i.e. future percentage of city flooded divided by historical percentage of city flooded)	FLP	Newcastle University
FLFUNEWI	Changes in the 10 year return period of annual maximum daily discharge (Q10)	FLF	Newcastle University

Table 4: Hazard indicators included in the RAMSES data model.

2.9.2 Generation of aggregated hazard indices

When appropriate, the aggregation of the individual hazard indicators considered within each impact chain was performed basing on a multiplicative utility function – a so-called *deprivation index* –. This is an approach to data aggregation commonly used by previous indicator-based vulnerability assessments (Balica et al., 2009; Charlotte Vinchon et al., 2011; Füssel, 2009).

In general terms, geometric aggregation of indicators into composed indexes is considered a better alternative to arithmetic aggregation because its outputs are more robust across different weighting, standardisation and normalisation methods commonly used for data pre-processing (El-Zein and Tonmoy, 2015; Merz et al., 2013; Tonmoy et al., 2014). Additionally, the multiplicative aggregation minimises compensability of scores more than the additive option (Guillaumont and Simonet, 2011; Nardo, M. et al., 2008; Nardo et al., 2005). This is considered to be an important advantage of the geometric aggregation approach, considering that with the additive method a deficit in one dimension could be offset by a surplus of identical magnitude in another (El-Zein and Tonmoy, 2015; Nardo, M. et al., 2008). More complex geometric aggregation methods, such as the reversed geometric average (Guillaumont and Simonet, 2011) or the Condorcet approach based on pairwise comparisons (El-Zein and Tonmoy, 2015), can reduce compensability even further, but the use of these sophisticated methods increase the difficulty for communicating results.

Hazard indices, *H*, are thus estimated for each impact chain using the following formula:

$$H_{ct} = \sqrt[I]{h_{c1} \times h_{c2} \times \ldots \times h_{cI}} \quad (2.1)$$

or, generically:

$$H_{ct} = \prod_{i=1}^{I} h_{ci}^{1/I} \quad (2.2)$$

where H_{ct} = hazard score for city *c* under climate threat *t*; h_{ci} = value of hazard factor *i* in city *c; I* = total number of hazard factors (i.e. indicators) considered.

All hazard scores were standardised and re-scaled (H'_{ct}) applying the methods described in Section 4.5, prior to aggregation with the exposure and vulnerability indices to calculate risks. Results for all EU Urban Audit cities are presented in Figure 40 to Figure 41.

The maps in Sections 2.9.3 - 2.9.4 all use the following legend:

HAZARD
- Higher hazard (> quantile 0.75)
- Medium to higher hazard (Median to quantile 0.75)
- Medium to lower hazard (quantile 0.25 to Median)
- Lower hazard (< quantile 0.25)

2.9.3 Combined heatwave hazard index

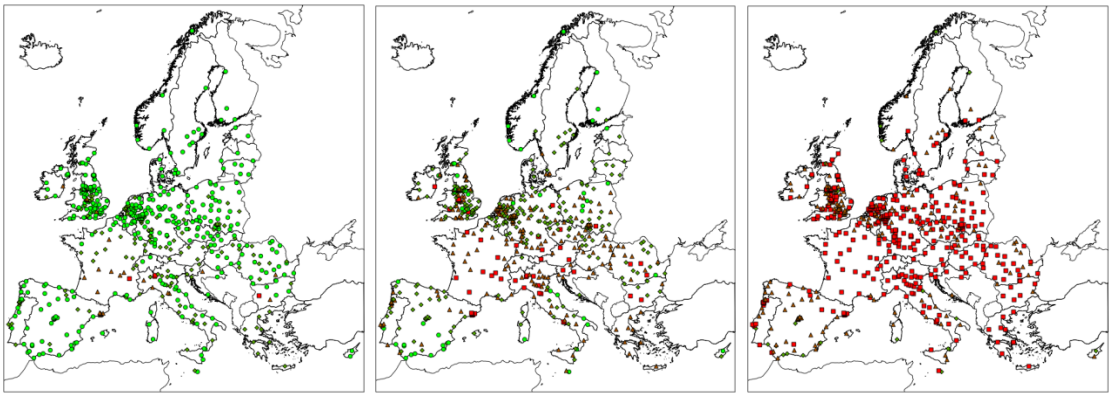

Figure 40: Combined heatwave hazard index for the low (left), medium (centre) and high (right) impact scenarios.

The heatwave hazard index shown in Figure 40 combine information on (1) the change in the percentage of heatwave days (i.e. difference between future and historical percentage of heatwave days); (2) the changes in maximum temperature of heatwaves (i.e. difference between the maximum temperature felt during a heatwave in the future period and in the historical period divided), and; (3) the Intensity of the Urban Heat Island (UHI) effect based on 8-day averaged daily mean land surface temperature during summer months. Whereas the 1st and 2nd indices combined in the composed heatwave index are produced under climate change scenarios, the indicator on UHI intensity is derived from observed data.

Interestingly, urban areas such as Milano, Monza, Grenoble, Paris, Bordeaux, London and Sofia show combined heatwave indexes that are persistently high across all scenarios. This is mostly related to the strong UHI effect in these areas. In turn, other cities from the southernmost cities from the Iberian Peninsula and some Mediterranean islands show low hazard scores across all scenarios. This is motivated by a comparatively inferior aggravation of the changes in maximum temperature of heatwaves across scenarios as well as by a much lower UHI effect, due to the arid context where these cities are located (e.g. in practical terms the absence of vegetation in the peri-urban area makes the UHI unperceivable in a number of cities located in the lower latitudes of the EU. Many of these cities even show a negative thermal gradient during the summer months, meaning that temperatures in the city centres are on average cooler that in the surrounding non-urbanised areas, as discussed in Section 5.1 below).

2.9.4 Combined drought hazard index

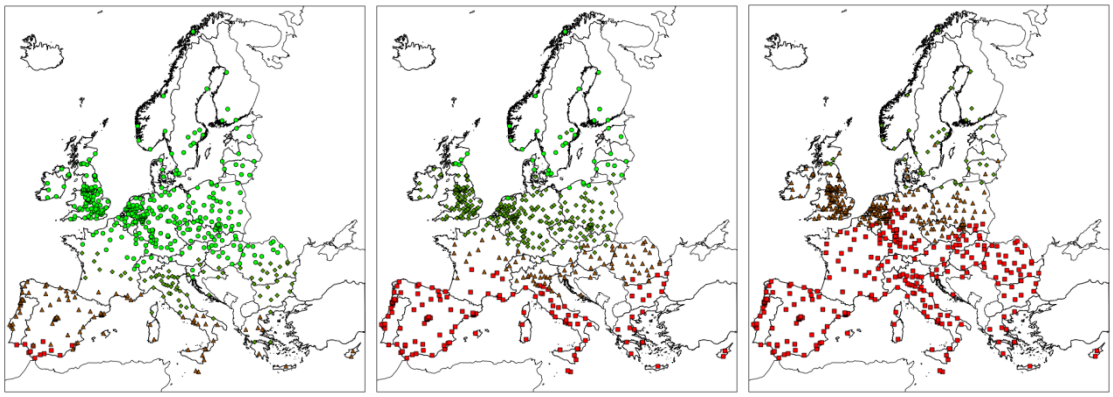

Figure 41: Combined drought hazard index for the low (left), medium (centre), and high (right) impact scenarios.

The drought hazard index shown in Figure 41 combines the scores for (1) the relative change on the DSI-12 indicator and (2) the probability for any given month in the future to be above the maximum historical DSI-12 indicator for low (left), medium (centre) and high (right) impact scenarios. Looking across scenarios, it is clear that drought hazard under climate change projections should be considered a priority in those cities located in the Mediterranean macro-region. This is particularly true if one considers that this is an area where the economic activity is highly dependent on water abstraction, both for irrigated agriculture as well as for tourism-related activities.

3 Climate change exposure assessment

Simply put, assessing exposure to climate change at this scale of analysis entails determining the total amount of people and assets potentially threatened by a given climate change-driven hazard within each urban area. Relying on the hazard data produced on Section 2, this project has followed different analytical choices to derive exposure information, as described below.

3.1 Data model

The **exposure indicators** used in this research aim to quantify as far as possible the total amount of population or assets that could be potentially affected by the climate impacts driven or intensified by climate change. In some cases the threats considered in this study show a spatially explicit distribution within cities (e.g. flooding), whereas in other cases the spatial variability at this scale of analysis is null or negligible (e.g. heatwaves and droughts). In the latter situation indicators such as the total population and assets included within cities have been used as exposure proxies. In the former situation, three alternative data scenarios have been faced: (1) whenever spatially explicit information on hazard distribution was available (e.g. coastal flooding), an estimation of the area potentially affected within each city was produced basing on GIS overlays (Boettle et al., 2016); (3) whenever the information allowed to derive some spatial data, but these were not considered to have enough quality for a detailed geographically-explicit assessment (e.g. pluvial flooding), it was assumed that population and assets are evenly distributed over the urban area as a preliminary estimate; (3) whenever spatially explicit information for hazards was not available (e.g. fluvial flooding), no exposure indicator was considered in the comparative evaluation of risks.

Table 5 lists the exposure indicators that have been considered within our risk analysis:

Exposure indicators			
Code	**Description**	**Threat[6]**	**Source**
DE1001V	Population on the 1st of January (last figure available 2004 to 2013), total	HW, DR	Urban Audit
SA1001	Number of conventional dwellings	HW, DR	Urban Audit
EC2021V	All companies	DR	Urban Audit
PEOFLPTECI	Estimated additional population potentially exposed to flooding using 0.9, 1.2 and 1.5 change factors for hourly rainfall for 10 year return period	FLP	Tecnalia R&D basing on data provided by Newcastle University and Urban Audit
COFLPIKI	Coastal flooding. Percentage of the city cluster potentially flooded due to a 100 year coastal storm surge event (Boettle et al., 2016).	FLC	PIK - Postdam Institute for Climate Impact Research

Table 5: Exposure indicators included in the RAMSES data model.

[6] DR: Droughts
FLF: Fluvial Flooding
FLP: Pluvial Flooding
FLC: Coastal Flooding
HW: Heatwaves

3.2 Exposure scoring

The exposure indices, *E*, are estimated for each impact chain using the following formula:

$$E_{ct} = \sqrt[J]{e_{c1} \times e_{c2} \times \ldots \times e_{cJ}} \quad (3.1)$$

or, generically:

$$E_{ct} = \prod_{j=1}^{J} e_{cj}^{1/J} \quad (3.2)$$

where E_{ct} = exposure score for city *c* under climate threat *t*; e_{cj} = value of exposure factor *j* in city *c; J* = total number of exposure factors (i.e. indicators) considered;

All exposure scores were subsequently standardised and re-scaled (E'_{ct}) prior to aggregation with the hazard and vulnerability indices to calculate risks, as shown in Section 4.5 below. Results for all EU Urban Audit cities are presented in Figure 42 to Figure 44.

The maps shown in Figure 42, Figure 43 and Figure 44 (right) all use the following legend:

EXPOSURE
- Higher exposure (> quantile 0.75)
- Medium to higher exposure (Median to quantile 0.75)
- Medium to lower exposure (quantile 0.25 to Median)
- Lower exposure (< quantile 0.25)

3.2.1 Combined exposure indices to heatwaves and droughts

Figure 42 includes a cartographic representation of the combined exposure indices to heatwaves (left) and droughts (right).

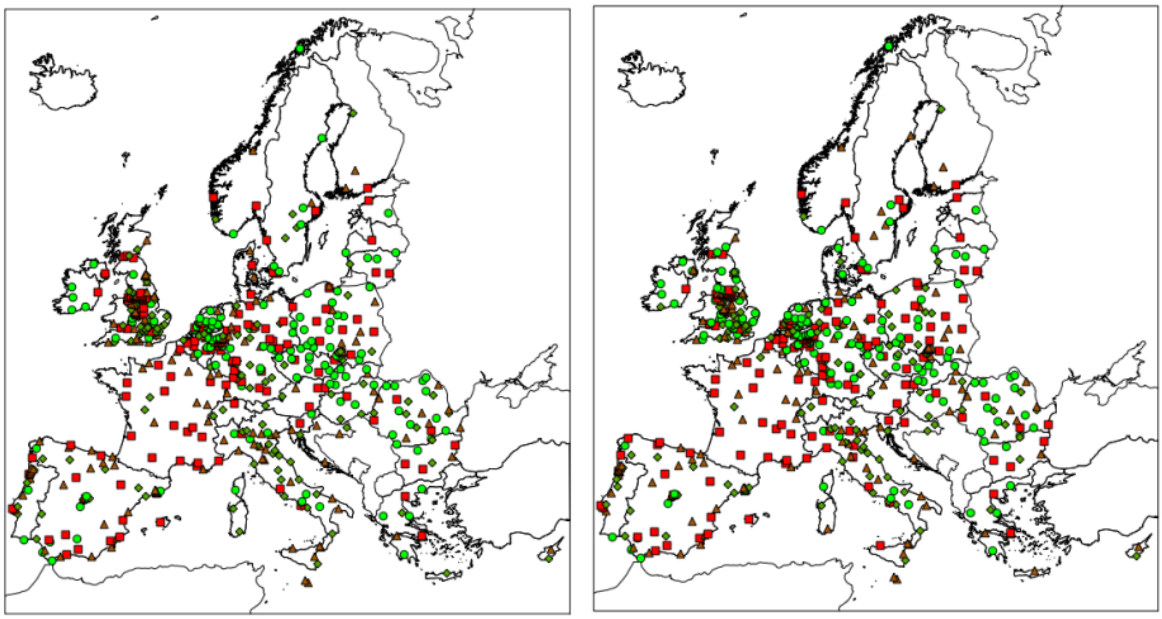

Figure 42: Combined exposure indices to heatwaves (left) and droughts (right).

Given the spatial level of our analysis, and considering the scale at which heatwaves express and propagate, exposure to this hazard is considered to equally affect all population and assets within cities, without performing further evaluations based on spatially-explicit modelling tools. Accordingly, the heatwave exposure index represented in the map to the left in Figure 42 combines information on the demographic size of cities – total population – and assets – number of conventional dwellings –. Both indicators are combined in a composite index illustrating the relative position of European cities in terms of their potential exposure to heatwaves.

The map to the right in Figure 42 provides a very similar indicator for droughts. In this case the exposure index represents a tri-dimensional construct including the number of companies within each city, alongside the total population and conventional dwellings. As claimed on Section 3.1 above, the inclusion of the economic dimension is related to the nature of this impact chain. This is because it is expected that the growing drought episodes expected during this century in many parts of Europe will affect urban comfort to the same extent that they will disturb economic activity within cities (Knutson et al., 1998; Stefano et al., 2015).

Essentially, both heatwave and exposure indices show a similar spatial distribution pattern across the EU. Larger urban areas are more exposed to both hazards, as they host more population and more assets potentially affected by these phenomena. This seems an obvious consequence of the very nature of both hazards and the impact transfer mechanisms that operate within these impact chains. This characteristic should nonetheless be accepted and considered within a pan-European policy framework as a relevant criterion to set priorities and allocate resources.

3.2.2 Exposure index to pluvial floods

The standardised exposure index to pluvial floods shown in Figure 43 is based on an estimate on the additional population potentially exposed to flooding using 0.9 (left), 1.2 (medium) and 1.5 (right) change factors for hourly rainfall for 10 year return period.

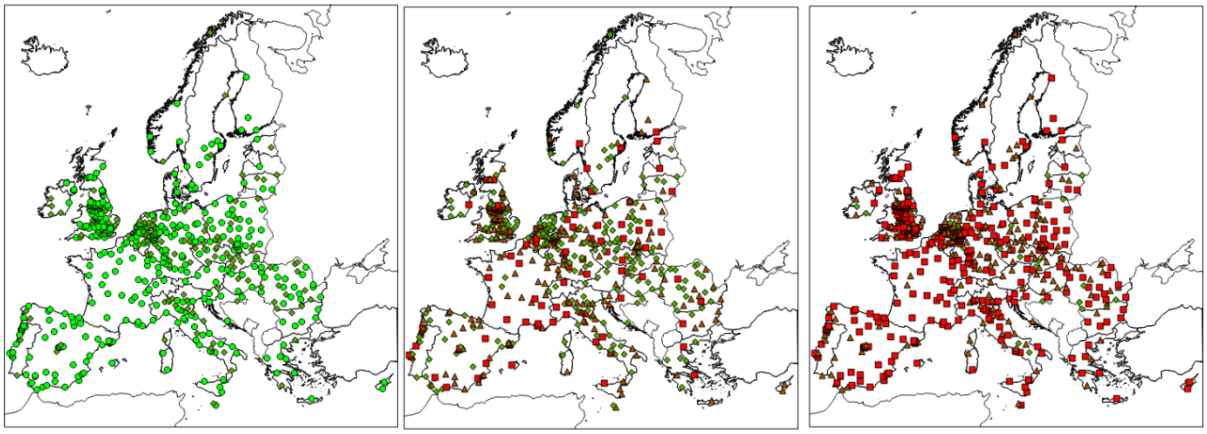

Figure 43: Exposure index to pluvial floods for the low (left), medium (centre), and high (right) impact scenarios.

The fluvial floods exposure index was derived by, firstly, calculating the extra area potentially affected by pluvial floods assuming a homogenous distribution of impacts over the entire urban area –

i.e. relative changes were multiplied by the total area of cities to calculate the extra area potentially flooded within each city – and, secondly, calculating the extra population affected based on average population densities – thus assuming a homogeneous distribution of population within the entire city area –. These are bold assumptions that do not preclude the utilization of the standardized index as a relative indicator of urban exposure to pluvial floods within a comparative risk analysis, if one considers that the bias introduced by the assumptions are equally applied to all the observations.

Similarly – and coherently – with the structural distribution of pluvial flood hazards shown in Figure 27, the standardised exposure index presented in Figure 43 shows a rather stable and generalised increase of urban exposure to pluvial floods under the three low (left), medium (centre) and high (right) impact scenarios. Most cities in the high impact scenario (right) are classified in the upper quartile (>0.75). Reversely, virtually all cities in the low impact scenario (left) are classified in the lower quartile (<0.25).

Thus the most expressive distribution of cities in terms of potential exposure to pluvial floods can be found within the medium impact scenario (Figure 43, centre). Although a higher variability can be easily recognised under this scenario, this variability does not seem to follow a well-defined spatial pattern. Broadly speaking, it could be claimed that drawing a diagonal line across Europe from the British Isles to the Strait of Sicily, those cities located to the North of this line show comparatively higher exposure rates to pluvial floods that those located to the South. This seems, however, a rather weak spatial pattern that could be biased by the methodological shortcomings of the pluvial hazard calculation described on Section 2.7 above, as well as by the assumptions made in the exposure analysis itself.

3.2.3 Exposure index to coastal floods

Contrary to previous exposure indices, the indicator informing on potential exposure to coastal floods shown in Figure 44 (right) is based on the outputs provided by a spatially-explicit model provided by RAMSES Deliverable 1.2: Development of a library of impact functions and general uncertainty measures, Part II: Library of Flood Damage Functions and Protection Measures (Boettle et al., 2016), which is also shown in Figure 44 (left). The flooding model was run for one single impact scenario.

This indicator ranks cities according to the potentially flooded area under a 100 year coastal storm surge event. Although the derivation of potentially flooded areas is based on a digital elevation model and thus no specific information about existing flood protection measures – such as existing dikes – have been considered, this proxy provides a harmonised and comparable measure of the relative level of exposure that the major coastal urban areas in Europe.

The maps shown in Figure 44 prove that highest exposure levels correspond to the urban areas located in the Atlantic Basin, from the Baltic to the Gulf of Biscay, across the North Sea and the British Isles, and affect in particular the coastal cities of the Netherlands (with around 80% of the city cluster potentially flooded due to a 100 year coastal storm surge event), alongside the cities of Bremerhaven in Germany and Le Havre in France. Both these cities have more than 20% of their areas potentially flooded due to a 100 year costal storm surge event.

In the Mediterranean the most exposed urban areas are those located over the Tirrenian-Ligurian seas (in particular Livorno, with more than 10% of the urban area potentially flooded due to a 100 year costal storm surge event) and the North Adriatic sea, in particular the cities of Rimini (around 10% of the urban area potentially flooded due to a 100 year costal storm surge event) and Venice, with 37% of the city cluster potentially flooded due to a 100 year costal storm surge event.

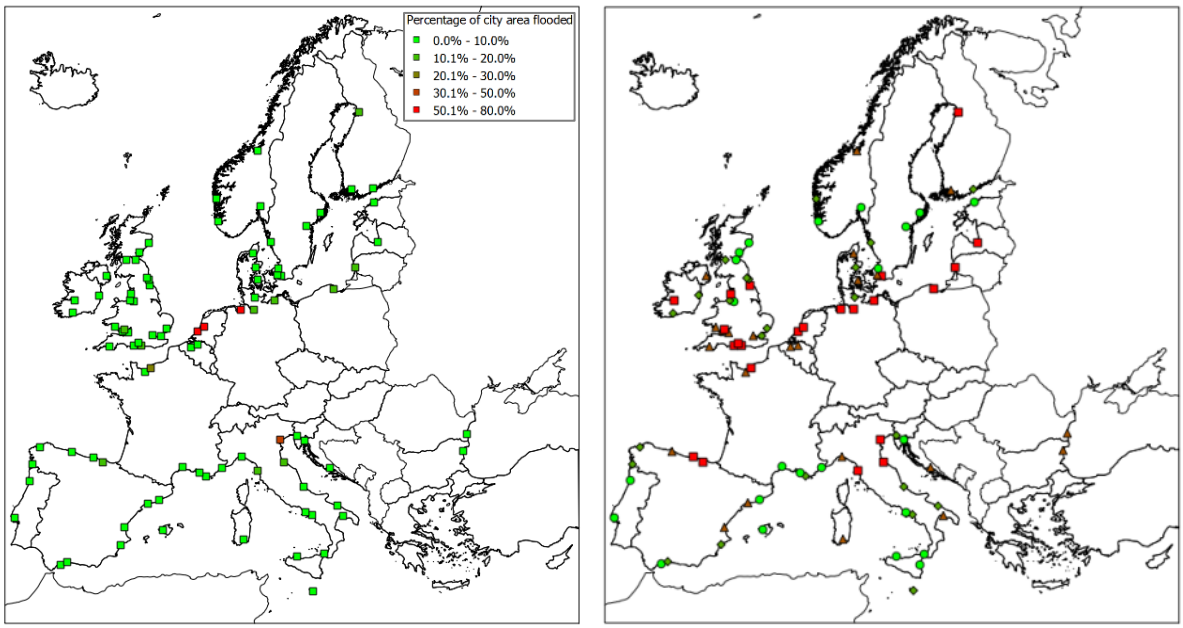

Figure 44: Percentage of the city cluster potentially flooded due to a 100 year coastal storm surge event, according to Boettle et al. (2016) *(left), and derived exposure index to coastal floods (right).*

4 Indicator-based Vulnerability Assessment

An Indicator-based Vulnerability Assessment (IBVA) for European cities enables consideration of the potential impacts caused by changes in the climate change hazards presented in Section 2. It helps to shed light on the key challenges that specific groups of cities face from this perspective, in order to better deal with the expected impacts at a European level. This knowledge is a necessary step towards the development of effective EU policies for urban adaptation (EEA, 2012). In order to support the development of successful and cost-effective adaptation strategies such policies require additional integrated and cross-sectoral climate change vulnerability assessments that identify, characterize and cluster cities according to the magnitude of the climatic hazards faced and their levels of exposure to such potential threats, as well as their intrinsic sensitivity to them and the degree of preparedness that cities have to deal with climate change (DG Environment, 2014).

4.1 Methodology

The high level indicator-based vulnerability assessment methodology is based on a sequential implementation of a number of analytical steps shown in Figure 45.

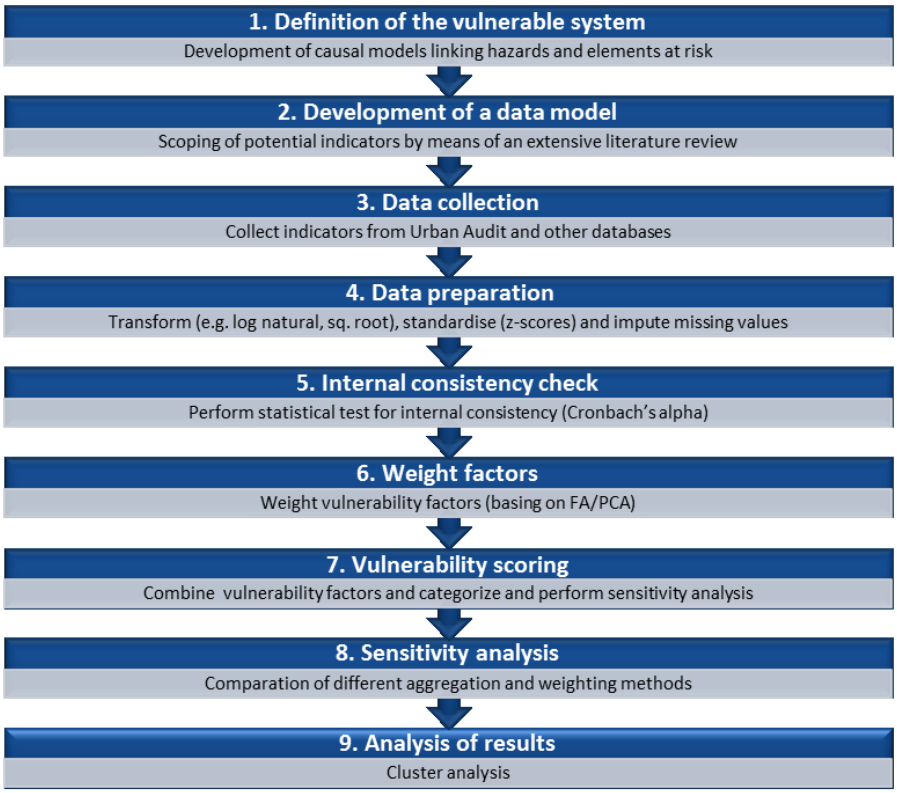

Figure 45: Analytical sequence followed in our indicator-based vulnerability analysis[7].

[7] Adapted from (Tapsell, Penning-Rowsell, Tunstall, & Wilson, 2002; Wolf & McGregor, 2013)

The analytical sequence starts with the characterisation of the different impact chains – i.e. the causal relations linking the potential impacts and its receptors –. It then continues with the development of a data model capturing the different system elements of the impact chains. The sequence follows with the generation of a well-structured database including comparable indicators. The data are subsequently classified and pre-processed for statistical soundness. Additionally, an internal consistency check based on statistical measures of reliability is also performed.

The first analytical step deals with the reduction of redundancy among vulnerability indicators. This has been achieved through the utilisation of weights computed through statistical data reduction techniques. The vulnerability scores were subsequently generated as a geometric aggregation of the weighted vulnerability indicators.

A sensitivity assessment was performed on vulnerability scores. Eventually, cities were grouped on statistically homogeneous clusters to ease the interpretation of results. Vulnerability scores were combined later on with hazard and exposure data, delivering a risk index for all cities under each impact chain, presented in Section 5.

This analytical sequence has been applied on the 571 cities included in the GISCO Urban Audit 2004 Database[8] for heatwaves, droughts and pluvial floods. In the case of coastal flooding the assessment was performed on the 92 coastal cities included in the GISCO Urban Audit 2004 Database for which exposure data were available. In the case of fluvial flooding the assessment was performed for the 365 Urban Audit cities with water courses with at least 500km2 catchment area (see Section 2.7.2 above for additional details). The analysis was performed utilising the R software for statistical computing v3.1.3.

4.2 Definition of the vulnerable system

Typically, indicator –based vulnerability assessments rely on the identification of a number of factors shaping the vulnerabilities to climate change threats within the specific domains of the urban systems that are being analysed, like e.g. certain areas, communities or social groups, or specific sub-systems the built environment, the infrastructures or other components (Birkmann and Wisner, 2006; Birkmann et al., 2013; Burton, 2012; Carreño et al., 2007; Carter et al., 2014; Charlotte Vinchon et al., 2011; Cutter et al., 2003, 2009; Guillaumont and Simonet, 2011; Preston, 2012; Villagrán-De-Leon, 2006). Kienberger et al. (2013) have recently proposed a framework to characterise climate change vulnerability assessments according to spatial, time and dimensional criteria.

The literature provides a number of inventories of explanatory factors that potentially increase or alleviate the impacts of climate change within any of the complex socio-environmental components that define complex urban systems (Cutter et al., 2008, 2010; Jacobs et al., 2012; Schauser et al., 2010). These explanatory factors were organised in different categories and represented in a series of schematic figures summarising the causal structure of vulnerability and risk within each impact chain. Such representations of the vulnerable systems were inspired by Downing's 'causal chain of hazard development' (Downing, 1990) and Wisner and Blaikie's 'Pressure and Release model' (Wisner et al.,

[8] The dataset was downloaded in spring 2014.

1994). These inputs were used as a reference framework for developing 'RAMSES causal model of climate change risk construction', or more succinctly, 'impact chains'.

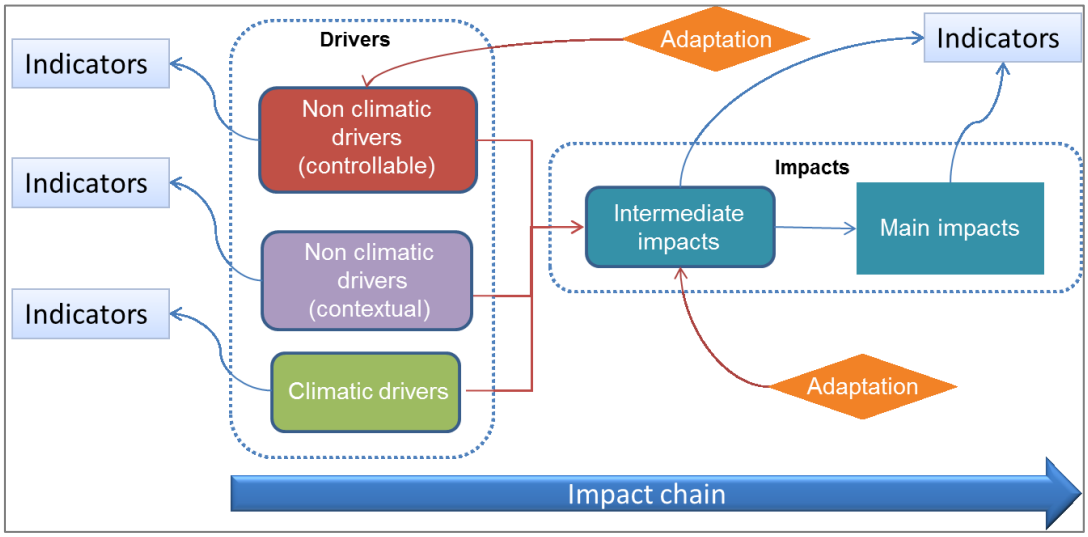

Figure 46: A generic impact model representing the causal structure of vulnerability and risk under climate change.

4.3 Data model

A comprehensive literature review, presented in Appendix B, allowed researchers to produce a generic inventory of indicators that could be used within the assessment. In total, 18 generic categories and more than 90 different types of indicators could be identified. Table 6 summarises these findings:

Category of indicators	No. of papers
Social structure	
(DEM) Demographic structure, dynamics, health status (life expectancy, age dependency ratios, fertility rates, population growth, family and household structure, nutrition, special needs populations, etc.)	36
(EDU) Education, skills and knowledge (Training, literacy, enrolment ratios, knowledge of foreign language, community knowledge, etc.)	24
(ETN) Race and/or ethnicity (immigration rates, community cohesion, language barriers, etc.)	6
Governance	
(RIG) Human rights (including minorities and press freedom)	2
(GEN) Gender status (gender ratios, gender income equality, entitlement and participation of women in public life)	10
(GOV) Quality of government (including participation of citizens, social organizations and institutions, community values, political stability, corruption, trust in authorities, volunteering, etc.)	25
(POL) Plans, policies and instruments (policies, tools, incentives and disincentives, zoning and building standards, conservation programmes, adaptation measures/plans, environment expenses, disaster relief systems, early warning systems, etc.)	15
(AWA) Risk perception and social behaviour (e.g. recycling rates, awareness, risk training, etc.)	11
Socio-economic status	
(INC) Socio-economic conditions and entitlement (GDP per capita, income, rent per capita, inequality, poverty, social cohesion, homeless, occupation in low-income activities, unemployment and related indicators)	40
(ECO) Macro-economic indicators (GDP, budget surplus, financial assets, debt payments, investments, international trade, business rates, economic structure, economic diversity, etc.)	17
(INS) Risk transfer schemes (including social security systems, social transfers, insurance and social-oriented expenditures)	10

(HOU) Access to housing (ownership, renters, median home loan repayment, etc.)	3
Access to technology	
(TEC) Technology (R&D expenditure, patents, human resources in R&D, etc.)	11
Built environment	
(INF) Infrastructures (availability, quality or lack thereof, including characteristics of networks, medical facilities, etc.)	28
(BUI) Characteristics of the building stock (housing typologies, densities, etc.)	14
Exposed assets[9] (transport density, km of coastline, exposed population, location of hot spots, accessibility indexes, isolation of communities, etc.)	24
Natural capital and ecosystem services	
(RES) Ecosystem services (land use, resource productivity, agricultural production, fishing resources, etc.)	25
(CON) Environmental status (environmental degradation, emissions, endangered species, etc.)	9
Historical records[9]	
Past events (Number of disasters and catastrophic events, including personal and economic damages)	6
Climatic indices (observed climatic trends)	30

Table 6: Categories of indicators used in literature to assess local vulnerability to climate change.

The Scoping Diagram shown in Figure 47 provides a visual representation of the critical dimensions considered in our IBVA.

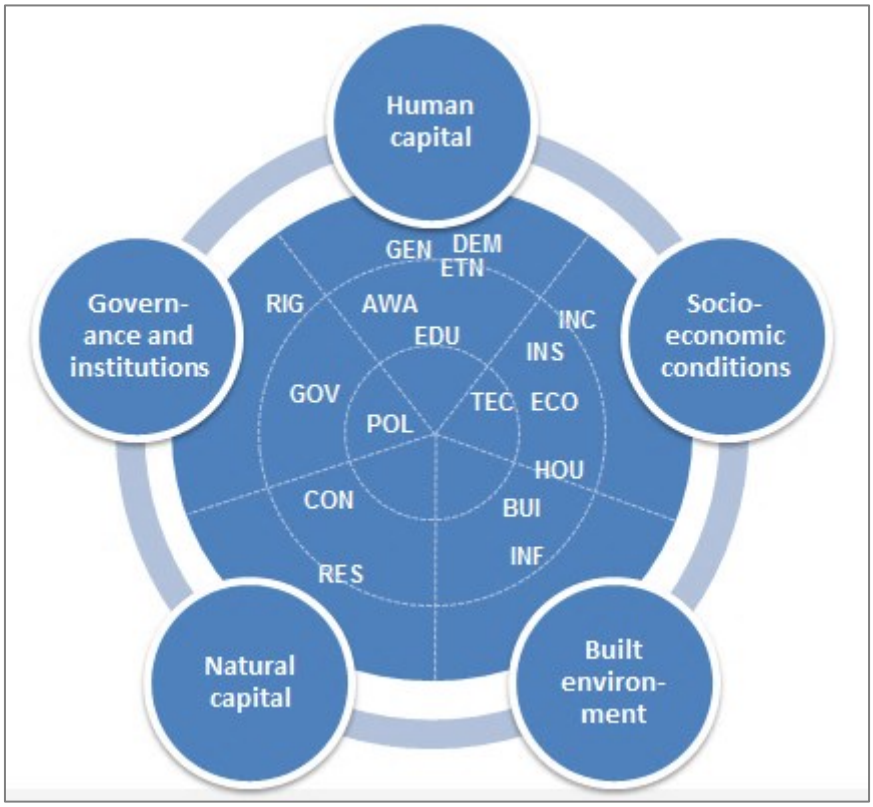

Figure 47: Ramses scoping diagram for the vulnerability dimension of risk.

[9] These dimensions are not considered in our data model as part of the vulnerability component.

4.4 Data collection

The vulnerability indicators illustrate the characteristics of the potential receptors of the climate change impacts in terms of their sensitivity to such impacts and their "capacity to resist, cope or adapt to them". Vulnerability indicators have been thus classified into two separate groups influencing vulnerability in the opposite direction, namely 'sensitivity' and 'adaptive capacity'. All the vulnerability indicators have been included in one of these specific categories depending on a simple dichotomous classification criterion: those indicators that according to the literature are thought to unequivocally increase the vulnerability of the exposed elements as their value/magnitude increase have been classified as sensitivity indicators (e.g. as the share of elder population increase, cities become more vulnerable to heatwaves); reversely, the indicators that reduce vulnerability as their value/magnitude increase have been classified as adaptive capacity indicators (e.g. larger shares of green/blue areas are thought to reduce urban vulnerability to heatwaves, as both land cover classes increase the thermal comfort of the surrounding areas).

Besides, as a general criterion for redundancy reduction, indicators that are built basing on the same background variables and characterise contradictory or mutually exclusive socio-economic, environmental or social trends (e.g. share of soil sealed area vs share of total green/blue area) have been included only once in the data model, either within the sensitivity or within the adaptive capacity category, as relevant.

In all cases data coverage and comparability, rather than precision and accuracy, have been the main selection criteria. The data coverage threshold for the vulnerability indicators has been set on a 50% of cities included. In order to increase data coverage as far as possible a flexible approach was adopted with regard to temporal harmonisation. In practice, this implied that the indicators were collected for the last available year over the period 2004 to 2014.

Socio-demographic indicators of exposure and vulnerability drew heavily on existing datasets, many from the Urban Audit database. This database provides a good comparable set of indicators with European coverage including basic information on cities, and it has been frequently used by previous climate change vulnerability assessments performed at this scale (EEA, 2012).

Some of the variables included in the Urban Audit database were combined to each other or with other variables to produce new indicators. Such newly developed indicators used within the vulnerability assessment are listed below:

- **Population growth rate** over the period 2004-2012, basing on DE1001V - Population on the 1st of January, total, retrieved from Urban Audit.
- **Population density**: total resident population per square km. Indicator built basing on GISCO GIS layers and Urban Audit population data: DE1001V - Population on the 1st of January, total.
- **Health status:** Number of deaths per year under 65 due to diseases of the circulatory or respiratory systems per 1000 inhabitants, based on Urban Audit data: SA2013V - Number of deaths per year under 65 due to diseases of the circulatory or respiratory systems and DE1001V - Population on the 1st of January, total.
- **Education:** Proportion of working age population qualified at level 5 or 6 ISCED, basing on Urban Audit data: TE2031V - Persons (aged 25-64) with ISCED level 5 or 6 as the highest level of education and population data: DE1058V - Population on the 1st of January, 25-34

years, total; DE1061V - Population on the 1st of January, 35-44 years, total; DE1064V - Population on the 1st of January, 45-54 years, total; DE1025V - Population on the 1st of January, 55-64 years, total.

- **Economic diversification:** Shannon index of economic diversity, basing on Urban Audit data on Employment (jobs) in NACE sectors (EC2008V to EC2038V).
- **Use of water resources:** Water consumption (m^3 per year per capita), basing on Urban Audit data: EN3003V - Total use of water - m^3 and DE1001V - Population on the 1st of January, total.

A major limitation in this indicator-based vulnerability assessment has been the scarcity of comparable data needed to characterise European cities along some specific dimensions of vulnerability. This is a limitation frequently mentioned by many of the indicator –based vulnerability assessments reviewed in this work (Charlotte Vinchon et al., 2011; Jacobs et al., 2012; Jeremy Carter et al., 2012).

In particular, there is a lack of comparable data assessing the degree to which cities and citizens are aware and are already taking specific steps towards climate change adaptation. As a result, some proxy indicators providing relevant information on this dimension were produced within our assessment. City commitment to adapt was verified through the participation in on-going initiatives such as Mayors Adapt. A proxy indicator on the potential degree of awareness within cities was produced basing on recursive Internet searches[10], thanks to the functionality of Google custom search API, as shown below:

- **City participating in Mayors Adapt initiative**, basing on the information available at http://mayors-adapt.eu/taking-action/participating-cities/. Accessed 23 July 2015
- **Google hits for the string "city name & climate change"** (hits per thousand inhabitants). Search performed in April 2015 using the Custom Search JSON/Atom API by Google
- **Google hits for the string "city name & climate change & heatwave"** (hits per million inhabitants). Search performed in April 2015 using the Custom Search JSON/Atom API by Google
- **Google hits for the string "city name & climate change & urban heat island"** (hits per million inhabitants). Search performed in April 2015 Custom Search JSON/Atom API by Google
- **Google hits for the string "city name & climate change & flood"** (hits per million inhabitants). Search performed in April 2015 using the Custom Search JSON/Atom API by Google
- **Google hits for the string "city name & climate change & drought"** (hits per million inhabitants). Search performed in April 2015 using the Custom Search JSON/Atom API by Google
- **Google hits for the string "city name & climate change & sea level rise"** (hits per million inhabitants). Search performed in April 2015 using the Custom Search JSON/Atom API by Google

In total, 135 indicators have been collected or derived, of which 58 have been so far included in the data model. These indicators were selected following a quality criterion based on relevance and

[10] All the internet searches were performed in all the official languages spoken in each city. Resulting hits were standardised by population and outliers were removed for data consistency.

interpretability (according to the literature), coverage (more than a half of the cities included), and reduced redundancy (i.e. avoiding indicators that measure similar socio-economic trends).

Table 8 (Sensitivity) and Table 8 (Adaptive Capacity) present the vulnerability indicators included in the data model:

Vulnerability indicators – sensitivity				
Code	**Description**	**Threat**	**Source**	**Relevance**
EEASEALI	Mean soil sealing [%] of UMZ 2006 of core city (EEA 2012)	FLP,FLF	EEA, 2012	(Balica et al., 2012)
EN2002V	Number of days ozone O_3 concentrations exceed 120 µg/m³	HW	Urban Audit	(ASC, 2014)
EN2005V	Number of days particulate matter PM10 concentrations exceed 50 µg/m³	HW	Urban Audit	(ASC, 2014)
EN2025V	Accumulated ozone concentration in excess 70 µg/m³	HW	Urban Audit	(ASC, 2014)
EN2026V	Annual average concentration of NO_2 (µg/m³)	HW	Urban Audit	(ASC, 2014)
EN2027V	Annual average concentration of PM10 (µg/m³)	HW	Urban Audit	(ASC, 2014)
EN3010V	Price of a m³ of domestic water - Euro	DR	Urban Audit	(DG Regio, 2009)
DE3002I	Proportion of households that are 1-person households	HW	Urban Audit	(Uejio et al., 2011; Wolf and McGregor, 2013)
DE3005I	Proportion of households that are lone-parent households	HW	Urban Audit	(Klein Rosenthal et al., 2014)
DE3008I	Proportion of households that are lone-pensioner households	HW	Urban Audit	(Klein Rosenthal et al., 2014; Uejio et al., 2011)
DE3016I	Lone parent households per 100 households with children aged 0-17	HW	Urban Audit	(ARUP, 2014; Klein Rosenthal et al., 2014; Wolf and McGregor, 2013)
EC1020I	Unemployment rate	HW,FLP,FLF,FLC,DR	Urban Audit	(Cutter et al., 2009; Lee, 2014)
DE2003I	Non-EU foreigners as a proportion of population	HW,FLP,FLF,FLC,DR	Urban Audit	(Cutter et al., 2009; El-Zein and Tonmoy, 2015; Kaźmierczak and Cavan, 2011; Wilhite and Hayes, 2005)
DE1040I	Proportion of population aged 0-4 years	FLP,FLF,FLC,HW	Urban Audit	(Cutter et al., 2009; Lee, 2014)
DE1055I	Proportion of population aged 75 years and over	FLP,FLF,FLC,HW	Urban Audit	(Cutter et al., 2009; Lee, 2014)
EN5101ITECI	Population density: total resident pop. per square km. Indicator built basing on GISCO GIS layers and Urban Audit population data (DE1001V - Population on the 1st of January, total)	HW,DR	Tecnalia R&I	(ARUP, 2014; Iglesias et al., 2009; Stefano et al., 2015; Wolf and McGregor, 2013)
SA2013TECI	Number of deaths per year under 65 due to diseases of the circulatory or respiratory systems per 1000 inhabitants, based on Urban Audit data: SA2013V - Number of deaths per year under 65 due to diseases of the circulatory or respiratory systems and DE1001V - Population on the 1st of January, total	HW	Tecnalia R&I	(ASC, 2014; Wolf and McGregor, 2013)
EN3003TECI	Total use of water (m³ per capita per year) basing on Urban Audit data: EN3003V - Total use of water - m³ and DE1001V - Population on the 1st of January, total	DR	Tecnalia R&I	(Stefano et al., 2015)
DE1001TECI	Population growth rate over the period 2004-2012, basing on DE1001V - Population on the 1st of January, total retrieved from Urban Audit	DR	Tecnalia R&I	(Knutson et al., 1998; Stefano et al., 2015)

Table 7: Sensitivity indicators included in RAMSES data model.

Vulnerability indicators – adaptive capacity				
Code	**Description**	**Threat**	**Source**	**Relevance**
EEAGRBLI	Green/blue urban area [%] UMZ 2006 of core city (EEA 2012)	HW	EEA, 2012	(Uejio et al., 2011)
EC3039V	Median disposable annual household income - EUR	HW,FLP,FLF,FLC,DR	Urban Audit	(Johnson et al., 2012; Koks et al., 2015)
EC3040V	Average disposable annual household income - EUR	HW,FLP,FLF,FLC,DR	Urban Audit	(Balica et al., 2012; Johnson et al., 2012; Koks et al., 2015)
SA1007I	Proportion of households living in houses	HW	Urban Audit	(ARUP, 2014; ASC, 2014; Uejio et al., 2011)
SA1022V	Average area of living accommodation - m²/person	HW	Urban Audit	(ARUP, 2014)
PS3090TECV	Most people can be trusted (synthetic index 0-100)	HW,FLP,FLF,FLC,DR	Urban Audit	(Kuhlicke et al., 2011)
PS3120TECV	City committed to fight against climate change (synthetic index 0-100)	HW,FLP,FLF,FLC,DR	Urban Audit	(EEA, 2012)
TE2031TECI	Proportion of working age population qualified at level 5 or 6 ISCED, basing on Urban Audit data: TE2031V - Persons (aged 25-64) with ISCED level 5 or 6 as the highest level of education and population data: DE1058V - Population on the 1st of January, 25-34 years, total; DE1061V - Population on the 1st of January, 35-44 years, total; DE1064V - Population on the 1st of January, 45-54 years, total; DE1025V - Population on the 1st of January, 55-64 years, total	HW,FLP,FLF,FLC,DR	Tecnalia R&I	(Brooks et al., 2005)
AWGCCTECI	Google hits for the string "climate change" (hits per thousand inhabitants). Search performed in April 2015 using the Custom Search JSON/Atom API by Google	HW,FLP,FLF,FLC,DR	Tecnalia R&I	New indicator
AWGHWTECI	Google hits for the string "city name & climate change & heatwave" (hits per million inhabitants). Search performed in April 2015 using the Custom Search JSON/Atom API by Google	HW	Tecnalia R&I	New indicator
AWGUHITECI	Google hits for the string "city name & climate change & urban heat island" (hits per million inhabitants). Search performed in April 2015 Custom Search JSON/Atom API by Google	HW	Tecnalia R&I	New indicator
AWGFLOTECI	Google hits for the string "city name & climate change & flood" (hits per million inhabitants). Search performed in April 2015 using the Custom Search JSON/Atom API by Google	FLP,FLF	Tecnalia R&I	New indicator
AWGDROTECI	Google hits for the string "city name & climate change & drought" (hits per million inhabitants). Search performed in April 2015 using the Custom Search JSON/Atom API by Google	DR	Tecnalia R&I	New indicator
AWGSLRTECI	Google hits for the string "city name & climate change & sea level rise" (hits per million inhabitants). Search performed in April 2015 using the Custom Search JSON/Atom API by Google	FLC	Tecnalia R&I	New indicator
ECSHADIVTECI	Shannon index of economic diversity, basing on Urban Audit data on Employment (jobs) in NACE sectors (EC2008V to EC2038V)	DR	Tecnalia R&I	New indicator
MAYADTECV	City participating in Mayors Adapt initiative, basing on http://mayors-adapt.eu/taking-action/participating-cities/. Accessed 23 July 2015	HW,FLP,FLF,FLC,DR	Tecnalia R&I	New indicator

Table 8: Adaptive capacity indicators included in RAMSES data model.

Appendix A provides a more detailed overview of the data model, including the number of variables used to characterise each vulnerability dimension, as well as the weights and the transformation methods used in each case.

4.5 Data preparation

Data preparation was performed on all the hazard, exposure and vulnerability indicators based on a sequential implementation of the following steps:

1. **Overall quality check:** All the indicators were visually supervised for atypical values. All anomalous values (e.g. values expressed in the wrong scale or including unexpected characters) were removed from the distribution. Additionally, statistical outliers (i.e. values laying beyond the threshold set at 1.5 times the interquartile range) were removed for those indicators built basing on Internet searches.
2. **Transformation of variables**: Sample normalisation is a prerequisite for a number of the statistical tests that are usually performed within indicator –based vulnerability assessments (Adger et al., 2004; Cutter et al., 2010; Jun et al., 2013; Müller et al., 2011). Most of the previous works reviewed by this project used any form of data transformation before aggregation (Lee, 2014; Müller et al., 2011; e.g. Tapsell et al., 2002). Similarly, all the variables included in our data model were transformed in order to normalise data distributions. Different transformation methods were tested for each variable (log method, square roots method, square method, cubic root method and quadratic root method). The transformation method that mostly reduced skewness within the distributions was selected. In those cases when the original data were less skewed than the transformed versions, the original figures were kept. Appendix A summarises the statistical transformation method applied to each variable, if any.
3. **Standardisation of variables**: Standardisation makes statistically consistent the aggregation of variables expressed in different units of measures and scales, preventing one specific variable having under or over influence on the final aggregated score (Koks et al., 2015). All the variables included in the vulnerability assessments were standardised as Z-scores, using the following formula:

$$z = \frac{x - \mu}{\sigma}$$

4. **Re-scaling of variables**: For simplicity, all variables were further re-scaled to a new scale ranging from 1 to 2, based on the minimum and maximum values of the distribution. In the case of the hazard variables belonging to any of the three impact scenarios, the minimum value used for the standardisation of the single observations belonging to any of the scenarios considered was the minimum value recorded under the low impact scenario, whereas the maximum was set as the maximum value under the high impact scenario. The formulation is as follows:

$$s = \frac{x - min(x)}{max(x) - min(x)} + 1$$

5. **Imputation of missing values**: Finally, all the missing values were imputed through Single Imputation (median substitution), as a simple operational way of reducing the bias in data analysis (Nardo et al., 2005).

4.6 Internal consistency check

Internal consistency tests assess scale reliability and internal consistency of uni-dimensional constructs basing on the correlation between the individual indicators combined in such constructs. More specifically, consistency tests evaluate if the individual indicators are measuring the latent phenomenon properly (Nardo, M. et al., 2008). For these reasons, testing for internal consistency is a necessary step towards the construction of composite indicators, in particular for those based on weights derived by Factor Analysis (Fekete, 2009).

Cronbach's alpha (C-alpha) is one of the most popular coefficients of reliability. Even if strictly speaking C-alpha is not a measure of uni-dimensionality (Nardo, M. et al., 2008), this coefficient has been widely used as internal consistency test by a number previous works to build vulnerability and resilience indexes to climate change (Cutter et al., 2014; Fekete, 2009). Table 9 shows the C-alpha scores for the indicator-based vulnerability assessment and the number of variables considered in each impact chain.

Threat	Vulnerability dimension	Number of variables included	Standardised Cronbach's alpha
Multi-threat	**Sensitivity**	**19**	**0.66**
Droughts	Sensitivity	6	0.30
Heatwaves	Sensitivity	15	0.61
Pluvial flooding	Sensitivity	5	-0.27[11]
Fluvial flooding	Sensitivity	5	-0.30[11]
Coastal flooding	Sensitivity	4	0.41
Multi-threat	**Adaptive capacity**	**16**	**0.58**
Droughts	Adaptive capacity	9	0.51
Heatwaves	Adaptive capacity	12	0.51
Pluvial flooding	Adaptive capacity	8	0.53
Fluvial flooding	Adaptive capacity	8	0.57
Coastal flooding	Adaptive capacity	8	0.51

Table 9: Internal consistency analysis of the vulnerability indicators.

The C-alpha value for all the 16 variables included in the adaptive capacity dimension was 0.58. The C-alpha value for those variables (19) informing on urban sensitivity was 0.66. These moderate values suggest acceptable levels of internal consistency for the purpose of building a composite index at the European scale (Cho and Kim, 2015; Scheurich et al., 2000).

Similarly to previous research on the construction of composite vulnerability/resilience indexes, we did not expect the individual threat-specific sub-indices to produce high C-alpha values (Cutter et al., 2014), in particular if one considers that some of our proxy indicators included in the distribution are

[11] Negative values are explained by the consideration of the percentage of green/blue urban in the urban morphological zone of core city (EEAGRBLI) as a sensitivity indicator. This is a morphological index that does not keep any structural relation to the remaining socio-economic indices considered in the sensitivity construct. If this specific indicator is excluded from the computation of the sensitivity indices to pluvial and fluvial flood hazards, the C-alpha value becomes much higher, around 0.45 in both cases, which consistent with the values obtained for the remaining sensitivity indices.

derived from physical and morphological features, or from surveys and indirect sources tracking the perception of citizens and city commitment to adapt.

4.7 Weighting procedure

Appling equal weighting to all the variables combined in composite indicators could introduce an element of double counting into the index, as a result of insufficient knowledge of the causal relations among the variables (Nardo, M. et al., 2008). The alternative is to test indicators for statistical correlation and find the most appropriate weighting procedure that takes account of such latent relations among the variables. In our work the individual variables included in the two dimensions of vulnerability (sensitivity and adaptive capacity) have been weighted separately basing on a combination of Factor Analysis (FA) and Principal Component Analysis (PCA).

FA and PCA are two methods commonly used for reducing the dimensionality of a dataset by reducing its internal redundancy. The goal is to account for the highest possible variance in the data using the smallest possible number of factors. This implies that this method assign lower weights to all the variables that share a certain level of explanatory capacity (i.e. are collinear). On the contrary, those variables that hold a larger amount of explanatory capacity are allocated higher weights. Consequently, this weighting procedure should be understood as a method for reducing redundancy in the data model, rather than as a method for defining the *relative importance* of the different variables contributing to the composite sub-indices of sensitivity and adaptive capacity.

The methodology applied for FA follows the standard procedure (e.g. Nardo et al., 2005). FA was run on all sensitivity and adaptive capacity variables. Basing on the correlation structure shown by all variables, a certain number of latent factors were extracted basing on PCA. The number of factors to extract was decided according to the following criteria: (1) number of factors with eigen values larger than one; (2) number of factors with individual contribution to overall variance by more than 10%, and; (3) number of factors with cumulative contribution to overall variance by more than 60%. Varimax rotation was used in order to maximize the variance of loadings, simplifying the interpretation (Fekete, 2009; Kaźmierczak and Cavan, 2011).

Weights were defined basing on the matrix of factor loadings after rotation: first, square factor loadings are computed; subsequently, weighted intra-factor loadings are calculated by dividing the square factor loadings by the proportion of variance explained by each factor; then across-factor weighted loadings are generated by dividing intra-factor weighted loads by the proportion of variance explained by each factor in relation to the total cumulative variance explained by all factors; subsequently those individual indicators with the highest factor loadings across all factors are selected and re-scaled to unity, as final weights. This method weighted the final city sensibility and adaptive capacity scores by both the individual component loading of the indicator and the total amount of explained variance of the factor in which each indicator was included (Frazier et al., 2014; Nicoletti et al., 1999). Appendix A summarises the weights attributed to each variable.

It is important to emphasise that despite the use of different values to weight the variables included in the sensitivity and adaptive capacity dimensions, the final contribution of each of these components to the final risk score presented on Section 5 remained proportional, as shown in the following figure:

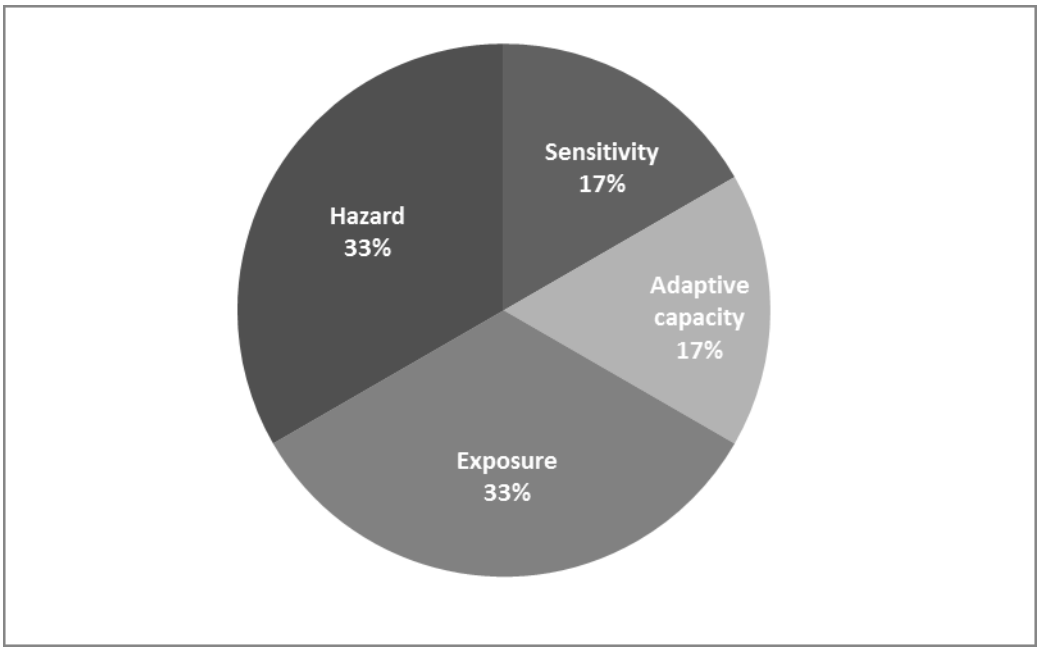

Figure 48: Contribution of the different components of risk to the final risk score[12].

4.8 Vulnerability scoring

Similarly to hazard and exposure indices, sensitivity and adaptive capacity indices under each impact chain were also estimated through geometric aggregation of the individual indicators shown on Table 7 and Table 8, using the following formulas:

$$S_{ct} = \prod_{i=1}^{I} s_{ci}^{w_i} \quad (4.1)$$

where S_{ct} = sensitivity score for city *c* under climate threat *t*; s_{ci} = value of sensitivity factor *i* for threat *t* in city *c*; w_i = weight of sensitivity factor *i* obtained by means of FA/PCA*; I* = total number of sensitivity factors considered;

$$AC_{ct} = \prod_{j=1}^{J} ac_{cj}^{w_j} \quad (4.2)$$

where AC_{ct} = adaptive capacity score for city *c* under climate threat *t*; ac_{cj} = value of adaptive capacity factor *j* for threat *t* in city *c*; w_j = weight of adaptive capacity factor *j* obtained by means of FA/PCA*; J* = total number of adaptive capacity factors considered.

The sensitivity (S'_{ct}) and adaptive capacity (AC'_{ct}) scores were standardised and re-scaled prior to aggregation with the hazard indices as vulnerability scores, using the following formula:

$$V_{ct} = \frac{S'_{ct}}{AC'_{ct}} \quad (4.3)$$

where V_{ct} = vulnerability score for city *c* under climate threat *t*;

[12] Whenever hazard data were not available (e.g. coastal floods), the exposure and vulnerability components contributed proportionally to the final risk score. Similarly, when exposure data were not accessible (e.g. fluvial floods), hazard and vulnerability contributed proportionally to the final risk score.

Finally, the vulnerability scores were standardised and re-scaled (V'_{ct}) again prior to aggregation with the hazard indices to quantify relative risks, as described in Section 4.5.

Results for all EU Urban Audit cities are presented in Figure 49 and Figure 50. The indicators shaping each impact chain and vulnerability dimension are listed on Table 7 and Table 8 above.

It is important to emphasise that the maps presented in Figure 49 and Figure 50 do not provide any explicit information on the relative intensity of the climate threats that could be potentially faced by the urban areas, which in our assessment are considered within the hazard and exposure dimensions discussed on Sections 2 and 3. Indeed, the maps presented in Figure 49 and Figure 50 summarise the intrinsic capacity of cities to cope and respond to hypothetical climate threats, regardless of the actual hazards and exposure levels faced by each city.

Maps presented in in Figure 49 and Figure 50 all use the following legend:

VULNERABILITY
- Higher vulnerability (> quantile 0.75)
- Medium to higher vulnerability (Median to quantile 0.75)
- Medium to lower vulnerability (quantile 0.25 to Median)
- Lower vulnerability (< quantile 0.25)

4.8.1 Combined vulnerability indices

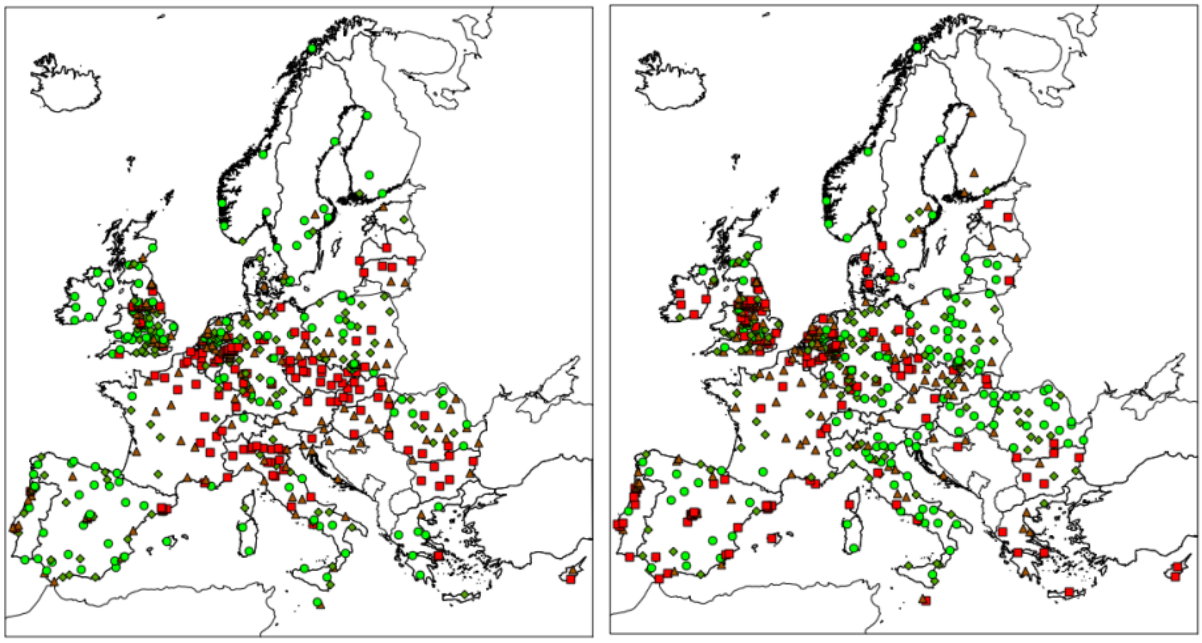

Figure 49: Vulnerability indices to heatwaves (left) and droughts (right).

The vulnerability indices shown in Figure 49 summarise all the relevant dimensions that are considered to shape the vulnerability to climate change for heatwaves (left) and droughts (right). The data allowed the computation of the vulnerability scores for all the 571cities included in the Urban Audit database, for both impact chains (see Appendix A for additional details on the data model).

Cities showing comparatively higher vulnerability to heatwaves are located in the central area of the EU and the southernmost regions of the New Member States, as well as on the Baltic republics. These are the regions where a combination of socio-economic and physical features that potentially increase urban sensitivity to heatwaves is mostly found. In contrast, cities with the lowest vulnerability scores

scatter over the peripheral regions of the EU, with large internal differences in counties such as Italy and the United Kingdom.

The spatial pattern is less obvious in relation to droughts (right). In this case, the areas with the highest vulnerability scores lay in the westernmost countries, some regions in Eastern Germany, Bulgaria, Cyprus and Greece. Still, there are huge internal differences within countries such as Spain and the UK. In these areas there does not seem to be an obvious spatial pattern.

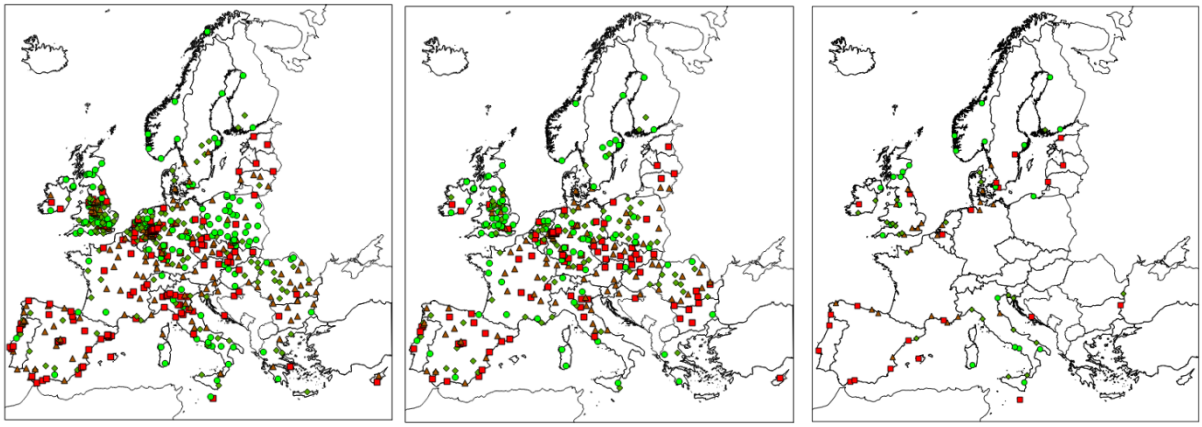

Figure 50: Vulnerability indices to pluvial floods (left), fluvial floods (centre), and coastal floods (right).

Figure 50 shows the vulnerability indices for pluvial floods (left), fluvial floods (centre) and coastal floods (right). The vulnerability indices were computed for all the 571 Urban Audit cities in the case of pluvial floods, the 365 Urban Audit cities with water courses with at least 500km2 catchment area (see Section 2.7.2 above for additional details), in the case of fluvial floods, and 92 coastal cities for which exposure data were accessible (see Boettle et al., 2016 for details on how this indicator was generated), in the case of coastal floods. Appendix A provides additional details on the data model.

Due to the great overlaps between the indicators used to characterise the sensitivity and adaptive capacity to pluvial and fluvial floods, these impact chains show very similar profiles on the vulnerability scores across all the cities considered in each analysis (571 cities for pluvial floods and 365 cities for fluvial floods). In both cases there seems to be an absence of a clear spatial pattern in the distribution of vulnerability scores.

Vulnerability values seem to be mixed and scattered even within the different countries, which calls for a higher resolution analysis. Nonetheless, lower values seem to predominate in the British Isles and the Scandinavian countries, whereas higher vulnerability scores seem to be distributed over the Mediterranean countries (with the exception of the cities located in the Italian Mezzogiorno), the Bohemian (Czech Republic, Slovakia and Austria) area, and eastern Danubian regions (Romania, Bulgaria).

On the contrary, vulnerability to coastal floods shows shown in Figure 50 (right) show a more defined spatial pattern. Cities laying over the Atlantic coast, western Mediterranean and the Baltic show relatively higher vulnerability scores, whereas cities located in Italian Peninsula, the UK and the Scandinavian countries tend to have lower vulnerability to coastal floods.

4.9 Sensitivity analysis

A sensitivity analysis comparing alternative weighting and aggregation procedures was performed. The analysis based on a comparison between the two alternative aggregation (geometric vs arithmetic) and weighting (FA/PCA weights vs equal weights) methods. Pearson's, Spearman's and Kendall's correlation indexes were calculated for all the alternative computations for vulnerability scores. This was done for all threats.

Multi-threat vulnerability scores were also assessed comparing the multi-threat scores generated by means of an ex-ante combination of the individual indicators versus an ex-post combination of the threat-specific vulnerability values into multi-threat scores (as in Preston et al., 2008). Table 10 to Table 12 show the resulting Pearson's correlation scores for all these methods. The outcomes of the sensitivity analysis show very consistent results of the vulnerability assessment across all the possible aggregation approaches considered here.

Aggregation method			**Additive**							
	Weights		**FA/PCA**				**Proportional**			
		Threats	**Multi-threat**	**Droughts**	**Floods (all types)**	**Heatwaves**	**Multi-threat**	**Droughts**	**Floods (all types)**	**Heatwaves**
Multiplicative	**FA/PCA**	**Multi-threat**	**0.98**	0.48	0.59	0.92	**0.91**	0.53	0.62	0.90
		Droughts	0.50	**0.99**	0.63	0.38	0.52	**0.90**	0.64	0.37
		Floods (all types)	0.59	0.65	**0.99**	0.62	0.64	0.80	**0.96**	0.58
		Heatwaves	0.93	0.37	0.62	**0.99**	0.90	0.46	0.66	**0.94**
	Proportional	**Multi-threat**	**0.91**	0.49	0.63	0.89	**0.99**	0.59	0.67	0.93
		Droughts	0.54	**0.90**	0.76	0.47	0.60	**0.99**	0.76	0.45
		Floods (all types)	0.61	0.67	**0.95**	0.65	0.67	0.79	**0.99**	0.61
		Heatwaves	0.90	0.33	0.57	**0.92**	0.92	0.42	0.60	**0.99**

Table 10: Results of the sensitivity analysis for vulnerability scores (Pearson's coefficient of correlation) – multiplicative vs additive aggregation.

Aggregation method			**Ex-ante aggregation**			
			Additive		**Multiplicative**	
		Weights	**FA/PCA**	**Proportional**	**FA/PCA**	**Proportional**
Ex-post aggregation	**Additive**	**FA/PCA**	**0.88**	0.87	0.85	0.85
		Proportional	0.87	**0.92**	0.86	0.91
	Multiplicative	**FA/PCA**	0.88	0.88	**0.88**	0.88
		Proportional	0.86	0.91	0.86	**0.92**

Table 11: Results of the sensitivity analysis for multi-threat vulnerability scores (Pearson's coefficient of correlation) –ex-ante vs ex-post aggregation.

Weights			Proportional							
	Aggregation method		Multiplicative				Additive			
		Threats	Multi-threat	Droughts	Floods (all types)	Heatwaves	Multi-threat	Droughts	Floods (all types)	Heatwaves
FA/PCA	Multiplicative	Multi-threat	**0.92**	0.56	0.62	0.90	**0.91**	0.53	0.62	0.90
		Droughts	0.52	**0.91**	0.66	0.36	0.52	**0.90**	0.64	0.37
		Floods (all types)	0.63	0.80	**0.96**	0.56	0.60	0.80	**0.96**	0.58
		Heatwaves	0.91	0.47	0.65	**0.94**	0.90	0.46	0.56	**0.94**
	Additive	Multi-threat	**0.91**	0.54	0.61	0.90	**0.92**	0.53	0.64	0.91
		Droughts	0.49	**0.90**	0.67	0.33	0.50	**0.92**	0.66	0.36
		Floods (all types)	0.63	0.76	**0.95**	0.57	0.65	0.78	**0.97**	0.60
		Heatwaves	0.89	0.47	0.65	**0.92**	0.90	0.47	0.67	**0.94**

Table 12: Results of the sensitivity analysis for vulnerability scores (Pearson's coefficient of correlation) – FA/PCA vs proportional weights.

4.10 Analysis of results

A K-Means Cluster Analysis has been performed to understand the spatial pattern of vulnerabilities across the different threats. This method partitions cities into a given number of *k* groups such that the sum of squares from points to the assigned cluster centres is minimised.

A key issue when conducting cluster analysis is the decision on the number of clusters to extract. In this case, the 'elbow criterion', based on the curvature of the within group variance (showin in Figure 51), was followed to select the number of clusters to distinguish within our analysis.

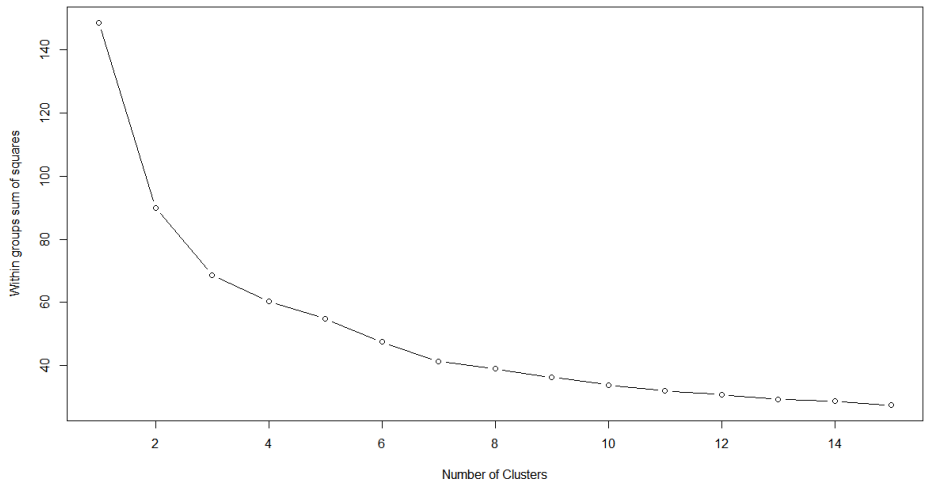

Figure 51: Vulnerability clusters – The within groups variance represented by the sum of squares.

The cluster analysis grouped cities according to the values of the resulting vulnerability indices to the different climate change hazards. For the sake of simplicity, differences between specific flood types (i.e. pluvial, fluvial and coastal) were disregarded in this analysis. Figure 52 shows the resulting spatial structure for the assessed cities considering 7 clusters.

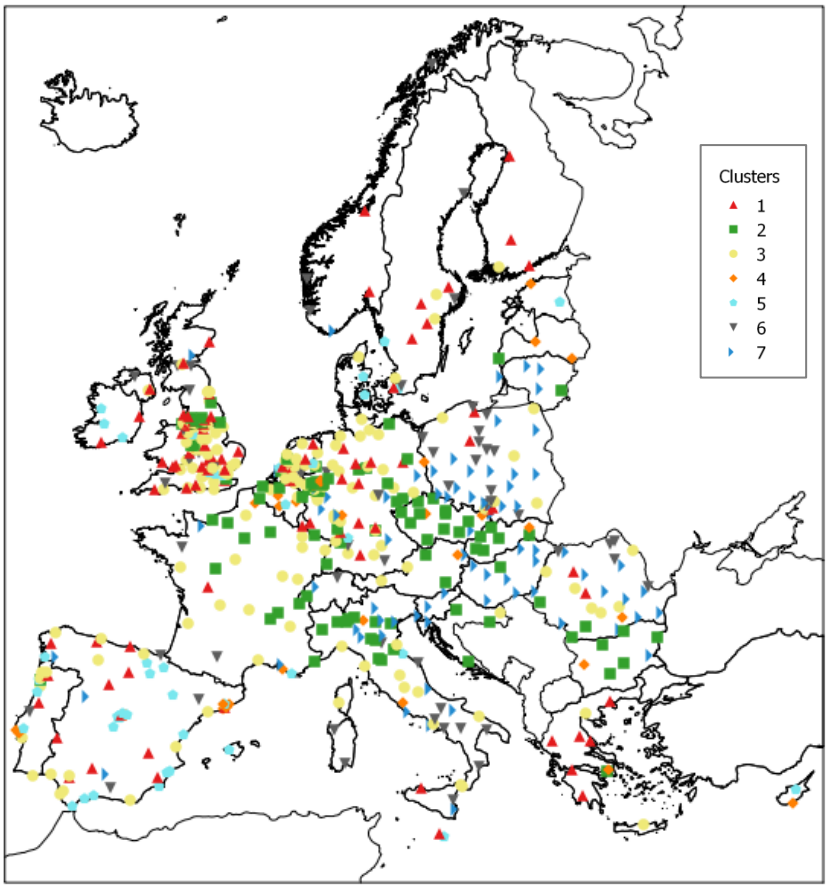

Figure 52: City clusters based on different combinations of threat-specific vulnerability scores.

Cluster 1 includes cities with medium to low vulnerabilities to heatwaves, droughts and floods. In contrast, Cluster 2 includes cities with medium to high vulnerabilities to these same threats. Cluster 3 includes cities with average vulnerabilities to heatwaves and droughts and medium to low vulnerabilities to floods. Cluster 4 includes cities with relatively high vulnerabilities to the three potential threats, thus deserving an in-depth vulnerability assessment. Cluster 5 includes cities with relatively high vulnerability to droughts, medium to high vulnerabilities to floods and medium to high vulnerabilities to heatwaves. Cluster 6 includes cities with low vulnerabilities to droughts and floods and medium to low vulnerabilities to heatwaves. Cluster 7 includes cities with medium to low vulnerabilities to droughts and floods, and medium to high vulnerabilities to heatwaves.

Whereas clusters 1, 2 and to a limited extent also 7 could be said to follow a rather coherent spatial distribution, cities included in clusters 3, 4, 5 and 6 do not show any traceable pattern at all. This comes in recognition that (1) different combinations of vulnerabilities are possible and do not depend upon the geographic characteristics of the regions where cities belong and the nature of hazards being faced, and (2) that urban vulnerability to climate change does not necessarily mirror the structural socio-economic patterns behind most of the indicators combined in the vulnerability indices;

vulnerability score are also a result of a number of dimensions entirely in the hands of local administrations, such as increasing awareness and implementing soft actions towards adaptation. Although in our analysis the former factors could only be captured through proxy indices based on Internet searches, results illustrate the importance of considering awareness and governance factors within climate change vulnerability assessments.

5 Risk scoring: ranking cities according to the relative magnitude of climate change-driven risks

The hazard, exposure and vulnerability indices have been combined to inform on the relative level of risk faced by each city under each impact chain. A risk score, R_{ct}, for each city, c, and climate change threat, t, is calculated as:

$$R_{ct} = \sqrt[3]{H'_{ct} \times V'_{ct} \times E'_{ct}} \quad (5.1)$$

where the standardised hazard score H'_{ct}, standardised exposure score E'_{ct} and standardised vulnerability score V'_{ct} are aggregated as a risk score R_{ct}. R_{ct} is standardised and re-scaled for visualisation as R'_{ct}.

Thus, the risk indices have been generated as the intersection of hazard, exposure and vulnerability scores.

Figure 53 to Figure 57 present the resulting relative risk indices for the Urban Audit cities under a low (left), medium (centre) and high (right) impact scenarios for all the impact chains considered in this work. Maps shown in Figure 53 to Figure 57 all use the following legend:

RISK
- Higher risk (> quantile 0.75)
- Medium to higher risk (median to quantile 0.75)
- Medium to lower risk (quantile 0.25 to median)
- Lower risk (< quantile 0.25)

5.1 Heatwave risk

Figure 53 shows the relative heatwave risk levels for the 571 Urban Audit cities under a low (left), medium (centre) and high (right) impact scenarios. These maps provide clear evidence that the cities where potential heatwave risks are more incumbent under the three climate scenarios are those located over the central continental European belt, which extends from central France to Romania and Bulgaria, with a few ramifications to the west (UK), southern Greece, and up North to the Baltic Republics. This is motivated by a combined increased probability or intensity in the expected heatwaves, coupled with a comparatively more severe UHI effect in those areas and/or relatively higher levels of exposed population, as well as with relatively higher levels of vulnerability scores.

In contrast, most cities laying in the Iberian Peninsula, Scandinavia and the Mediterranean regions show medium to lower levels in the combined heatwave risk scores. In the Mediterranean cities this is mainly due to a reduced intensity of the UHI effect. The natural climate in this region is characterized by dry hot summers and therefore these urban areas are better adapted to high temperatures. The effectiveness of the *adaptation measures* in place in these cities – related to urban morphology, types of vegetation, shade artefacts, etc. – is perceivable on the observed thermal gradient during summer months, which in most cases is less acute than in northern latitudes, and can sometimes be even negative. This holds for the following list of cities: Bari, Marbella, Reggio di Calabria, Alicante/Alacant, Almeria, Huelva, Cagliari, Lefkosia, Toledo, Malaga, Rimini, Setubal, Valletta and Taranto. In the Scandinavian cities lower heatwave risk scores are mostly explained by a lesser intensity and frequency of heatwave events under the three climate change scenarios.

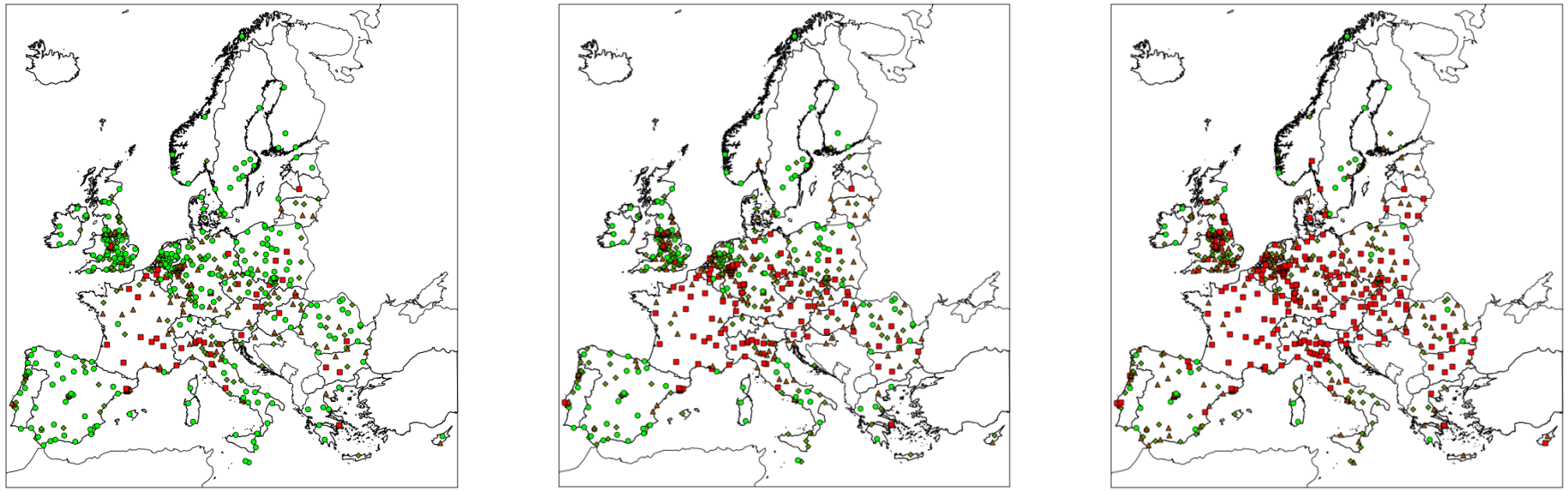

Figure 53: Heatwave risk for the low (left), medium (centre) and high (right) impact scenarios.

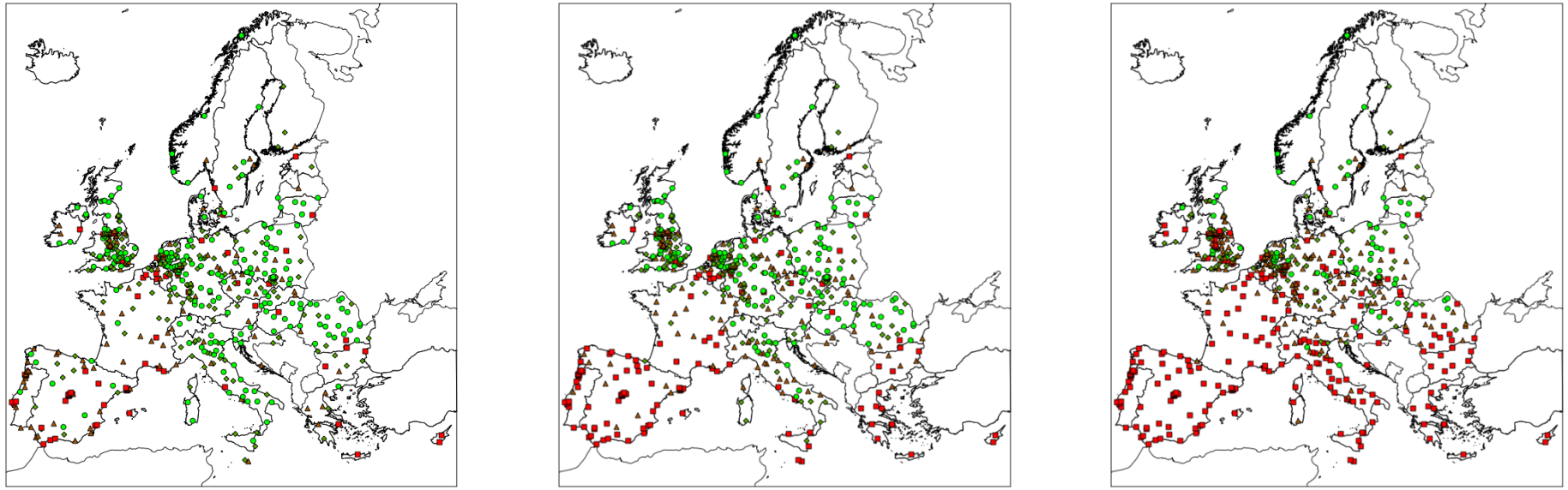

Figure 54: Drought risk for the low (left), medium (centre) and high (right) impact scenarios.

5.2 Drought risk

Figure 54 shows the relative drought risk levels for the 571 Urban Audit cities under a low (left), medium (centre) and high (right) impact scenarios. These relative risk maps represent the intersection of hazard, exposure and vulnerability indices. Thus, the resulting risk scores consider issues such as: (1) the relative change on the expected severity and frequency of droughts under the three climate change impact scenarios; (2) the level of exposure of each city – dependant on its dimension –, and; (3) the resulting vulnerability scores.

The maps clearly show a gradual and steady increase on the risk levels from the low to the high impact scenario. This suggests that the dominant underlying component shaping risk scores is drought hazard, which shows a quite similar increase pattern along the low, medium and high scenarios (see Figure 41). The spatial pattern of both hazard and risk scores depict a situation in which most cities located around the Mediterranean and Black sea basins, in particular those located in the Iberian Peninsula and Greece, face comparatively higher risk levels than those cities located in Central and Northern Europe within all the three scenarios.

5.3 Pluvial flood risk

Climate models, run at standard resolution, cannot simulate intense hourly rainfall and since Europe-wide future climate model simulations at convection-permitting scales do not yet exist, there are no reliable projections of future intense hourly rainfall for Europe. Therefore, the assessment of future changes in the pluvial flooding hazard could not follow a similar methodology to the other impacts in this report and was done using a sensitivity analysis (where the same rainfall changes where applied to all cities), with severe implications to the interpretation of the risk results (see Section 2.6 above for additional details).

Figure 55 classify the 571 Urban Audit cities according to their relative pluvial flood risk levels under a low (left), medium (centre) and high (right) impact scenarios derived from a sensitivity analysis where different changes in rainfall intensity were applied. According to the map shown on Figure 55 (left), some of the cities that have a comparatively higher risk level under a low impact scenario are those included in the conurbations of large Mediterranean cities like Barcelona (e.g. Santa Coloma de Gramenet, L'Hospitalet de Llobregat, Mataro, Terrassa, Badalona, Sabadell), Lisbon (Sintra and Vila Franca de Xira), and Madrid (Fuenlabrada, Mostoles, Getafe). This is motivated by the combination of consistently high vulnerability scores and relatively high pluvial hazard and exposure values. A similar reasoning also holds for some Baltic (Riga, Daugavpils, Tallinn, Liepaja) and German (Ludwigshafen am Rhein, Duisburg, Herne, Frankfurt (Oder), Gelsenkirchen, Mulheim a.d.Ruhr) cities. The only two capital cities falling in this category would be Brussel and Prague.

Reversely, a small group of Urban Audit cities show pluvial flood risk levels that fall persintently below the 0.25 percentile, also under a high impact scenario (Figure 55, right). These cities are scattered in different countries across Europe, particularly in the Netherlands (Utrecht, Groningen, Arnhem, Nijmegen, Zwolle), Norway (Bergen, Trondheim, Kristiansand and Tromso), Poland (Torun, Opole, Gorzow, Wielkopolski, Czestochowa, Plock, Gliwice, Bytom, Tychy, Wloclawek, Chorzow, Legnica, Grudziadz), and the United Kingdom (Exeter, Plymouth, Warrington, Warwick and Carlisle). The only major cities that are classified in this low risk category under the three impact scenarios are

Stockholm and Bratislava. All these cities combine comparatively low vulnerability scores and relatively low hazard and exposure indices to pluvial floods.

Looking at the medium impact scenario shown in the central map in Figure 55, it becomes apparent that the cities that have relatively higher risk scores are the same ones as those having comparatively higher risk in the low impact scenario. The same motivations that have been mentioned above, namely consistently high vulnerability scores and relatively high pluvial hazard and exposure values, also hold under this high impact scenario for this specific group of cities. Additionally, a number of large urban areas, including Bucuresti, London (greater city), Athina, Roma, Wien are also classified in the higher risk class. The reason can be found in the standardised exposure indices to pluvial flooding, which due to the assumptions made in its computation (see Section 3.2.2 for details) are structurally higher in such larger urban agglomerations, which is not necessarily associated to higher hazard levels in such areas.

In general terms, according to the classification of cities in relation to their relative levels of risk to pluvial flooding under a medium impact scenario shown in Figure 55 (centre), it seems that those cities that have comparatively lower levels of risk to pluvial floods seem to predominate in the western (UK, Ireland, the Netherlands, Germany) and northern regions of Europe (Nordic countries). But even in these areas the distribution patterns are quite irregular, with an uneven distribution of risk scores for this specific impact chain over these two macroregions. A paradigmatic example is the UK, where all risk categories are represented by a similar number of cities.

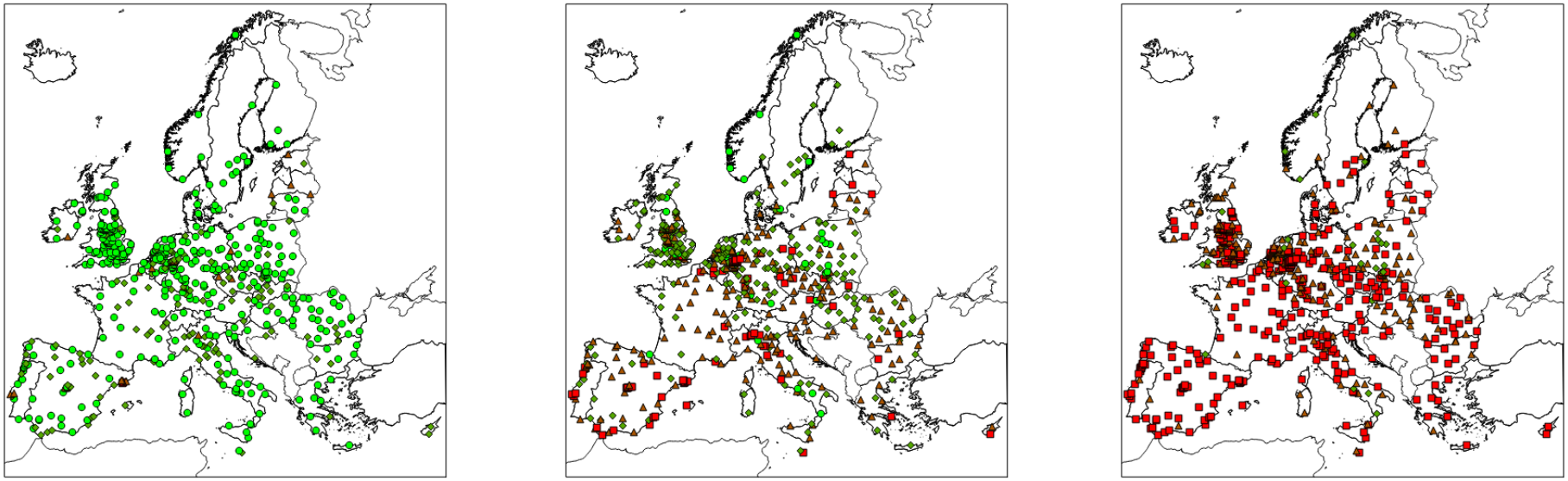

Figure 55: Pluvial flood risk for the low (left), medium (centre) and high (right) impact scenarios.

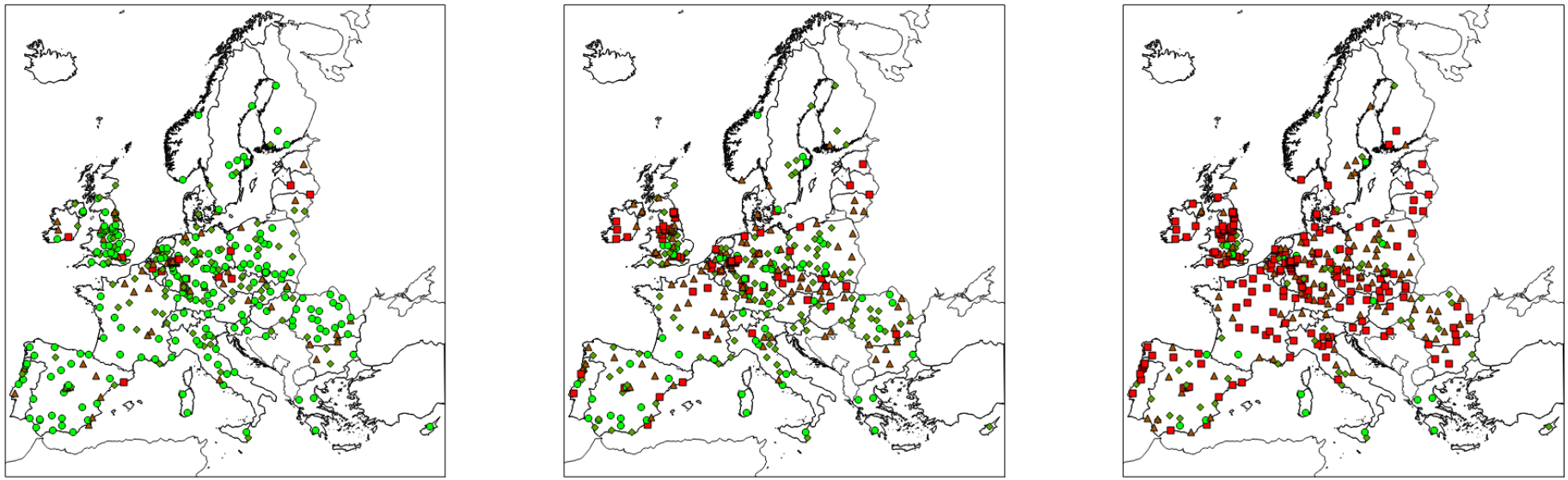

Figure 56: Fluvial flood risk for the low (left), medium (centre) and high (right) impact scenarios

5.4 Fluvial flood risk

The maps shown in Figure 56 classify a total of 365 cities with water courses with at least 500km^2 catchment area (see Section 2.7.2 above for additional details on the selection method) in four categories of risk under a low (left), medium (centre) and high (right) impact scenarios.

Considering that the fluvial risk construct lacks of a specific exposure dimension, the resulting risk scores are highly conditioned by the vulnerability values to this specific threat. Indeed, cities showing comparatively higher risk values under the low impact scenario (Figure 56, left), such as Riga, Santa Coloma de Gramenet, Daugavpils, Bruxelles / Brussel, Gelsenkirchen, Waterford, Oberhausen, Liege, Hamm, Ludwigshafen am Rhein, Praha, Karlovy Vary, Duisburg, Gravesham, Getafe, Offenbach am Main, and Frankfurt (Oder)) all show structurally higher levels of vulnerability to fluvial floods.

As shown in the right map included in Figure 56, some other cities, such as Larisa, Potsdam, Wycombe, Sassari, Murcia, Ioannina, Warwick, Toulouse, Bratislava, Stockholm, Kalamata, Wloclawek, Catania, Munster, Nijmegen, San Sebastian/Donostia, Granada and Cagliari find themselves in the opposite situation (i.e. lower risk level under a high impact scenario). All these areas are characterised by lower vulnerability levels to this climate threat, which contributes to moderate the final risk scores, even though in some of these urban areas (e.g. Wycombe, Warwick, Stockholm, Munster, Nijmegen) the hazard indices to fluvial floods are not negligible under a high impact scenario.

However, the most diverse and expressive situation can be found in the medium impact scenario representation shown in Figure 56 (centre). According to this map, the cities that hold comparatively higher risk levels to fluvial flooding could be classified in three different groups:

1. cities showing higher vulnerability and higher to average hazard scores to fluvial flooding: e.g. Riga, Daugavpils, Bruxelles / Brussel, Waterford, Gelsenkirchen, Oberhausen, Ludwigshafen am Rhein, Hamm, Duisburg Wirral, Liege, Dortmund, Karlovy Vary, Limerick, Gravesham, Offenbach am Main, Bottrop, Slough, Antwerpen, Tartu, Witten, Koszalin, Bochum, Bremerhaven, Reims, Salzgitter, Krefeld, Nurnberg, Neuss, Zaanstad, Heilbronn, Paris and Saint-Etienne;
2. cities characterised by higher vulnerability values and moderate or even lower hazard scores, which are essentially the same ones mentioned above when referring to the low impact scenario: e.g. Santa Coloma de Gramenet, Praha, Bucuresti, Getafe, Frankfurt (Oder), Ostrava, Presov, Aveiro, Bergamo, Wien, Plzen, Mostoles, Vila Franca de Xira, Zilina, Cartagena, Moers, Castellon de la Plana/Castello de la Plana and Budapest;
3. cities with higher hazard scores and average to lower vulnerability scores: Middlesbrough, Cork, Kirklees, Crewe and Nantwich, Galway, Hagen, Telford and Wrekin, London (greater city), Salford, Malmo, Newcastle upon Tyne, Essen, Preston, North Tyneside, Lubeck and South Tyneside.

It is also interesting to emphasise the particularities of those cities classified in the low to average risk class under a medium impact scenario, according to Figure 56 (centre). This category results from the combination of lower vulnerability scores with higher hazard scores, including cities such as Rennes, Worcester, Trondheim, Wycombe and Lund, as well as from the integration of lower hazard scores with comparatively higher vulnerabilities to fluvial flooding, a sub-category represented by cities such as Jerez de la Frontera and Lefkosia.

5.5 Coastal flood risk

Figure 57 presents the resulting coastal flood risk index for 92 Urban Audit cities across Europe. As discussed in Section 3.2.3 above, no impact scenarios were used in this case. Results suggest higher levels of coastal flood risk in those cities located over the Atlantic, including most part of cities over the coasts of Portugal, Spain, France, England and the Baltic republics, but excluding the Scandinavian countries, where both hazard and vulnerability levels are inferior. In general terms, the coastal cities located in the Mediterranean region face higher risk levels, especially in Spain, but also in the northernmost extreme of Italian Adriatic Sea, including the cities of Rimini and Venezia.

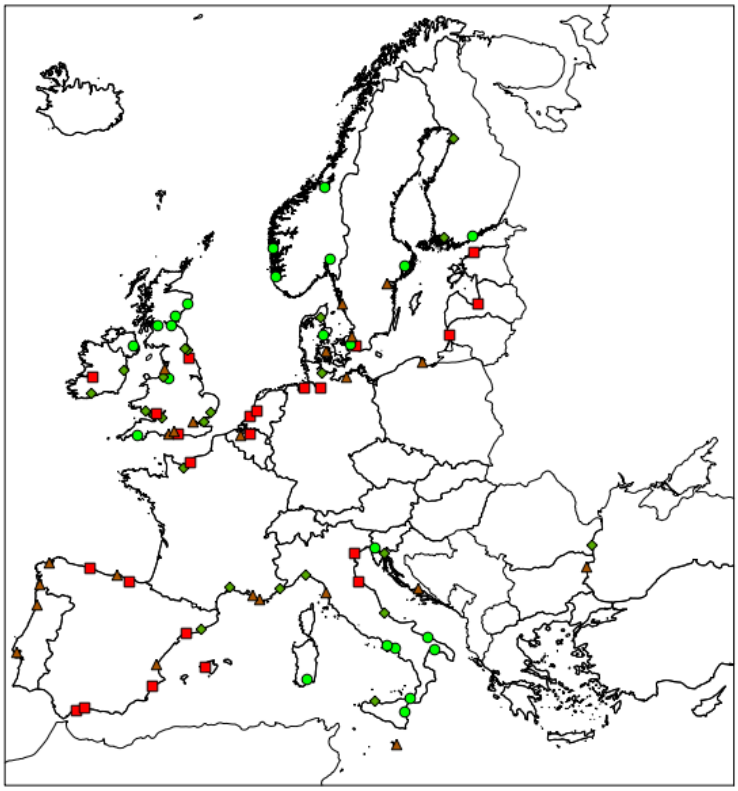

Figure 57: Coastal flood risk index.

6 Conclusions

Increasing availability of continental and global datasets has enabled the development and successful application of an EU-wide climate change risk analysis for urban areas, based on the combination of hazard, exposure and vulnerability indices derived from state-of-the-art climate modelling techniques and the most recent environmental and socio-economic data available. This has been applied to all 571 Urban Audit cities, enabling their climate change risks to be compared relative to one another.

The hazard, exposure, vulnerability and risk scores obtained applying this methodology rank cities in a consistent, relative, scale for each impact chain. This scoring methodology can be used to assess the relative priorities for cities in terms of most significant threats, or whether to focus on measures to manage a risk, further characterise a hazard or decrease vulnerability. National and EU policy makers are able to use this information to inform the prioritisation of investment in particular risks and between different urban areas.

Risk is not just a function of hazard and exposure levels, but also of socio-economic vulnerabilities. For instance, focusing on the heatwaves example it becomes apparent that some cities have relatively lower hazard scores but higher exposure – such as Madrid, Sevilla, Murcia – and/or vulnerability – like Bruxelles / Brussel, Antwerpen, Gent, Zlin, Nitra, Karlovy Vary, Kladno–, whilst other cities have relatively higher hazard and lower exposure – including Novara, Ruda Slaska, Cork, Campobasso, Kavala– and/or vulnerability – such as Barcelona, Genova, Munchen, Dublin, Cardiff –. Similar conclusions could be drawn focusing on other climate-driven threats, as thoroughly discussed on Section 5 above.

This provides important information on the nature of the potential adaptation strategies that could be put in place in each type of cities – whether to focus on engineered adaptation such as flood defences and/or strengthening socio-economic capabilities that might include education programmes. Although the resolution level of this research does not allow to draw any general conclusion in this respect, the methodology itself is scalable and can thus be applied to evaluate risks at multiple levels.

At this scale of analysis our findings allow to draw the following general conclusions:

- **Heat and drought risks** are significant in some places but show regional variability, as socio-economic vulnerability does. Under the high impact hazard results, increases in heatwave hazards and peak temperatures are prevalent across all EU cities. Vulnerabilities to heatwaves are related to socio-economic conditions, environmental quality, morphological aspects, and awareness and engagement levels. Higher vulnerabilities and risks tend to concentrate in the central area of the EU, extending from France along the Rhine, Danube and Po valleys, across the Bohemian plain, including also a large part of German cities.
- Typically cities in Northern European latitudes are less susceptible to unprecedented **droughts** than those in Southern latitudes. Most notably, the variability in hazards exceeds those reported by previous analyses which have only been based upon a small number of model results. Accordingly, cities exposed to higher risk levels tend to predominate in the southern latitudes. This is also a natural consequence of the distribution of vulnerabilities to this threat, which is driven by morphological, demographic, economic, social, and awareness and commitment factors.
- In terms of changes in the **pluvial flooding** hazard, the differences in the percentage of city flooded can vary considerably between cities (even though the same change factor for the

rainfall was applied for all cities). For example a 50% increase in hourly rainfall (for a 10 year return period) causes changes in percentage of city flooded between 18% and 75% which is partially due to the different elevations within each city (besides the different absolute rainfall values that a 50% increase associates with).

- The UK (and parts of Scandinavia) have the most impacted cities in terms of changes in **fluvial flooding** hazard while most of the Mediterranean region does not see any increases, even in the high impact scenario.
- In terms of exposure to **coastal flooding**, which has been characterised in this report through the percentage of urban area exposed to floods due to coastal storm surge events, the most impacted cities would be those from the Netherlands (more than 50% of the urban area flooded) and those cities located over the costs of Frieseland and Flanders.
- Vulnerability to floods (all types) is function of place-specific morphological aspects, socio-economic conditions, awareness levels and city engagement to fight climate change. The combination of all these factors depicts a very contextual situation that call for a more detailed assessment of urban vulnerabilities to floods. This also holds for flood risks, which are evenly distributed across European cities, and thus call for a more detailed assessment at higher spatial resolutions.

6.1 Advances in high level climate change risk analysis

This high level approach provides helpful comparative information, however its very nature means that it inevitably will not suitable for local risk analysis, or emergency planning. The approach developed in RAMSES has made significant advances on previous high level climate change risk analysis in that it has:

- provided a high level climate change risk analysis that captures information on hazard, exposure and vulnerability in urban areas;
- integrated information from multiple climate change hazards;
- analysed over 50 of the latest generation of climate model runs to explore the variability in climate changes;
- exploited cloud computing power to model hydrodynamic processes using the new pan-Europe 25m DEM for the flood modelling;
- developed a coherent, flexible, stable, scalable, transparent and very robust model to assess vulnerabilities and risks at different scales based on indicators – but not dependent on any particular indicator –;
- developed a data model for vulnerability assessments based on a dichotomous classification of vulnerability factors that minimises redundancy and simplifies interpretation;
- delivered a ranking of European cities relative to each other in terms of their vulnerabilities and risks, with respect to a number of pre-defined climate change –driven hazards;
- clustered European cities in a number of coherent and homogeneous groups according to the type and intensity of the vulnerabilities and risks faced by each city.

6.2 Contribution to RAMSES project

This task has provided a high level overview of risks to European cities and contributes to the overall RAMSES aim to develop a set of innovative methods and tools that will quantify the impacts of climate change in EU cities. The work contributes to two of the four RAMSES objectives: (1) A strategic frame for evidence-based adaptation decision-making. A pragmatic and standardised framework for decision making using comparable climate change impact assumptions, impact and adaptation costs while taking account of uncertainty, and (2) Multi-level analysis–as local administrative units, cities will be used to develop adaptation (and more generally sustainable development) strategies from the bottom-up/top-down, that can be aggregated to consider costs at the national, EU and international levels. The different layers of hazard, climate and vulnerability information provide contextual information for more detailed studies in WP3 and other RAMSES WPs.

6.3 Research priorities for high level climate change risk analysis

Despite recent substantial improvements in EU-wide or global datasets – particularly remote sensing and satellite data, there is still potential for improvements in data that could greatly enhance the accuracy of broad scale climate change risk analysis:

- Higher spatial resolution, and in particular greater vertical accuracy, of DEMs that cover the continent would improve flood model accuracy.
- Accurate surveys of river depth and width for fluvial flood modelling.
- Improved understanding of interactions between different sources of flooding, but coastal and fluvial interactions in delta and estuary cities in particular.
- More extensive and readily accessible meteorological records (especially hourly rainfall) and river gauging data will help improve the statistical analysis of extreme events. European-wide future projections of changes in hourly precipitation would also be ideal; this seems an unrealistic goal using current climate models and therefore more research needs to be done for finding alternative ways of estimating future changes in intense rainfall.
- OpenStreetMap provides great potential to complement high resolution DEMs for pluvial flood risk analysis as the two combined would enable complex urban features to be modelled. This is already feasible where data exists – but this is typically on an individual city basis only and limited only to detailed risk assessments. As computing power increases the potential to exploit such large and detailed datasets is in reach of a high level analysis.
- At the continental scale there is limited data on the impacts and costs of extreme events. An EU database of observations from extreme events could be used to construct city specific and/or national damage functions that relate the magnitude of a hazard to damages. Such functions have been developed by the insurance industry but these are generally commercially sensitive, and only include insured losses. Public datasets such as EMDAT record events and headline impacts but provide insufficient information to construct detailed functions. Similarly several countries have collated depth-damage relationships for flooding (e.g. Penning-Rowsell et al., 2013) but approaches differ and coverage or data access across Europe is limited.

- A major gap in assessing vulnerability is an understanding of what has been done 'on the ground' in each city. For example, how high are existing flood defences, what design standards have been employed for urban drainage *etc*. In this study, we have assessed adaptive capacity (via a number of proxy indicators) to capture this, but a database, possibly crowdsourced by individual cities and inhabitants who provide information on risk management interventions via an App or a similar tool, would enable much more rigorous risk analysis.
- Further work should also consider a wider range of impacts and exposures. For example, there is currently no Europe-wide coverage of all infrastructure – but disruption to infrastructure causes a number of cascading impacts that magnify climate change risks.
- An interdisciplinary research programme for "Broad Scale Climate Risk Modelling" would help galvanise a number of activities and innovations that have been developed here and in other research. Sectorally, initiatives such as the Global Earthquake Model have brought together the earthquake community and provided a focal point for data and simulation innovation. Drawing from these and other experiences an EU programme could deliver a flexible, scalable and integrated set of climate risk and resilience modelling tools.
- Neither the indicator-based vulnerability assessment nor the integrated risk analysis presented here can be used to make absolute comparisons between different risks. The nature of the calculation means that an identical score could have very different implications for e.g. flooding and heatwaves. Similarly, this method does not enable comparison between different study areas if those risks are calculated independently. These limitations call for the development of a new generation of indicator-based vulnerability – and, to some extent, risk analysis – that enable cross-temporal, cross-threat and cross-scale comparisons by means of standard units of measure and absolute scales.
- Along these lines, further research is needed on the key determinants of climate change – related risks. Whereas there is a vast range of literature that characterise climate change – driven impacts building on the theoretical factors shaping risks at different spatial scales, such factors have not been characterised enough through 'disaster case studies' (Gall et al., 2014). It is thus difficult to build accurate and realistic climate change impact scenarios at the city level basing on the underlying risk factors alone.
- Furthermore, there is much room for improvement in defining more operational ways for managing socio-economic uncertainties within traditional IBVAs. The two main methodological approaches traditionally used in social sciences to handle uncertainty, namely the development of socio-economic scenarios and the construction of probabilistic models have limitations, are demanding in terms of time and resource consumption, and are difficult to communicate and combine with climatic data. Additional research on this topic should focus on the development of alternative simplified approaches for managing socio-economic uncertainties and link those with the traditional methods used by climate science.
- Similarly, further research is needed in order to understand the structural relations of the different components of risk at different scales. There is little evidence that the same structural relations among the different risk factors that have been documented in this study hold for all types of cities in different regions across the EU. It might well be the case that comparable underlying factors imply different levels of risk for different groups of cities. A possible way forward in this respect would be the elaboration of intermediate –level vulnerability and risk analysis based on more homogeneous groups of cities.

7 References

Adger W N, Brooks N, Bentham G, Agnew M, Eriksen S, 2004, "New indicators of vulnerability and adaptive capacity", Tyndall Centre for Climate Change Research, Norwich, UK, http://tyndall.ac.uk/sites/default/files/Adger W. N ., Brooks, N. , Kelly, M., Bentham, S. and Eriksen, S. (2004) New indicators of vulnerability and adaptive capacity (tr7).pdf

Alfieri L, Burek P, Feyen L, Forzieri G, 2015, "Global warming increases the frequency of river floods in Europe" *Hydrology and Earth System Sciences* **19**(5) 2247–2260

ARUP, 2014, "Reducing urban heat risk: A study on urban heat risk mapping and visualisation", London

ASC, 2014, "Adatation indicator set for the NAP"

Balica S F, Douben N, Wright N G, 2009, "Flood vulnerability indices at varying spatial scales." *Water science and technology : a journal of the International Association on Water Pollution Research* **60**(10) 2571–80, http://www.ncbi.nlm.nih.gov/pubmed/19923763

Balica S F, Wright N G, van der Meulen F, 2012, "A flood vulnerability index for coastal cities and its use in assessing climate change impacts" *Natural Hazards* **64**(1) 73–105, http://link.springer.com/10.1007/s11069-012-0234-1

Ban N, Schmidli J, Schär C, 2014, "Evaluation of the convection-resolving regional climate modeling approach in decade-long simulations" *Journal of Geophysical Research: Atmospheres* **119**(13) 7889–7907, http://doi.wiley.com/10.1002/2014JD021478

Ban N, Schmidli J, Schär C, 2015, "Heavy precipitation in a changing climate: Does short-term summer precipitation increase faster?" *Geophysical Research Letters* **42**(4) 1165–1172, http://doi.wiley.com/10.1002/2014GL062588

Barredo J I, 2007, "Major flood disasters in Europe: 1950–2005" *Natural Hazards* **42**(1) 125–148, http://link.springer.com/10.1007/s11069-006-9065-2

Birkmann J, Cardona O D, Carreño M L, Barbat a. H, Pelling M, Schneiderbauer S, Kienberger S, Keiler M, Alexander D, Zeil P, Welle T, 2013, "Framing vulnerability, risk and societal responses: The MOVE framework" *Natural Hazards* **67**(2) 193–211

Birkmann J, Wisner B, 2006, "Measuring the un-measurable: The Challenge of Vulnerability", http://www.ihdp.unu.edu/file/get/3962.pdf

Blenkinsop S, Fowler H J, 2007, "Changes in European drought characteristics projected by the PRUDENCE regional climate models" *International Journal of Climatology* **27**(12) 1595–1610, http://doi.wiley.com/10.1002/joc.1538

Boettle M, Costa L, Vousdoukas M, Voukouvalas E, Foster G, Costa H, Kriewald S, Zhou B, Chen P-Y, Kropp J P, Rybski D, 2016, "Coastal Floods in European Cities: Damage and Adaptation Functions"

Brooks N, Neil Adger W, Mick Kelly P, 2005, "The determinants of vulnerability and adaptive capacity at the national level and the implications for adaptation" *Global Environmental Change* **15**(2) 151–163, http://linkinghub.elsevier.com/retrieve/pii/S0959378004000913

Burton C G, 2012 *The Development of Metrics for Community Resilience to Natural Disasters*, University of South Carolina

Cardona O D, 2005, "A System of Indicators for Disaster Risk Management in the Americas", in *250th Anniversary of the 1755 Lisbon Earthquake*

Carreño M L, Cardona O D, Barbat A H, 2007, "A disaster risk management performance index" *Natural Hazards* **41**(1) 1–20, http://link.springer.com/10.1007/s11069-006-9008-y

Carter J G, Cavan G, Connelly A, Guy S, Handley J, Kazmierczak A, 2014, "Climate change and the city: Building capacity for urban adaptation" *Progress in Planning*, http://linkinghub.elsevier.com/retrieve/pii/S0305900614000397

Charlotte Vinchon, Carreño M-L, Contreras-Mojica D M, Kienberger S, Schneiderbauer S, Alexander D, Barbat A H, Cardona O D, Decker B, Eidsvig U, Papathoma-Köhle M, Miniati R, Pratzler-Wanczura S, Ulbrich T, Vangelsten B V, Welle T, 2011, "Assessing vulnerability to natural hazards in Europe: From Principles to Practice. A manual on concept, methodology and tools", MOVE Project.Methods for the Improvement of Vulnerability Assessment in Europe, http://www.move-fp7.eu

Cho E, Kim S, 2015, "Cronbach's Coefficient Alpha: Well Known but Poorly Understood" *Organizational Research Methods* **18**(2) 207–230, http://orm.sagepub.com/cgi/doi/10.1177/1094428114555994

Cutter S L, Ash K D, Emrich C T, 2014, "The geographies of community disaster resilience" *Global Environmental Change* **29** 65–77, http://www.sciencedirect.com/science/article/pii/S0959378014001459

Cutter S L, Barnes L, Berry M, Burton C, Evans E, Tate E, Webb J, 2008, "A place-based model for understanding community resilience to natural disasters" *Global Environmental Change* **18**(4) 598–606, http://linkinghub.elsevier.com/retrieve/pii/S0959378008000666

Cutter S L, Boruff B J, Shirley W L, 2003, "Social vulnerability to environmental hazards" *Social Science Quarterly* **84**(2) 242–261

Cutter S L, Burton C G, Emrich C T, 2010, "Disaster Resilience Indicators for Benchmarking Baseline Conditions" *Journal of Homeland Security and Emergency Management* **7**(1), http://www.degruyter.com/view/j/jhsem.2010.7.1/jhsem.2010.7.1.1732/jhsem.2010.7.1.1732.xml

Cutter S L, Emrich C T, Webb J J, Morath D, 2009, "Social Vulnerability to Climate the Literature Social Vulnerability to Climate Literature. Final Report to Oxfam America"

Dankers R, Feyen L, 2009, "Flood hazard in Europe in an ensemble of regional climate scenarios" *Journal of Geophysical Research: Atmospheres* **114**(16)

DG Environment, 2014, "Background note to the Climate Change Committee: Bridging the Adaptation Knowledge Gap – priorities for research, demonstration and innovation" 1–9

DG Regio, 2009, "Regions 2020 - Climate change challenges for European regions. Background Document to Commission Staff Working Document SEC(2008)"

Downing T E, 1990, "Assessing Socioeconomic Vulnerability To Famine: Frameworks, Concepts, and Applications" *FEWS Working Paper 2.1* (March) 1–129

Dumbser M, Toro E F, 2011, "On universal Osher-type schemes for general nonlinear hyperbolic conservation laws" *Communications in Computational Physics* **10**(3) 635–671

EEA, 2012, "Urban adaptation to climate change in Europe. Challenges and opportunities for cities together with supportive national and European policies", Luxembourg

El-Zein A, Tonmoy F N, 2015, "Assessment of vulnerability to climate change using a multi-criteria outranking approach with application to heat stress in Sydney" *Ecological Indicators* **48** 207–217, http://www.sciencedirect.com/science/article/pii/S1470160X14003677

Fekete A, 2009, "Validation of a social vulnerability index in context to river-floods in Germany" *Natural Hazards and Earth System Science* **9**(2) 393–403

Fischer E M, Schär C, 2010, "Consistent geographical patterns of changes in high-impact European heatwaves" *Nature Geoscience* **3**(6) 398–403, http://dx.doi.org/10.1038/ngeo866

Forzieri G, Feyen L, Rojas R, Flörke M, Wimmer F, Bianchi A, 2014, "Ensemble projections of future streamflow droughts in Europe" *Hydrology and Earth System Sciences* **18**(1) 85–

108, http://www.hydrol-earth-syst-sci.net/18/85/2014/

Foudi S, Osés-Eraso N, Tamayo I, 2015, "Integrated spatial flood risk assessment: The case of Zaragoza" *Land Use Policy* **42** 278–292, http://linkinghub.elsevier.com/retrieve/pii/S0264837714001720

Frazier T G, Thompson C M, Dezzani R J, 2014, "A framework for the development of the SERV model: A Spatially Explicit Resilience-Vulnerability model" *Applied Geography* **51** 158–172, http://linkinghub.elsevier.com/retrieve/pii/S0143622814000745

Füssel H-M, 2009, "Review and quantitative analysis of indices of climate change exposure, adaptive capacity, sensitivity and impacts. Capacity, Sensitivity, and Impacts, Background note to the World Development Report 2010"

Gall M, Nguyen K, Cutter S L, 2014, "Integrated research on disaster risk: is it really integrated?" *International Journal of Disaster Risk Reduction* 1–13, http://dx.doi.org/10.1016/j.ijdrr.2015.01.010

Glenis V, McGough A S, Kutija V, Kilsby C, Woodman S, 2013, "Flood modelling for cities using Cloud computing" *Journal of Cloud Computing: Advances, Systems and Applications* **2**(1) 7, http://www.journalofcloudcomputing.com/content/2/1/7

Godunov S K, 1959, "Finite Difference Method for Numerical Computation of Discontinuous Solutions of the Equations of Fluid Dynamics" *Matematicheski Sbornik* **47** 271–306

Guillaumont P, Simonet C, 2011, "Designing an index of structural vulnerability to climate change", http://meteo.vnu.edu.vn/bmkt/Danida/References/Vulnerability/Designing an index of structural vulnerability to climate change.pdf

Hailegeorgis T T, Thorolfsson S T, Alfredsen K, 2013, "Regional frequency analysis of extreme precipitation with consideration of uncertainties to update IDF curves for the city of Trondheim" *Journal of Hydrology* **498** 305–318, http://linkinghub.elsevier.com/retrieve/pii/S0022169413004629

Harten A, Lax P D, Leer B van, 1983, "On Upstream Differencing and Godunov-Type Schemes for Hyperbolic Conservation Laws" *SIAM Review* **25**(1) 35–61, http://epubs.siam.org/doi/abs/10.1137/1025002

Hijmans R J, Cameron S E, Parra J L, Jones P G, Jarvis A, 2005, "Very high resolution interpolated climate surfaces for global land areas" *International Journal of Climatology* **25**(15) 1965–1978, http://doi.wiley.com/10.1002/joc.1276

Holsten A, Kropp J, 2012, "An integrated and transferable climate change vulnerability assessment for regional application" *Natural hazards*, http://link.springer.com/article/10.1007/s11069-012-0147-z

Iglesias A, Moneo M, Quiroga S, 2009 *Coping with Drought Risk in Agriculture and Water Supply Systems* Eds A Iglesias, A Cancelliere, D A Wilhite, L Garrote, and F Cubillo (Springer Netherlands, Dordrecht), http://link.springer.com/chapter/10.1007/978-1-4020-9045-5_11

IPCC, 2001, "Climate change 2001: impacts, adaptation, and vulnerability: contribution of Working Group II to the third assessment report of the Intergovernmental Panel" Eds J J McCarthy, O F Canziani, N A Leary, D J Dokken, and K S White

IPCC, 2012, "Managing the Risks of Extreme Events and Disasters to Advance Climate Change Adaptation. A Special Report of Working Groups I and II of the Intergovernmental Panel on Climate Change" Eds C B Field, V Barros, T F Stocker, and Q Dahe, Cambridge University Press, Cambridge, UK, and New York, NY, USA, http://ebooks.cambridge.org/ref/id/CBO9781139177245

IPCC, 2013, "Climate Change 2013: The Physical Science Basis. Contribution of Working Group I to the Fifth Assessment Report of the Intergovernmental Panel on Climate Change. Summary for Policymakers" Ed V B and P M M Stocker, T.F., D. Qin, G.-K. Plattner, M. Tignor, S. K. Allen, J. Boschung, A. Nauels, Y. Xia, Cambridge University

Press, Cambridge, United Kingdom and New York, NY, USA

IPCC, 2014 *Climate Change 2014: Impacts, Adaptation, and Vulnerability. Part A: Global and Sectoral Aspects. Contribution of Working Group II to the Fifth Assessment Report of the Intergovernmental Panel on Climate Change* Eds C B Field, V R Barros, D J Dokken, K J Mach, M D Mastrandrea, T E Bilir, M Chatterjee, K L Ebi, Y O Estrada, R C Genova, B Girma, E S Kissel, A N Levy, S MacCracken, P R Mastrandrea, and L L White (Cambridge University Press, Cambridge, United Kingdom and New York, NY, USA)

Jacobs C, Kazmierczak A, Krellenberg K, Kuhlicke C, Peltonen L, 2012, "Urban Vulnerability Indicators A joint report of ETC-CCA and ETC-SIA"

Jeremy Carter, Connelly A, Handley J, Lindley S, 2012, "European Cities in a Changing Climate: Exploring climate change hazards, impacts and vulnerabilities", Centre for Urban and Regional Ecology, The University of Manchester

Johnson D P, Stanforth A, Lulla V, Luber G, 2012, "Developing an applied extreme heat vulnerability index utilizing socioeconomic and environmental data" *Applied Geography* **35**(1-2) 23–31, http://linkinghub.elsevier.com/retrieve/pii/S014362281200032X

Jun K-S, Chung E-S, Kim Y-G, Kim Y, 2013, "A fuzzy multi-criteria approach to flood risk vulnerability in South Korea by considering climate change impacts" *Expert Systems with Applications* **40**(4) 1003–1013, http://linkinghub.elsevier.com/retrieve/pii/S0957417412009748

Kaźmierczak A, Cavan G, 2011, "Surface water flooding risk to urban communities: Analysis of vulnerability, hazard and exposure" *Landscape and Urban Planning* **103**(2) 185–197, http://linkinghub.elsevier.com/retrieve/pii/S0169204611002404

Kendon E J, Roberts N M, Fowler H J, Roberts M J, Chan S C, Senior C A, 2014, "Heavier summer downpours with climate change revealed by weather forecast resolution model" *Nature Climate Change* **4**(7) 570–576, http://www.nature.com/doifinder/10.1038/nclimate2258

Kienberger S, Blaschke T, Zaidi R Z, 2013, "A framework for spatio-temporal scales and concepts from different disciplines: The 'vulnerability cube'" *Natural Hazards* **68**(3) 1343–1369

Klein Rosenthal J, Kinney P L, Metzger K B, 2014, "Intra-urban vulnerability to heat-related mortality in New York City, 1997-2006." *Health & place* **30C** 45–60, http://www.ncbi.nlm.nih.gov/pubmed/25199872

van der Knijff J M, Younis J, De Roo A P J, 2010, "LISFLOOD: a GIS-based distributed model for river basin scale water balance and flood simulation" *International Journal of Geographical Information Science* **24**(2) 189–212, http://www.tandfonline.com/doi/abs/10.1080/13658810802549154

Knutson C, Hayes M, Phillips T, 1998, "How to reduce drought risk", Western Drought Coordination Council, Lincoln, Nebraska

Kocornik-Mina A, Mcdermott T, Michaels G, Rauch F, 2015, "Flooded cities", Centre for Climate Change Economics and Policy and Grantham Research Institute on Climate Change and the Environment, London, UK

Koks E E, Jongman B, Husby T G, Botzen W J W, 2015, "Combining hazard, exposure and social vulnerability to provide lessons for flood risk management" *Environmental Science & Policy* **47** 42–52, http://linkinghub.elsevier.com/retrieve/pii/S1462901114002056

Kuhlicke C, Scolobig A, Tapsell S, Steinführer A, De Marchi B, 2011, "Contextualizing social vulnerability: findings from case studies across Europe" *Natural Hazards* **58**(2) 789–810, http://link.springer.com/10.1007/s11069-011-9751-6

Kunreuther H, Heal G, Allen M, Edenhofer O, Field C B, Yohe G, 2013, "Risk management and climate change" *Nature Climate Change* **3**(5) 447–450, http://www.nature.com/doifinder/10.1038/nclimate1740

Lee Y-J, 2014, "Social vulnerability indicators as a sustainable planning tool" *Environmental Impact Assessment Review* **44** 31–42, http://linkinghub.elsevier.com/retrieve/pii/S0195925513000802

van Leer B, 1979, "Towards the ultimate conservative difference scheme. V. A second-order sequel to Godunov's method" *Journal of Computational Physics* **32**(1) 101–136

van Leer B, 1984, "On the Relation Between the Upwind-Differencing Schemes of Godunov, Engquist–Osher and Roe" *SIAM Journal on Scientific and Statistical Computing* **5**(1) 1–20, http://epubs.siam.org/doi/abs/10.1137/0905001

Lissner T K, Holsten A, Walther C, Kropp J P, 2012, "Towards sectoral and standardised vulnerability assessments: the example of heatwave impacts on human health" *Climatic Change* **112**(3-4) 687–708, http://link.springer.com/10.1007/s10584-011-0231-5

Liu J, Dietz T, Carpenter S R, Alberti M, Folke C, Moran E, Pell A N, Deadman P, Kratz T, Lubchenco J, Ostrom E, Ouyang Z, Provencher W, Redman C L, Schneider S H, Taylor W W, 2007, "Complexity of coupled human and natural systems" *Science (New York, N.Y.)* **317**(5844) 1513–1516

Merz M, Hiete M, Comes T, Schultmann F, 2013, "A composite indicator model to assess natural disaster risks in industry on a spatial level" *Journal of Risk Research* **16**(April 2014) 1077–1099, http://www.tandfonline.com/doi/abs/10.1080/13669877.2012.737820

Müller a., Reiter J, Weiland U, 2011, "Assessment of urban vulnerability towards floods using an indicator-based approach – a case study for Santiago de Chile" *Natural Hazards and Earth System Science* **11**(8) 2107–2123, http://www.nat-hazards-earth-syst-sci.net/11/2107/2011/

Nardo, M., Saisana M, Saltelli A, Tarantola. S, 2008 *Handbook on Constructing Composite Indicators: Methodgy and User Guide* (OECD Publishing, Paris, France)

Nardo M, Saisana M, Saltelli A, Tarantola S, 2005, "Tools for composite indicators building", EC. Joint Research Centre, Ispra (VA), Italy

Nicholls R J, de la Vega-Leinert A C, 2008, "Implications of Sea-Level Rise for Europe's Coasts: An Introduction" *Journal of Coastal Research* **242** 285–287, http://www.bioone.org/doi/abs/10.2112/07A-0002.1

Nicoletti G, Scarpetta S, Boyland O, 1999, "Summary Indicators of Product Market Regulation with an Extension to Employment Protection Legislation", OECD, http://www.oecd.org/eco/eco

Osher S, Solomon F, 1982, "Upwind Difference Schemes for Hyperbolic Systems of Conservation Laws" *Mathematics of Computation* **38**(158) pp. 339–374, http://www.jstor.org/stable/2007275

Oudin L, Andreassian V, Perrin C, Michel C, Moine N L, 2008, "Spatial proximity, physical similarity, regression and ungauged catchments: A comparison of regionalisation approaches based on 913 French catchments" *Water Resources Research* **44** 1–15

Panagos P, Ballabio C, Borrelli P, Meusburger K, Klik A, Rousseva S, Tadić M P, Michaelides S, Hrabalíková M, Olsen P, Aalto J, Lakatos M, Rymszewicz A, Dumitrescu A, Beguería S, Alewell C, 2015, "Rainfall erosivity in Europe" *Science of The Total Environment* **511** 801–814, http://linkinghub.elsevier.com/retrieve/pii/S004896971500011X

Penning-Rowsell E C, Priest S J, Parker D J, Morris J, Tunstall S M, Viavatenne C, Chatterton J, D. O, 2013 *Flood and Coastal Erosion Risk Management. A manual for economic appraisal* (Routledge, London)

Prein A F, Langhans W, Fosser G, Ferrone A, Ban N, Goergen K, Keller M, Tölle M, Gutjahr O, Feser F, Brisson E, Kollet S, Schmidli J, van Lipzig N P M, Leung R, 2015, "A review on regional convection-permitting climate modeling: Demonstrations, prospects, and challenges" *Reviews of Geophysics* **53**(2) 323–361, http://doi.wiley.com/10.1002/2014RG000475

Preston B L, 2012, "Climate Change Vulnerability Assessment: From Conceptual Frameworks to Practical Heuristics", http://www.csiro.au/en/Organisation-Structure/Flagships/Climate-Adaptation-Flagship/CAF-

Preston B L, Smith T F, Brooke C, Gorddard R, Measham T g., Withycombe G, Mcinnes K, Abbs D, Beveridge B, Morrison C, 2008, "Mapping Climate Change Vulnerability in the Sydney Coastal Councils Group. Prepared for the Sydney Coastal Councils Group"

Reckien D, Flacke J, Dawson R J, Heidrich O, Olazabal M, Foley A, Hamann J J-P P, Orru H, Salvia M, Gregorio Hurtado S, Geneletti D, Pietrapertosa F, de Gregorio Hurtado S, Geneletti D, Pietrapertosa F, 2014, "Climate change response in Europe: What's the reality? Analysis of adaptation and mitigation plans from 200 urban areas in 11 countries" *Climatic Change* **122** 331–340, http://link.springer.com/10.1007/s10584-013-0989-8

Ricardo-AEA, 2013, "Adaptation Strategies for European Cities"

Rojas R, Feyen L, Bianchi A, Dosio A, 2012, "Assessment of future flood hazard in Europe using a large ensemble of bias-corrected regional climate simulations" *Journal of Geophysical Research: Atmospheres* **117**(D17) n/a–n/a, http://doi.wiley.com/10.1029/2012JD017461

Roudier P, Andersson J C M, Donnelly C, Feyen L, Greuell W, Ludwig F, 2016, "Projections of future floods and hydrological droughts in Europe under a +2°C global warming" *Climatic Change* **135**(2) 341–355, http://link.springer.com/10.1007/s10584-015-1570-4

Salinas J L, Laaha G, Rogger M, Parajka J, Viglione A, Sivapalan M, Blöschl G, 2013, "Comparative assessment of predictions in ungauged basins – Part 2: Flood and low flow studies" *Hydrology and Earth System Sciences* **17**(7) 2637–2652, http://www.hydrol-earth-syst-sci.net/17/2637/2013/

Schauser I, Otto S, Schneiderbauer S, Harvey A, Hodgson N, Robrecht H, Morchain D, Schrander J, Khovanskaia M, Prutsch A, Mccallum S, 2010, "Urban Regions: Vulnerabilities, Vulnerability Assessments by Indicators and Adaptation Options for Climate Change Impacts. Scoping Study", European Topic Centre on Air and Climate Change (ETC/ACC), Bilthoven, The Netherlands

Scheurich A, Müller M J, Wetzel H, Anghelescu I, Klawe C, Ruppe A, Lörch B, Himmerich H, Heidenreich M, Schmid G, Hautzinger M, Szegedi A, 2000, "Reliability and validity of the German version of the European Addiction Severity Index (EuropASI)." *Journal of Studies on Alcohol* **61**(6) 916–919, http://www.jsad.com/doi/10.15288/jsa.2000.61.916

Smith A, Sampson C, Bates P, 2015, "Regional flood frequency analysis at the global scale" *Water Resources Research* **51**(1) 539–553, http://doi.wiley.com/10.1002/2014WR015814

Stefan Greiving et al., 2011, "ESPON Climate. Climate Change and Territorial Effects on Regions and Local Economies. Applied Research 2013/1/4. Final Report | Version 31/5/2011"

Stefano L De, Tánago I G, Ballesteros M, Urquijo J, Blauhut V, James H, Stahl K, Stefano L De, Tánago I G, Ballesteros M, Blauhut V, Stagge J H, Stahl K, 2015, "Methodological Approach Considering Different Factors Influencing Vulnerability – Pan-European Scale", DROUGHT-R&SPI (Fostering European Drought Research and Science-Policy Interfacing) - ENV.2011.1.3.2-2. Tecnical Report No. 26.

Tapsell S M, Penning-Rowsell E C, Tunstall S M, Wilson T L, 2002, "Vulnerability to flooding: health and social dimensions." *Philosophical transactions. Series A, Mathematical, physical, and engineering sciences* **360** 1511–1525

Terenzi A, Wigström A ., 2014, "RAMSES – D9.1. Stakeholder Survey Report"

Tonmoy F N, El-Zein A, Hinkel J, 2014, "Assessment of vulnerability to climate change using indicators: a meta-analysis of the literature" *Wiley Interdisciplinary Reviews: Climate Change* **5**(6) 775–792, http://onlinelibrary.wiley.com/doi/10.1002/wcc.314/full

Turner B L, Kasperson R E, Matson P A, McCarthy J J, Corell R W, Christensen L, Eckley N,

Kasperson J X, Luers A, Martello M L, Polsky C, Pulsipher A, Schiller A, 2003, "A framework for vulnerability analysis in sustainability science." *Proceedings of the National Academy of Sciences of the United States of America* **100**(14) 8074–9, http://www.pnas.org/content/100/14/8074.short

Turner B L, Matson P a, McCarthy J J, Corell R W, Christensen L, Eckley N, Hovelsrud-Broda G K, Kasperson J X, Kasperson R E, Luers A, Martello M L, Mathiesen S, Naylor R, Polsky C, Pulsipher A, Schiller A, Selin H, Tyler N, 2003, "Illustrating the coupled human-environment system for vulnerability analysis: three case studies." *Proceedings of the National Academy of Sciences of the United States of America* **100**(14) 8080–8085

Uejio C K, Wilhelmi O V, Golden J S, Mills D M, Gulino S P, Samenow J P, 2011, "Intra-urban societal vulnerability to extreme heat: the role of heat exposure and the built environment, socioeconomics, and neighborhood stability." *Health & place* **17**(2) 498–507, http://www.ncbi.nlm.nih.gov/pubmed/21216652

UN-Habitat, 2011, "Cities and Climate Change: Global Report on Human Settlements"

Villagrán-De-Leon J C, 2006, "Vulnerability: A conceptual and methodological review", http://scholar.google.com/scholar?hl=en&btnG=Search&q=intitle:Vulnerability:+A+conceptual+and+methodological+review#0

Wilhite D A, Hayes M J, 2005, "The Basics of Drought Planning: A 10-Step Process" 15

Wisner B, Blaikie P, Cannon T, Davis I, 1994 *At risk: natural hazards, people's vulnerability and disasters* (Routledge, London)

Wolf T, McGregor G, 2013, "The development of a heat wave vulnerability index for London, United Kingdom" *Weather and Climate Extremes* **1**(August 2003) 59–68, http://linkinghub.elsevier.com/retrieve/pii/S2212094713000054

World Bank, 2010, "Cities and Climate Change: An Urgent Agenda", Washington DC

Zhou B, Rybski D, Kropp J P, 2013, "On the statistics of urban heat island intensity" *Geophysical Research Letters* **40**(20) 5486–5491

Appendix A: Data model

Code	Description	Number of cities[13]	Weights per impact chain					Transformation method
			HW	DR	FLP	FLF	FLC	
HWDAYSUNEWI	Relative change on the percentage of days classified as heatwaves days between 1951-2000 and 2051-2100 for low, medium and high impact scenarios	571	0.33	-	-	-	-	Untransformed
HWMAXUNEWI	Change in the maximum daily maximum temperature between 1951-2000 and 2051-2100 (units: ºC) for low, medium and high impact scenarios	571	0.33	-	-	-	-	Untransformed
UHIPIKI	UHI intensity based on 8-day averaged daily mean land surface temperature (LST, i.e. skin surface temperature) data during summer months (June-August) 2006-2013. Data from MODIS (MOD11A2, MYD11A2) datasets (Zhou et al., 2013).	571	0.33	-	-	-	-	Square method
DSI12RCUNEWI	Relative change on the DSI-12 indicator (2051-2100 over 1951-2000) for low, medium and high impact scenarios	571	-	0.50	-	-	-	Untransformed
DSI12PROBUNEWI	Probability for any given month in the future to be above the maximum historical DSI-12 indicator (2051-2100 over 1951-2000) for low, medium and high impact scenarios	571	-	0.50	-	-	-	Untransformed
FLPUNEWI	Changes in the percentage of city flooded using 0.9, 1.2 and 1.5 change factors for hourly rainfall for 10 year return period	571	-	-	1.00	-	-	Untransformed
FLFUNEWI	Changes in the 10 year return period of annual maximum daily discharge (Q10)	365	-	-	-	1.00	-	Untransformed

Table 13:Transformation method and weights applied to each variable included in the hazard indices.

[13] Including imputed values.

Code	Description	Number of cities[14]	Weights per impact chain					Transformation method
			HW	DR	FLP	FLF	FLC	
DE1001V	Population on the 1st of January (last figure available 2004 to 2013), total	571	0.50	0.33	-	-	-	Log method
SA1001V	Number of conventional dwellings	571	0.50	0.33	-	-	-	Square root method
EC2021V	All companies	571	-	0.33	-	-	-	Log method
PEOFLPTECI	Estimated additional population potentially exposed to flooding using 0.9, 1.2 and 1.5 change factors for hourly rainfall for 10 year return period	571	-	-	1.00	-	-	Untransformed
COFLPIKI	Coastal flooding. Percentage of the city cluster potentially flooded due to a 100 year coastal storm surge event (Boettle et al., 2016).	92	-	-	-	-	1.00	Log method

Table 14:Transformation method and weights applied to each variable included in the exposure indices.

[14] Including imputed values

Code	Description	Number of cities[15]	Weights per impact chain					Transformation method
			HW	DR	FLP	FLF	FLC	
EEASEALI	Mean soil sealing [%] of UMZ 2006 of core city (EEA 2012)	571	-	-	0.21	0.22	-	Quadratic root method
EN2002V	Number of days ozone O^3 concentrations exceed 120 µg/m³	571	0.07	-	-	-	-	Log method
EN2005V	Number of days particulate matter PM10 concentrations exceed 50 µg/m³	571	0.06	-	-	-	-	Log method
EN2025V	Accumulated ozone concentration in excess 70 µg/m³	571	0.07	-	-	-	-	Square root method
EN2026V	Annual average concentration of NO^2 (µg/m³)	571	0.09	-	-	-	-	Square root method
EN2027V	Annual average concentration of PM10 (µg/m³)	571	0.05	-	-	-	-	Square root method
EN3010V	Price of a m³ of domestic water - Euro	571	-	0.15	-	-	-	Log method
DE3002I	Proportion of households that are 1-person households	571	0.07	-	-	-	-	Untransformed
DE3005I	Proportion of households that are lone-parent households	571	0.08	-	-	-	-	Log method
DE3008I	Proportion of households that are lone-pensioner households	571	0.06	-	-	-	-	Square root method
DE3016I	Lone parent households per 100 households with children aged 0-17	571	0.07	-	-	-	-	Square root method
EC1020I	Unemployment rate	571	0.12	0.23	0.29	0.29	0.39	Log method
DE2003I	Non-EU foreigners as a proportion of population	571	0.06	0.05	0.29	0.29	0.39	Log method
DE1040I	Proportion of population aged 0-4 years	571	0.05	-	0.09	0.08	0.11	Square root method
DE1055I	Proportion of population aged 75 years and over	571	0.05	-	0.12	0.12	0.11	Square root method
EN5101ITECI	Population density: total resident pop. per square km. Indicator built basing on GISCO GIS layers and Urban Audit population data (DE1001V - Population on the 1st of January, total)	571	0.08	0.18	-	-	-	Log method
SA2013TECI	Number of deaths per year under 65 due to diseases of the circulatory or respiratory systems per 1000 inhabitants, based on Urban Audit data: SA2013V - Number of deaths per year under 65 due to diseases of the circulatory or respiratory systems and DE1001V - Population on the 1st of January, total	571	0.02	-	-	-	-	Log method
EN3003TECI	Total use of water (m³ per capita per year) basing on Urban Audit data: EN3003V - Total use of water - m³and DE1001V - Population on the 1st of January, total	571	-	0.18	-	-	-	Square root method
DE1001TECI	Population growth rate over the period 2004-2012, basing on DE1001V - Population on the 1st of January, total retrieved from Urban Audit	571	-	0.21	-	-	-	Square method

Table 15:Transformation method and weights applied to each variable included in the sensitivity indices.

[15] Including imputed values

Code	Description	Number of cities[16]	Weights per impact chain					Transformation method
			HW	DR	FLP	FLF	FLC	
EEAGRBLI	Green/blue urban area [%] UMZ 2006 of core city (EEA 2012)	571	0.27	-	-	-	-	Untransformed
EC3039V	Median disposable annual household income - EUR	571	0.06	0.08	0.11	0.11	0.13	Log method
EC3040V	Average disposable annual household income - EUR	571	0.06	0.08	0.11	0.11	0.11	Untransformed
SA1007I	Proportion of households living in houses	571	0.06	-	-	-	-	Square root method
SA1022V	Average area of living accommodation - m²/person	571	0.03	-	-	-	-	Untransformed
PS3090TECV	Most people can be trusted (synthetic index 0-100)	571	0.10	0.08	0.11	0.11	0.10	Square method
PS3120TECV	City committed to fight against climate change (synthetic index 0-100)	571	0.10	0.08	0.11	0.11	0.10	Square method
TE2031TECI	Proportion of working age population qualified at level 5 or 6 ISCED, basing on Urban Audit data: TE2031V - Persons (aged 25-64) with ISCED level 5 or 6 as the highest level of education and population data: DE1058V - Population on the 1st of January, 25-34 years, total; DE1061V - Population on the 1st of January, 35-44 years, total; DE1064V - Population on the 1st of January, 45-54 years, total; DE1025V - Population on the 1st of January, 55-64 years, total	571	0.09	0.11	0.16	0.16	0.17	Square method
AWGCCTECI	Google hits for the string "climate change" (hits per thousand inhabitants). Search performed in April 2015 using the Custom Search JSON/Atom API by Google	571	0.06	0.09	0.12	0.12	0.12	Square root method
AWGHWTECI	Google hits for the string "city name & climate change & heatwave" (hits per million inhabitants). Search performed in April 2015 using the Custom Search JSON/Atom API by Google	571	0.07	-	-	-	-	Square root method
AWGUHITECI	Google hits for the string "city name & climate change & urban heat island" (hits per million inhabitants). Search performed in April 2015 Custom Search JSON/Atom API by Google	571	0.04	-	-	-	-	Log method
AWGFLOTECI	Google hits for the string "city name & climate change & flood" (hits per million inhabitants). Search performed in April 2015 using the Custom Search JSON/Atom API by Google	571	-	-	0.13	0.13	-	Square root method

[16] Including imputed values

AWGDROTECI	Google hits for the string "city name & climate change & drought" (hits per million inhabitants). Search performed in April 2015 using the Custom Search JSON/Atom API by Google	571	-	0.09	-	-	-	Square root method
AWGSLRTECI	Google hits for the string "city name & climate change & sea level rise" (hits per million inhabitants). Search performed in April 2015 using the Custom Search JSON/Atom API by Google	571	-	-	-	-	0.12	Square root method
ECSHADIVTECI	Shannon index of economic diversity, basing on Urban Audit data on Employment (jobs) in NACE sectors (EC2008V to EC2038V)	571	-	0.27	-	-	-	Cubic root method
MAYADTECV	City participating in Mayors Adapt initiative, basing on http://mayors-adapt.eu/taking-action/participating-cities/. Accessed 23 July 2015	571	0.06	0.12	0.15	0.15	0.15	Log method

Table 16:Transformation method and weights applied to each variable included in the adaptive capacity indices.

Appendix B: Literature review

This Appendix provides a description on the literature review performed in this work. This review allowed researchers to: (1) select and characterise the most relevant impact chains to be considered in our assessment; (2) identify the most appropriate analytical methods and tools among the ones usually used to produce vulnerability and risk assessments at the urban and sub-urban levels, and; (3) choose the most meaningful indicators – and proxies – within each risk component.

The literature review was first based on a cross-reference research of scientific papers citing a reduced number of 'seminal papers' on vulnerability and risk assessment at the urban level. These papers are shown in Table 17.

Concept	Seminal paper / report
The Social Amplification of Risk	Kasperson, R. E., Renn, O., Slovic, P., Brown, H. S., Emel, J., Goble, R., … Ratick, S. (1988). The Social Amplification of Risk: A Conceptual Framework. Risk Analysis, 8(2), 177 – 187. doi:10.1111/j.1539-6924.1988.tb01168.x
Vulnerability and capability	Anderson and Woodrow (1989), in Downing, T. E. (1990). Assessing Socioeconomic Vulnerability To Famine: Frameworks, Concepts, and Applications. FEWS Working Paper 2.1, (March), 1 – 129.
Causal chain of hazard development	Dowing (1991). In Dowing, T. E., & Patwardhan, A. (2005). Assessing Vulnerability for Climate Adaptation. In Adaptation Policy Frameworks for Climate Change: Developing Strategies, Policies and Measures (pp. 69 – 89). Cambridge, UK, and New York, NY, USA: Cambridge University Press
The two sides of vulnerability: the Bohle model	Bohle (1993) In Villagrán-De-Leon, J. C. (2006). Vulnerability: A conceptual and methodological review (No. 4). SOURCE - Studies of the University: Research, Counsel, Education (p. 64).
Three dimensions of vulnerability	Bohle, H. G., Downing, T. E., & Watts, M. J. (1994). Climate change and social vulnerability. Global Environmental Change, 4(1), 37 – 48. doi:10.1016/0959-3780(94)90020-5
Pressure and Release model	Wisner, B., Blaikie, P., Cannon, T., & Davis, I. (1994). At risk: natural hazards, people' s vulnerability and disasters. London: Routledge.
The access model	Wisner, B., Blaikie, P., Cannon, T., & Davis, I. (1994). At risk: natural hazards, people' s vulnerability and disasters. London: Routledge.
Damage functions	Carreño, M.-L., Cardona, O. D., & Barbat, A. H. (2007). Urban Seismic Risk Evaluation: A Holistic Approach. Natural Hazards, 40(1), 137 – 172. doi:10.1007/s11069-006-0008-8
Vulnerability interactions and feedbacks	Carter TR, La Rovere EL, Jones RN, Leemans R, Mearns LO, Nakı´cenovı´c N, Pittock B, Semenov SM, Skea J (2001) Developing and applying scenarios. In: McCarthy JJ, Can- ziani OF, Leary NA, Dokken DJ, White KS (eds) Climate change 2001. Impacts, adaptation, and vulnerability. Cam- bridge University Press, Cambridge, pp 145 – 190
Operationalization	Tapsell, S. M., Penning-Rowsell, E. C., Tunstall, S. M., & Wilson, T. L. (2002). Vulnerability to flooding: health and social dimensions. Philosophical Transactions. Series A, Mathematical, Physical, and Engineering Sciences, 360, 1511 – 1525. doi:10.1098/rsta.2002.1013
Vulnerability framework	Turner, B. L., Kasperson, R. E., Matson, P. A., McCarthy, J. J., Corell, R. W., Christensen, L., … Schiller, A. (2003). A framework for vulnerability analysis in sustainability science. Proceedings of the National Academy of Sciences of the United States of America, 100(14), 8074 – 9. doi:10.1073/pnas.1231335100
Operationalization	Klein, R. J. T. (2003). Adaptation to climate variability and change: What is optimal and appropriate. In C. Giupponi & M. Shechter (Eds.), Climate Change in the Mediterranean: Socio-Economic Perspectives of Impacts, Vulnerability and Adaptation (pp. 32 – 50). Cheltenham, UK: Edward Elgar.

BBC model	Bogardi, J., & Birkmann, J. (2004). Vulnerability assessment: the first step towards sustainable risk reduction. In D. Malzahn & T. Plapp (Eds.), Disaster and Society – From Hazard Assessment to Risk Reduction (pp. 75 – 82). Berlin: Logos Verlag Berlin.
Determinants of adaptive capacity (awareness, ability, action)	Schröter, D., Acosta-Michlik, L., Reidsma, P., Metzger, M., & Klein, R. J. T. (2003). Modelling the vulnerability of eco-social systems to global change: human adaptive capacity to changes in ecosystem service provision. In Open meeting on the Human Dimensions of Global Change (pp. 1 – 7).
Operationalization	2003 Cutter, S. L., Boruff, B. J., & Shirley, W. L. (2003). Social vulnerability to environmental hazards. Social Science Quarterly, 84(2), 242–261. doi:10.1111/1540-6237.8402002
Integrated vulnerability assessment	GTZ (2004) In Lummen, N., Miller, D., & Yamada, F. (2012).
Eight step methodology for global change methodology assessments	Schröter, D., Polsky, C., & Patt, A. G. (2005). Assessing vulnerabilities to the effects of global change: an eight step approach. Mitigation and Adaptation Strategies for Global Change, 10(4), 573 – 595. doi:10.1007/s11027-005-6135-9
Operationalization	UNFCCC. (2005). Compendium on methods and tools to evaluate impacts of, and vulnerability and adaptation to, climate change. Draft Final Report.
General	Adger, W. N. (2006). Vulnerability. Global Environmental Change, 16(3), 268 – 281. doi:10.1016/j.gloenvcha.2006.02.006.
Nested hierarchy model of vulnerability	Smit, B., & Wandel, J. (2006). Adaptation, adaptive capacity and vulnerability. Global Environmental Change, 16(3), 282 – 292. doi:10.1016/j.gloenvcha.2006.03.008
Adaptation policy assessment	Füssel, H.-M., & Klein, R. J. T. (2006). Climate Change Vulnerability Assessments: An Evolution of Conceptual Thinking. Climatic Change, 75(3), 301 – 329. doi:10.1007/s10584-006-0329-3
The multidimensional framework for vunberability	Villagrán-De-Leon, J. C. (2006). Vulnerability: A conceptual and methodological review (No. 4). SOURCE - Studies of the University: Research, Counsel, Education (p. 64). Retrieved from http://scholar.google.com/scholar?hl=en&btnG=Search&q=intitle:Vulnerability:+A+conceptual+and+methodological+review#0
Vulnerability spanning damage potential,resistance,and resilience	Bogardi (2006) en Villagrán-De-Leon, J. C. (2006)
General	Eakin, H., & Luers, A. L. (2006). Assessing the Vulnerability of Social-Environmental Systems. Annual Review of Environment and Resources, 31(1), 365 – 394. doi:10.1146/annurev.energy.30.050504.144352.
Vulnerability vs resilience	Gallopín, G. C. (2006). Linkages between vulnerability, resilience, and adaptive capacity. Global Environmental Change, 16(3), 293 – 303. doi:10.1016/j.gloenvcha.2006.02.004
Key spheres of the concept of vulnerability	Birkmann, J., & Wisner, B. (2006). Measuring the un-measurable: The Challenge of Vulnerability (No. 5). SOURCE - Studies of the University: Research, Counsel, Education (p. 64). Retrieved from http://www.ihdp.unu.edu/file/get/3962.pdf
Links between climate change adaptation and disaster risk management communities	Thomalla, F., Downing, T., Spanger-Siegfried, E., Han, G., & Rockström, J. (2006). Reducing hazard vulnerability: Towards a common approach between disaster risk reduction and climate adaptation. Disasters, 30(1), 39 – 48. doi:10.1111/j.1467-9523.2006.00305.x
Resilience	The concept of resilience revisited. SB Manyena - Disasters, 2006 - Wiley Online Library

The vulnerability scoping diagram	Polsky, C., Neff, R., & Yarnal, B. (2007). Building comparable global change vulnerability assessments: The vulnerability scoping diagram. Global Environmental Change, 17(3-4), 472 – 485. doi:10.1016/j.gloenvcha.2007.01.005
Outcome and contextual vulnerability	O'Brien, K., Eriksen, S., Nygaard, L. P. and Schjolden, A. (2007) Why different interpretations of vulnerability matter in climate change discourses. Climate Policy 7, 73 – 88.
End-point / starting-point interpretation	Füssel, H.-M. (2007). Vulnerability: A generally applicable conceptual framework for climate change research. Global Environmental Change, 17(2), 155 – 167. doi:10.1016/j.gloenvcha.2006.05.002
General concepts	Füssel, H.M. (2007). Adaptation planning for climate change: concepts, assessment approaches, and key lessons, Sustainability Science, 2, 265 – 275, DOI 10.1007/s11625-007-0032-y.
Scoping diagram	Polsky, C., Neff, R., & Yarnal, B. (2007). Building comparable global change vulnerability assessments: The vulnerability scoping diagram. Global Environmental Change, 17(3-4), 472 – 485. doi:10.1016/j.gloenvcha.2007.01.005
Operationalization	UNISDR. (2008). Linking Disaster Risk Reduction and Poverty Reduction: Good Practices and Lessons Learned, A Publication of the Global Network of NGOs for Disaster Risk Reduction. Geneva: UN/ISDR secretariat.
Disaster resilience of place (DROP model)	Cutter, S. L., Barnes, L., Berry, M., Burton, C., Evans, E., Tate, E., & Webb, J. (2008). A place-based model for understanding community resilience to natural disasters. Global Environmental Change, 18(4), 598 – 606. doi:10.1016/j.gloenvcha.2008.07.013
Diamond analogy	Parker, D. and Tapsell, S. et al., (2009) Deliverable 2.1. Relations between different types of social and economic vulnerability. Final draft report submitted to EU project 'Enhancing resilience of communities and territories facing natural and na-tech hazards' (ENSURE).
Current and future determinants of vulnerability	Preston, A. Ben, Stafford-smith, M., & Lee, B. L. B. (2009). Framing vulnerability and adaptive capacity assessment: Discussion paper (No. 2) (p. 60). Retrieved from http://www.csiro.au/org/ClimateAdaptationFlagship.html
The CLUVA model for a vulnerability ladder	Jean-Baptiste, N., Kuhlicke, C., Kunath, A., & Kabisch, S. (2011). CLUVA Project. D2.11: Review and evaluation of existing vulnerability indicators in order to obtain an appropriate set of indicators for assessing climate related vulnerability. Helmholtz Centre for Environmental Research - UFZ.
Top-down and bottom-up approaches	Carter, T. R., & Mäkinen, K. (2011). Approaches to climate change impact, adaptation and vulnerability assessment: towards a classification framework to serve decision-making. MEDIATION Technical Report No. 2.1. Helsinki, Finland. Retrieved from http://mediation-project.eu/
Operationalization	Hinkel, J. (2011). "Indicators of vulnerability and adaptive capacity": Towards a clarification of the science – policy interface. Global Environmental Change. Retrieved from http://www.sciencedirect.com/science/article/pii/S0959378010000750
A classification framework	Carter, T. R., & Mäkinen, K. (2011). Approaches to climate change impact, adaptation and vulnerability assessment: towards a classification framework to serve decision-making. MEDIATION Technical Report No. 2.1. Retrieved from http://mediation-project.eu/
Construction of damage functions	ERN - Evaluación de Riesgos Naturales - América Latina. (2011). Probabilistic Modelling of Natural Risks at the Gobal Level: the Hybrid Loss Exceedance Curve. Development of Methodology and Implementation of Case Studies. Phase 1a. Colombia, Mexico and Nepal. ISDR.
Operationalization	Jacobs, C., Kazmierczak, A., Krellenberg, K., Kuhlicke, C., & Peltonen, L. (2012). Urban Vulnerability Indicators A joint report of ETC-CCA and ETC-SIA.
Assessment framework	Jones, R. N., & Preston, B. L. (2011). Adaptation and risk management. Wiley Interdisciplinary Reviews: Climate Change, 2(2), 296 – 308. doi:10.1002/wcc.97
Operationalization	EEA. (2012). Urban adaptation to climate change in Europe. Challenges and opportunities for cities together with supportive national and European policies. Luxembourg.

Conceptual model for indicator-based hazard assessment	Lung, T., Lavalle, C., & Hiederer, R. (2013). A multi-hazard regional level impact assessment for Europe combining indicators of climatic and non-climatic change. Global Environmental. Retrieved from http://www.sciencedirect.com/science/article/pii/S0959378012001409
The vulnerability cube	Kienberger, S., Blaschke, T., & Zaidi, R. Z. (2013). A framework for spatio-temporal scales and concepts from different disciplines: The "vulnerability cube." Natural Hazards, 68(3), 1343 – 1369. doi:10.1007/s11069-012-0513-x
Vulnerability, resilience and adaptation	Lei, Y., Wang, J., Yue, Y., Zhou, H., & Yin, W. (2013). Rethinking the relationships of vulnerability, resilience, and adaptation from a disaster risk perspective. Natural Hazards, 70(1), 609 – 627. doi:10.1007/s11069-013-0831-7
Catastrophe risk models	Michel-Kerjan, E., Hochrainer-Stigler, S., Kunreuther, H., Linnerooth-Bayer, J., Mechler, R., Muir-Wood, R., ⋯ Young, M. (2013). Catastrophe risk models for evaluating disaster risk reduction investments in developing countries. Risk Analysis : An Official Publication of the Society for Risk Analysis, 33(6), 984 – 99. doi:10.1111/j.1539-6924.2012.01928.x
CLIMSAVE Vulnerability approach	Dunford, R., Harrison, P. A., Jäger, J., Rounsevell, M. D. A., & Tinch, R. (2014). Exploring climate change vulnerability across sectors and scenarios using indicators of impacts and coping capacity. Climatic Change. doi:10.1007/s10584-014-1162-8
Lifehood resilience	Ifejika Speranza, C., Wiesmann, U., & Rist, S. (2014). An indicator framework for assessing livelihood resilience in the context of social – ecological dynamics. Global Environmental Change, 28, 109 – 119. doi:10.1016/j.gloenvcha.2014.06.005
Adaptive social system	Blair, B., Lovecraft, A. L., & Kofinas, G. P. (2014). Meeting institutional criteria for social resilience: a nested risk system model. Ecology and Society, 19(4), art36. doi:10.5751/ES-06944-190436
Operationalization	Dunford, R., Harrison, P. A., Jäger, J., Rounsevell, M. D. A., & Tinch, R. (2014). Exploring climate change vulnerability across sectors and scenarios using indicators of impacts and coping capacity. Climatic Change. doi:10.1007/s10584-014-1162-8
Operationalization	Tonmoy, F. N. (2014). Assessment of vulnerability to climate change: theoretical and methodological developments with applications to infrastructure and built environment A thesis submitted in fulfillment of the requirements for the degree of. The University of Sydney.
Operationalization	Bowyer, P., Bender, S., Rechid, D., & Schaller, M. (2014). Adapting to Climate Change: Methods and Tools for Climate Risk Management (p. 124). Germany: Climate Service Center.

Table 17:Seminal papers that were used to structure the literature review.

Basing on this list of seminal papers, a number of cross-reference searches were performed using the Google Academics and the Web Of Science tools. Alerts for new works citing these seminal papers were also created on both platforms in order to update the database throughout the analytical process.

Additionally, a number of complementary searches were performed using different combinations of keywords selected from the terminology relevant for this subject, such as: Adapt* AND vulnerability, Adapt* AND risk, Adapt* AND cities, Climate change AND vulnerability, Climate change AND risk, Climate change AND cities.

In total, we selected 176 papers. Around a half of these included indicators that were eventually classified in the subjects listed on Table 6. Table 18 enumerates all the papers included in our review.

IPCC Reports
IPCC. (2007). Climate Change 2007: Impacts, Adaptation and Vulnerability. Contribution of Working Group II to the Fourth Assessment Report of the Intergovernmental Panel on Climate Change. (M. L. Parry, O. F. Canziani, J. P. Palutikof, P. J. van der Linden, & C. E. Hanson, Eds.) (p. 976). Cambridge, UK: Cambridge University Press.
IPCC. (2012). Managing the Risks of Extreme Events and Disasters to Advance Climate Change Adaptation. A Special

Report of Working Groups I and II of the Intergovernmental Panel on Climate Change. (C. B. Field, V. Barros, T. F. Stocker, & Q. Dahe, Eds.) (p. 582). Cambridge, UK, and New York, NY, USA: Cambridge University Press. doi:10.1017/CBO9781139177245
IPCC. (2014). Climate Change 2014: Impacts, Adaptation, and Vulnerability. Part A: Global and Sectoral Aspects. Contribution of Working Group II to the Fifth Assessment Report of the Intergovernmental Panel on Climate Change. (C. B. Field, V. R. Barros, D. J. Dokken, K. J. Mach, M. D. Mastrandrea, T. E. Bilir, … L. L. White, Eds.) (p. 1132). Cambridge, United Kingdom and New York, NY, USA: Cambridge University Press.
IPCC. (2014). Climate Change 2014: Impacts, Adaptation, and Vulnerability. Part A: Global and Sectoral Aspects. Contribution of Working Group II to the Fifth Assessment Report of the Intergovernmental Panel on Climate Change. (C. B. Field, V. R. Barros, D. J. Dokken, K. J. Mach, M. D. Mastrandrea, T. E. Bilir, … L. L. White, Eds.) (p. 1132). Cambridge, United Kingdom and New York, NY, USA: Cambridge University Press.
Climate Change Vulnerability Assessments
1981 Timmerman, P. (1981). Vulnerability, Resilience and the collapse of Society. Institute for Environmental Studies. Retrieved from http://www.ilankelman.org/miscellany/Timmerman1981.pdf
1994 Blaikie, P., Cannon, T., Davis, I., & Wisner, B. (1994). At risk: natural hazards, people's vulnerability and disasters. London: Routledge.
1996 Adger, W. N. (1996). Approaches to vulnerability to climate chaneg (No. GEC 96-05) (p. 63).
1998 Clark, G. E., Moser, S. C., Ratick, S. J., Meyer, W. B., Emani, S., Jin, W., … Schwarz, H. E. (1998). Assessing the vulnerability of coastal communities to extreme storms:the case of Revere,MA,USAN. Mitigation and Adaptation Strategies for Global Change, 3, 59–82.
1999 Neil Adger, W. (1999). Social Vulnerability to Climate Change and Extremes in Coastal Vietnam. World Development, 27(2), 249–269. doi:10.1016/S0305-750X(98)00136-3
1999 Smeets, E., & Weterings, R. (1999). Environmental indicators: Typology and overview. Environmental Indicators: Typology and Overview.
2000 Kelly, P. M., & Adger, W. N. (2000). Theory and Practice in Assessing Vulnerability to Climate Change and Facilitating Adaptation, 325–352. doi:10.1023/A:1005627828199
2003 ECLAC. (2003). Handbook for Estimating the Socio-economic and Environmental Effects of Disasters.
2003 Turner, B. L., Kasperson, R. E., Matson, P. A., McCarthy, J. J., Corell, R. W., Christensen, L., … Schiller, A. (2003). A framework for vulnerability analysis in sustainability science. Proceedings of the National Academy of Sciences of the United States of America, 100(14), 8074–9. doi:10.1073/pnas.1231335100
2003 Brooks, N. (2003). Vulnerability, risk and adaptation: A conceptual framework (No. 38). Tyndall Centre for Climate Change Research Working …. Retrieved from https://ipcc-wg2.gov/AR5-tools/author/njlite/data/7793.pdf
2003 Schröter, D., Acosta-Michlik, L., Reidsma, P., Metzger, M., & Klein, R. J. T. (2003). Modelling the vulnerability of eco-social systems to global change: human adaptive capacity to changes in ecosystem service provision. In Open meeting on the Human Dimensions of Global Change (pp. 1–7). Retrieved from http://www.researchgate.net/publication/40126404_Modelling_the_vulnerability_of_eco-social_systems_to_global_change_Human_adaptive_capacity_to_changes_in_ecosystem_service_provision/file/9fcfd507db02985b9a.pdf
2003 Cutter, S. L., Boruff, B. J., & Shirley, W. L. (2003). Social vulnerability to environmental hazards. Social Science Quarterly, 84(2), 242–261. doi:10.1111/1540-6237.8402002
2004 O'Brien, K., Leichenko, R., Kelkar, U., Venema, H., Aandahl, G., Tompkins, H., … West, J. (2004). Mapping vulnerability to multiple stressors: climate change and globalization in India. Global Environmental Change, 14(4), 303–313. doi:10.1016/j.gloenvcha.2004.01.001
2004 Adger, W. N., Brooks, N., Bentham, G., Agnew, M., & Eriksen, S. (2004). New indicators of vulnerability and adaptive capacity (p. 128). Norwich, UK: Tyndall Centre for Climate Change Research. Retrieved from http://tyndall.ac.uk/sites/default/files/Adger W. N ., Brooks, N. , Kelly, M., Bentham, S. and Eriksen, S. (2004) New indicators of vulnerability and adaptive capacity (tr7).pdf
2005 Cardona, O. D. (2005). A System of Indicators for Disaster Risk Management in the Americas. In 250th Anniversary of the 1755 Lisbon Earthquake.

2005 Mechler, R. (2005). Cost-benefit analysis of natural disaster risk management in developing countries. Eschborn: Deutsche Gesellschaft für Technische Zusammenarbeit (GTZ); Federal Ministry for Economic Cooperation and Development.

2005 Schröter, D., Polsky, C., & Patt, A. G. (2005). Assessing vulnerabilities to the effects of global change: an eight step approach. Mitigation and Adaptation Strategies for Global Change, 10(4), 573–595. doi:10.1007/s11027-005-6135-9

2005 Dowing, T. E., & Patwardhan, A. (2005). Assessing Vulnerability for Climate Adaptation. In Adaptation Policy Frameworks for Climate Change: Developing Strategies, Policies and Measures (pp. 69–89). Cambridge, UK, and New York, NY, USA: Cambridge University Press.

2005 Brooks, N., Neil Adger, W., & Mick Kelly, P. (2005). The determinants of vulnerability and adaptive capacity at the national level and the implications for adaptation. Global Environmental Change, 15(2), 151–163. doi:10.1016/j.gloenvcha.2004.12.006

2006 Smit, B., & Wandel, J. (2006). Adaptation, adaptive capacity and vulnerability. Global Environmental Change, 16(3), 282–292. doi:10.1016/j.gloenvcha.2006.03.008

2006 Adger, W. N. (2006). Vulnerability. Global Environmental Change, 16(3), 268–281. doi:10.1016/j.gloenvcha.2006.02.006

2006 Füssel, H.-M., & Klein, R. J. T. (2006). Climate Change Vulnerability Assessments: An Evolution of Conceptual Thinking. Climatic Change, 75(3), 301–329. doi:10.1007/s10584-006-0329-3

2006 Eakin, H., & Luers, A. L. (2006). Assessing the Vulnerability of Social-Environmental Systems. Annual Review of Environment and Resources, 31(1), 365–394. doi:10.1146/annurev.energy.30.050504.144352

2006 Birkmann, J. (2006). Indicators and criteria for measuring vulnerability: Theoretical bases and requirements. In J. Birkmann (Ed.), Measuring vulnerability to natural hazards: towards disaster resilient societies (Vol. 02, pp. 55–77). Tokyo: United Nations University. Retrieved from Click here for full text: http://WX7CF7ZP2H.search.serialssolutions.com/?V=1.0&L=WX7CF7ZP2H&S=JCs&C=TC0000200027&T=marc

2006 Birkmann, J., & Wisner, B. (2006). Measuring the un-measurable: The Challenge of Vulnerability (No. 5). SOURCE - Studies of the University: Research, Counsel, Education (p. 64). Retrieved from http://www.ihdp.unu.edu/file/get/3962.pdf

2006 Villagrán-De-Leon, J. C. (2006). Vulnerability: A conceptual and methodological review (No. 4). SOURCE - Studies of the University: Research, Counsel, Education (p. 64). Retrieved from http://scholar.google.com/scholar?hl=en&btnG=Search&q=intitle:Vulnerability:+A+conceptual+and+methodological+review#0

2006 Metzger, M. J., & Schröter, D. (2006). Towards a spatially explicit and quantitative vulnerability assessment of environmental change in Europe. Regional Environmental Change. doi:10.1007/s10113-006-0020-2

2007 Polsky, C., Neff, R., & Yarnal, B. (2007). Building comparable global change vulnerability assessments: The vulnerability scoping diagram. Global Environmental Change, 17(3-4), 472–485. doi:10.1016/j.gloenvcha.2007.01.005

2007 Füssel, H.-M. (2007). Vulnerability: A generally applicable conceptual framework for climate change research. Global Environmental Change, 17(2), 155–167. doi:10.1016/j.gloenvcha.2006.05.002

2007 Manuel-Navarrete, D., Gómez, J. J., & Gallopín, G. (2007). Syndromes of sustainability of development for assessing the vulnerability of coupled human–environmental systems. The case of hydrometeorological disasters in Central America and the Caribbean. Global Environmental Change, 17(2), 207–217. doi:10.1016/j.gloenvcha.2006.07.002

2008 Preston, B. L., Smith, T. F., Brooke, C., Gorddard, R., Measham, T. g., Withycombe, G., … Morrison, C. (2008). Mapping Climate Change Vulnerability in the Sydney Coastal Councils Group. Prepared for the Sydney Coastal Councils Group (p. 124).

2009 Preston, A. Ben, Stafford-smith, M., & Lee, B. L. B. (2009). Framing vulnerability and adaptive capacity assessment: Discussion paper (No. 2) (p. 60). Retrieved from http://www.csiro.au/org/ClimateAdaptationFlagship.html

2009 Cutter, S. L., Emrich, C. T., Webb, J. J., & Morath, D. (2009). Social Vulnerability to Climate the Literature Social Vulnerability to Climate Literature. Final Report to Oxfam America (pp. 1–44).

2009 DG Regio. (2009). Regions 2020 - Climate change challenges for European regions. Background Document to Commission Staff Working Document SEC(2008) (pp. 1–27).

2009 Füssel, H.-M. (2009). Review and quantitative analysis of indices of climate change exposure, adaptive capacity, sensitivity and impacts. Capacity, Sensitivity, and Impacts, Background note to the World Development Report 2010.

Washington D.C.: World Bank.
2009 Khan, S., & Crozier, M. J. (2009). "Hazardscape": A Holistic Approach to Assess Tipping Points in Humanitarian Crises. In Annual Summer Academy on Social Vulnerability: "Tipping Points in Humanitarian Crises." Hohenkammer, Munich, Germany.
2009 Heltberg, R., Siegel, P. B., & Jorgensen, S. L. (2009). Addressing human vulnerability to climate change: Toward a "no-regrets" approach. Global Environmental Change, 19(1), 89–99. doi:10.1016/j.gloenvcha.2008.11.003
2010 Schauser, I., Otto, S., Schneiderbauer, S., Harvey, A., Hodgson, N., Robrecht, H., … Mccallum, S. (2010). Urban Regions: Vulnerabilities, Vulnerability Assessments by Indicators and Adaptation Options for Climate Change Impacts. Scoping Study. Bilthoven, The Netherlands: European Topic Centre on Air and Climate Change (ETC/ACC).
2010 Tapsell, S., Mccarthy, S., Faulkner, H., Alexander, M., Mccarthy, S., Faulkner, H., … Bianchizza, C. (2010). Social vulnerability to natural hazards: CapHaz-Net WP4 Report. London: Flood Hazard Research Centre – FHRC, Middlesex University. Retrieved from http://caphaz-net.org/outcomes-results/CapHaz- Net_WP4_Social-Vulnerability.pdf
2010 Koh, J. (2010). Assessing Local Vulnerability to Climate Change and its Implications: the Case of Gyeonggi-Do. In Resilient Cities.
2010 Füssel, H. (2010). How inequitable is the global distribution of responsibility, capability, and vulnerability to climate change: A comprehensive indicator-based assessment. Global Environmental Change. Retrieved from http://www.sciencedirect.com/science/article/pii/S0959378010000683
2011 Guillaumont, P., & Simonet, C. (2011). Designing an index of structural vulnerability to climate change (No. I 08) (p. 40). Retrieved from http://meteo.vnu.edu.vn/bmkt/Danida/References/Vulnerability/Designing an index of structural vulnerability to climate change.pdf
2011 Carter, T. R., & Mäkinen, K. (2011). Approaches to climate change impact, adaptation and vulnerability assessment: towards a classification framework to serve decision-making. MEDIATION Technical Report No. 2.1. Helsinki, Finland. Retrieved from http://mediation-project.eu/
2011 Jean-Baptiste, N., Kuhlicke, C., Kunath, A., & Kabisch, S. (2011). CLUVA Project. D2.11: Review and evaluation of existing vulnerability indicators in order to obtain an appropriate set of indicators for assessing climate related vulnerability. Helmholtz Centre for Environmental Research - UFZ.
2011 Hinkel, J. (2011). "Indicators of vulnerability and adaptive capacity": Towards a clarification of the science–policy interface. Global Environmental Change, 21, 198–208. Retrieved from http://www.sciencedirect.com/science/article/pii/S0959378010000750
2011 ERN - Evaluación de Riesgos Naturales - América Latina. (2011). Probabilistic Modelling of Natural Risks at the Gobal Level: the Hybrid Loss Exceedance Curve. Development of Methodology and Implementation of Case Studies. Phase 1a. Colombia, Mexico and Nepal. ISDR.
2012 Preston, B. L. (2012). Climate Change Vulnerability Assessment: From Conceptual Frameworks to Practical Heuristics (No. 16). Retrieved from http://www.csiro.au/en/Organisation-Structure/Flagships/Climate-Adaptation-Flagship/CAF-working-papers.aspx
2012 Lundgren, L., & Jonsson, A. (2012). Assessment of Social Vulnerability: A Literature review of vulnerability related to climate change and natural hazards (No. 9) (p. 20).
2012 Matyas, D., & Pelling, M. (2012). Disaster Vulnerability and Resilience: Theory, Modelling and Prospective. Report produced for the Government Office of Science, Foresight project "Reducing Risks of Future Disasters: Priorities for Decision Makers."
2012 Lummen, N., Miller, D., & Yamada, F. (2012). Integrated Vulnerability and Risk Assessment : Case Study in Coastal Communities , Jamaica. In 8th annual international conference of the international institute or infrastructure renewal and reconstruction (pp. 417–426). Kumamoto, Japan.
2013 Paul, S. K. (2013). Vulnerability concepts and its application in various fields: a review on geographical perspective. J. Life Earth Sci., 8, 63–81. Retrieved from http://banglajol.info.index.php/JLES
2012 EEA. (2012). Urban adaptation to climate change in Europe. Challenges and opportunities for cities together with supportive national and European policies (p. 148). Luxembourg.
2012 Jacobs, C., Kazmierczak, A., Krellenberg, K., Kuhlicke, C., & Peltonen, L. (2012). Urban Vulnerability Indicators A joint report of ETC-CCA and ETC-SIA (p. 178).

2013 Ford, J., & Berrang-Ford, L. (2013). How to track adaptation to climate change: a typology of approaches for national-level application. Ecology and …. Retrieved from http://seachangecop.org/sites/default/files/documents/2013 09 RA - How to Track Adaptation to Climate Change.pdf
2013 Dunford, R., Harrison, P. A., Jäger, J., Rounsevell, M. D. A., & Tinch, R. (2013). The CLIMSAVE Project: Report on assessment of vulnerability across Europe and the identification of vulnerability hotspots (pp. 1–38).
2013 Lung, T., Lavalle, C., & Hiederer, R. (2013). A multi-hazard regional level impact assessment for Europe combining indicators of climatic and non-climatic change. Global Environmental …. Retrieved from http://www.sciencedirect.com/science/article/pii/S0959378012001409
2013 Gómez-Baggethun, E., & Barton, D. N. (2013). Classifying and valuing ecosystem services for urban planning. Ecological Economics, 86, 235–245. doi:10.1016/j.ecolecon.2012.08.019
2013 Kabisch, N., & Haase, D. (2013). Landscape and Urban Planning Green spaces of European cities revisited for 1990 – 2006. Landscape and Urban Planning, 110, 113–122. doi:10.1016/j.landurbplan.2012.10.017
2013 Ciurean, R., Schröter, D., & Glade, T. (2013). Conceptual Frameworks of Vulnerability Assessments for Natural Disasters Reduction. In Approaches to Disaster Management - Examining the Implications of Hazards, Emergencies and Disasters (pp. 3–32). doi:10.5772/55538
2013 Merz, M., Hiete, M., Comes, T., & Schultmann, F. (2013). A composite indicator model to assess natural disaster risks in industry on a spatial level. Journal of Risk Research, 16(April 2014), 1077–1099. doi:10.1080/13669877.2012.737820
2013 Kienberger, S., Blaschke, T., & Zaidi, R. Z. (2013). A framework for spatio-temporal scales and concepts from different disciplines: The "vulnerability cube." Natural Hazards, 68(3), 1343–1369. doi:10.1007/s11069-012-0513-x
2014 Ahsan, M. N., & Warner, J. (2014). The socioeconomic vulnerability index: A pragmatic approach for assessing climate change led risks–A case study in the south-western coastal Bangladesh. International Journal of Disaster Risk Reduction, 8, 32–49. doi:10.1016/j.ijdrr.2013.12.009
2014 Krellenberg, K., Link, F., Welz, J., Harris, J., Barth, K., & Irarrazaval, F. (2014). Supporting local adaptation: The contribution of socio-environmental fragmentation to urban vulnerability. Applied Geography, 55, 61–70. doi:10.1016/j.apgeog.2014.08.013
2014 Carter, J. G., Cavan, G., Connelly, A., Guy, S., Handley, J., & Kazmierczak, A. (2014). Climate change and the city: Building capacity for urban adaptation. Progress in Planning. doi:10.1016/j.progress.2013.08.001
2014 Dunford, R., Harrison, P. A., Jäger, J., Rounsevell, M. D. A., & Tinch, R. (2014). Exploring climate change vulnerability across sectors and scenarios using indicators of impacts and coping capacity. Climatic Change. doi:10.1007/s10584-014-1162-8
2014 Tonmoy, F. N. (2014). Assessment of vulnerability to climate change: theoretical and methodological developments with applications to infrastructure and built environment A thesis submitted in fulfillment of the requirements for the degree of. The University of Sydney.
2014 Frazier, T. G., Thompson, C. M., & Dezzani, R. J. (2014). A framework for the development of the SERV model: A Spatially Explicit Resilience-Vulnerability model. Applied Geography, 51, 158–172. doi:10.1016/j.apgeog.2014.04.004
2014 Notre Dame Global Adaptation Index (2014)
2014 Lee, Y.-J. (2014). Social vulnerability indicators as a sustainable planning tool. Environmental Impact Assessment Review, 44, 31–42. doi:10.1016/j.eiar.2013.08.002
2014 ASC. (2014). Adatation indicator set for the NAP. London, UK: Committee on Climate Change.
2015 Kok, M., Lüdeke, M., Lucas, P., Sterzel, T., Walther, C., Janssen, P., … de Soysa, I. (2015). A new method for analysing socio-ecological patterns of vulnerability. Regional Environmental Change. doi:10.1007/s10113-014-0746-1
Resilience community
2006 Folke, C. (2006). Resilience: The emergence of a perspective for social-ecological systems analyses. Global Environmental Change, 16(3), 253–267. doi:10.1016/j.gloenvcha.2006.04.002
2007 Mayunga, J. S. (2007). Understanding and Applying the Concept of Community Disaster Resilience : A capital-based approach. In Summer academy for social vulnerability and resilience building (pp. 1–16). Munich, Germany.
2008 Cutter, S. L., Barnes, L., Berry, M., Burton, C., Evans, E., Tate, E., & Webb, J. (2008). A place-based model for

understanding community resilience to natural disasters. Global Environmental Change, 18(4), 598–606. doi:10.1016/j.gloenvcha.2008.07.013
2010 Cutter, S. L., Burton, C. G., & Emrich, C. T. (2010). Disaster Resilience Indicators for Benchmarking Baseline Conditions. Journal of Homeland Security and Emergency Management, 7(1). doi:10.2202/1547-7355.1732
2014 Ifejika Speranza, C., Wiesmann, U., & Rist, S. (2014). An indicator framework for assessing livelihood resilience in the context of social–ecological dynamics. Global Environmental Change, 28, 109–119. doi:10.1016/j.gloenvcha.2014.06.005
2014 Cutter, S. L., Ash, K. D., & Emrich, C. T. (2014). The geographies of community disaster resilience. Global Environmental Change, 29, 65–77. doi:10.1016/j.gloenvcha.2014.08.005
2014 Fiksel, J., Goodman, I., & Hecht, A. (2014). Resilience: Navigating toward a Sustainable Future. Solutions: For a Sustainable and Desirable Future, 5(5), 38–47. Retrieved from http://www.thesolutionsjournal.com/node/237208
2014 Blair, B., Lovecraft, A. L., & Kofinas, G. P. (2014). Meeting institutional criteria for social resilience: a nested risk system model. Ecology and Society, 19(4), art36. doi:10.5751/ES-06944-190436
2015 Serrao-Neumann, S., Crick, F., Harman, B., Schuch, G., & Choy, D. L. (2015). Maximising synergies between disaster risk reduction and climate change adaptation: Potential enablers for improved planning outcomes. Environmental Science & Policy, 50, 46–61. doi:10.1016/j.envsci.2015.01.017
2015 Gall, M., Nguyen, K., & Cutter, S. L. (2014). Integrated research on disaster risk: is it really integrated? International Journal of Disaster Risk Reduction, 1–13. doi:10.1016/j.ijdrr.2015.01.010
On the relation between vulnerability, adaptation and resilience
2006 Gallopín, G. C. (2006). Linkages between vulnerability, resilience, and adaptive capacity. Global Environmental Change, 16(3), 293–303. doi:10.1016/j.gloenvcha.2006.02.004
2013 Lei, Y., Wang, J., Yue, Y., Zhou, H., & Yin, W. (2013). Rethinking the relationships of vulnerability, resilience, and adaptation from a disaster risk perspective. Natural Hazards, 70(1), 609–627. doi:10.1007/s11069-013-0831-7
2010 Miller, F., Osbahr, H., & Boyd, E. (2010). Resilience and vulnerability: complementary or conflicting concepts. Ecology and …. Retrieved from http://aaaspolicyfellowships.org/sites/default/files/pdfs/Resilience and Vulnerability - Complementary or Conflicting Concepts.pdf
Specific hazards: Wildfires
2010 Paveglio, T. B., Carroll, M. S., & Jakes, P. J. (2010). Alternatives to evacuation during wildland fire: Exploring adaptive capacity in one Idaho community. Environmental Hazards, 9(4), 379–394. doi:10.3763/ehaz.2010.0060
Specific hazards: Floods
2002 Tapsell, S. M., Penning-Rowsell, E. C., Tunstall, S. M., & Wilson, T. L. (2002). Vulnerability to flooding: health and social dimensions. Philosophical Transactions. Series A, Mathematical, Physical, and Engineering Sciences, 360, 1511–1525. doi:10.1098/rsta.2002.1013
2009 Balica, S. F., Douben, N., & Wright, N. G. (2009). Flood vulnerability indices at varying spatial scales. Water Science and Technology : A Journal of the International Association on Water Pollution Research, 60(10), 2571–80. doi:10.2166/wst.2009.183
2009 Fekete, A. (2009). Validation of a social vulnerability index in context to river-floods in Germany. Natural Hazards and Earth System Science, 9(2), 393–403. doi:10.5194/nhess-9-393-2009
2011 Keogh, D. U., Apan, A., Mushtaq, S., King, D., & Thomas, M. (2011). Resilience , Vulnerability and Adaptive Capacity of an Inland Rural Town Prone to Flooding : A Climate Change Adaptation Case Study. Natural Hazards, 59(2), 699–723.
2011 Alexander, M., Viavattene, C., Faulkner, H., & Priest, S. (2011). Methods for creating a flood risk assessment tool: FRMRC Research Report SWP3.2 (pp. 1–19). Flood Hazard Research Centre, Middlesex University. Retrieved from www.floodrisk.org.uk
2011 Müller, a., Reiter, J., & Weiland, U. (2011). Assessment of urban vulnerability towards floods using an indicator-based approach – a case study for Santiago de Chile. Natural Hazards and Earth System Science, 11(8), 2107–2123. doi:10.5194/nhess-11-2107-2011
2011 Kaźmierczak, A., & Cavan, G. (2011). Surface water flooding risk to urban communities: Analysis of vulnerability, hazard and exposure. Landscape and Urban Planning, 103(2), 185–197. doi:10.1016/j.landurbplan.2011.07.008

2013 Jun, K.-S., Chung, E.-S., Kim, Y.-G., & Kim, Y. (2013). A fuzzy multi-criteria approach to flood risk vulnerability in South Korea by considering climate change impacts. Expert Systems with Applications, 40(4), 1003–1013. doi:10.1016/j.eswa.2012.08.013
2015 Akukwe, T. I., & Ogbodo, C. (2015). Spatial Analysis of Vulnerability to Flooding in Port Harcourt Metropolis, Nigeria. SAGE Open, 5(1). doi:10.1177/2158244015575558
2015 Foudi, S., Osés-Eraso, N., & Tamayo, I. (2015). Integrated spatial flood risk assessment: The case of Zaragoza. Land Use Policy, 42, 278–292. doi:10.1016/j.landusepol.2014.08.002
2015 Koks, E. E., Jongman, B., Husby, T. G., & Botzen, W. J. W. (2015). Combining hazard, exposure and social vulnerability to provide lessons for flood risk management. Environmental Science & Policy, 47, 42–52. doi:10.1016/j.envsci.2014.10.013
Specific hazards: Heat Island Effect
2011 Uejio, C. K., Wilhelmi, O. V, Golden, J. S., Mills, D. M., Gulino, S. P., & Samenow, J. P. (2011). Intra-urban societal vulnerability to extreme heat: the role of heat exposure and the built environment, socioeconomics, and neighborhood stability. Health & Place, 17(2), 498–507. doi:10.1016/j.healthplace.2010.12.005
2012 Johnson, D. P., Stanforth, A., Lulla, V., & Luber, G. (2012). Developing an applied extreme heat vulnerability index utilizing socioeconomic and environmental data. Applied Geography, 35(1-2), 23–31. doi:10.1016/j.apgeog.2012.04.006
2013 Aubrecht, C., & Özceylan, D. (2013). Identification of heat risk patterns in the U.S. National Capital Region by integrating heat stress and related vulnerability. Environment International, 56, 65–77. doi:10.1016/j.envint.2013.03.005
2013 Krüger, T., Held, F., Hoechstetter, S., Goldberg, V., Geyer, T., & Kurbjuhn, C. (2013). A new heat sensitivity index for settlement areas. Urban Climate, 6, 63–81. doi:10.1016/j.uclim.2013.09.003
2013 Depietri, Y., Welle, T., & Renaud, F. G. (2013). Social vulnerability assessment of the Cologne urban area (Germany) to heat waves: links to ecosystem services. International Journal of Disaster Risk Reduction, 6, 98–117. doi:10.1016/j.ijdrr.2013.10.001
2013 Wolf, T., & McGregor, G. (2013). The development of a heat wave vulnerability index for London, United Kingdom. Weather and Climate Extremes, 1(August 2003), 59–68. doi:10.1016/j.wace.2013.07.004
2014 Dugord, P.-A., Lauf, S., Schuster, C., & Kleinschmit, B. (2014). Land use patterns, temperature distribution, and potential heat stress risk – The case study Berlin, Germany. Computers, Environment and Urban Systems, 48, 86–98. doi:10.1016/j.compenvurbsys.2014.07.005
2014 Klein Rosenthal, J., Kinney, P. L., & Metzger, K. B. (2014). Intra-urban vulnerability to heat-related mortality in New York City, 1997-2006. Health & Place, 30C, 45–60. doi:10.1016/j.healthplace.2014.07.014
2014 ARUP. (2014). Reducing urban heat risk: A study on urban heat risk mapping and visualisation. London.
2015 El-Zein, A., & Tonmoy, F. N. (2015). Assessment of vulnerability to climate change using a multi-criteria outranking approach with application to heat stress in Sydney. Ecological Indicators, 48, 207–217. doi:10.1016/j.ecolind.2014.08.012
Specific hazards: Coastal Flooding
2010 Romieu, E., Welle, T., Schneiderbauer, S., Pelling, M., & Vinchon, C. (2010). Vulnerability assessment within climate change and natural hazard contexts: revealing gaps and synergies through coastal applications. Sustainability Science, 5(2), 159–170. doi:10.1007/s11625-010-0112-2
2011 Dutta, D. (2011). An integrated tool for assessment of flood vulnerability of coastal cities to sea-level rise and potential socio-economic impacts: a case study in Bangkok, Thailand. Hydrological Sciences Journal, 56(5), 805–823. doi:10.1080/02626667.2011.585611
2011 Yoo, G., Hwang, J. H., & Choi, C. (2011). Development and application of a methodology for vulnerability assessment of climate change in coastal cities. Ocean & Coastal Management, 54(7), 524–534. doi:10.1016/j.ocecoaman.2011.04.001
2012 Friedrich, E., & Kretzinger, D. (2012). Vulnerability of wastewater infrastructure of coastal cities to sea level rise: a South African case study. Water SA, 38(5), 755–764. Retrieved from http://www.scielo.org.za/scielo.php?script=sci_arttext&pid=S1816-79502012000500015&lng=en&nrm=iso&tlng=en
2012 Balica, S. F., Wright, N. G., & van der Meulen, F. (2012). A flood vulnerability index for coastal cities and its use in assessing climate change impacts. Natural Hazards, 64(1), 73–105. doi:10.1007/s11069-012-0234-1

2013 Davidson, J. L., Putten, I. E. Van, Leith, P., Nursey-bray, M., Madin, E. M., & Neil, J. (2013). Toward Operationalizing Resilience Concepts in Australian Marine, 18(3).
Specific hazards: Droughts
1982 Hashimoto, T., Stedinger, J. R., & Loucks, D. P. (1982). Reliability, resiliency, and vulnerability criteria for water resource system performance evaluation. Water Resources Research, 18(1), 14–20. doi:10.1029/WR018i001p00014
2005 Wilhite, D. A., & Hayes, M. J. (2005). The Basics of Drought Planning: A 10-Step Process.
2008 Kallis, G. (2008). Droughts. Annual Review of Environment and Resources, 33(1), 85–118. doi:10.1146/annurev.environ.33.081307.123117
2009 Iglesias, A., Moneo, M., & Quiroga, S. (2009). Coping with Drought Risk in Agriculture and Water Supply Systems. (A. Iglesias, A. Cancelliere, D. A. Wilhite, L. Garrote, & F. Cubillo, Eds.)Coping with Drought Risk in Agriculture and Water Supply Systems (Vol. 26, pp. 153–159). Dordrecht: Springer Netherlands. doi:10.1007/978-1-4020-9045-5

Table 18: List of papers reviewed for methods and indicators.